Late Triassic (early Carnian) palynology of the shallow stratigraphic core 7830/3-U-1, offshore Kong Karls Land, Northern Barents Sea

Kurt Inge Miljeteig

Thesis for master degree in Petroleum Geoscience

Department of Earth Science,

University of Bergen

June, 2016

Abstract

This study presents palynostratigraphic and palynofacies analyses from the shallow stratigraphic core 7830/3-U-1, drilled through the Snadd Formation (equivalent to De Geerdalen Formation) offshore Kong Karls Land in the northern Barents Sea, Norwegian Arctic. The Norwegian Petroleum Directorate have drilled several stratigraphic cores in the northern Barents Sea, which offer a unique insight into the Late Triassic stratigraphy and paleogeography of the region. This study constitutes a part of a broader palynostratigraphic investigation of the late Middle to Late Triassic of the Barents Sea, currently being undertaken at the University of Bergen, with the aim of improving the biostratigraphic resolution.

Thirty-one samples from the approximately 200 m long core were analysed for palynological purpose. The core yielded great diversity of well-preserved palynomorphs. The palynological association is considered to constitute a single assemblage which is assigned an early Late Triassic (early Carnian) age, consistent with previously published age constraints including Re-Os datings from the area.

Interpretation of sedimentological data, integrated with palynological and palynofacies data, indicates seven prograding parasequences, bounded by marine flooding surfaces, interpreted to range from offshore to delta front depositional environments. Palynofacies analysis suggest cycles of amorphous organic matter content and the presence of marine acritarchs (microplankton) strengthening the evidence of progradational parasequences deposited in a paralic environment. The high relative abundance of hinterland pollen types, e.g. bisaccate pollen, indicate transportation over large area. Spores are interpreted to reflect the local vegetation growing on the margins of the basin, such as abundant fern spores like *Deltoidospora*, *Dictyophyllidites* and *Leschikisporis* which were recorded and indicates a temperate and humid climate, consistent with previous interpretations of Late Triassic palaeoclimate on the northern Pangaean margin.

Acknowledgments

This thesis is at part of a Master Degree in Petroleum Geoscience at the University of Bergen, to which I owe gratitude to provide this project.

First of all, I would like to thank my supervisor Prof. Gunn Mangerud and my co-supervisor Dr. Niall William Paterson (Department of Earth Science, University of Bergen) for all their help, feedback, discussions and explanations.

I would also like to thank my co-supervisor Bjørn Anders Lundschien (Norwegian Petroleum Directory) for his advising during a core logging session. Special thanks goes to the NPD for giving me the opportunity to participate in a field course on the Triassic succession in Svalbard.

Thanks to Dr. Stijn De Schepper (Department of Earth Science, University of Bergen) for his theoretical introduction to palynological processing techniques and his lecture about dinoflagellates.

Thanks to Applied Petroleum Technology for giving me a practical introduction to palynological processing techniques and an introduction on Triassic palynomorphs.

Centrica Energi NUF, Chevron Norge AS, ConocoPhillips Skandinavia AS, Det Norske Oljeselskap ASA, Dong E&P Norge AS, ENI Norge AS, Lundin Norway AS, A/S Norske Shell and Statoil Petroleum AS. Thanks to you all for funding this project.

Finally, I would like to thank my family for support and motivation through the time writing the master thesis.

Bergen, 29th of May 2016

Kurt Inge Miljeteig

Kurt Inge Miljeteig

Table of Contents

1. Introduction

This thesis includes palynostratigraphic analysis and palynofacies data of the Upper Triassic succession in the northern Barents Sea (The Norwegian Arctic) (Fig. 1). The Triassic period has an approximate timespan of 50.9 Ma, 35.7 Ma of which is represented by the Late Triassic (Ogg, 2012). The Early and Middle Triassic represent considerably shorter intervals of time, with a timespan of 5.0 and 10.2 Ma, respectively (Fig. 2). There is a generally low resolution of the Arctic Late Triassic due to the lack of age-diagnostic macrofossils in the area. Ammonites are the best index fossils for subdivision of the Boreal Triassic because of their relatively rapid evolution, which provides a high resolution; however, they are rare to find in the current area and they are also facies dependent. This leads to uncertainty regarding correlation with zonations in other areas, like the Germanic and Alpine realm (Hochuli et al., 1989). Especially the resolution is low for the latest stage of the period, recently underlined by Vigran et al. (2014). However, a lot of the uncertainty is that the palynomorph assemblages are different between northern Barents Sea and Germanic/Alpine realm and the taxa have different ranges (Hochuli et al., 1989). Previous studies (e.g. Vigran et al. 2014) have shown that palynology is a useful tool that can contribute toward a higher resolution stratigraphy.

The geological data coverage from the Northern Barents Sea is relatively scarce, especially regarding palynology. However, Norwegian Petroleum Directorate have during the last decade drilled several stratigraphic shallow cores in the area providing a unique insight into the Upper Triassic sediments. Despite the number of papers published in recent years, it is important to improve the biostratigraphic resolution in order to get a more detailed zonation and age assessment of the sediments. This is also of importance for the petroleum industry, as dating is critical in all geological work, including better understanding of the depositional environment and establish paleogeographic models which again can give us a better understanding of e.g. where hydrocarbons are localized (Riis et al., 2008, Lundschien et al., 2014). Additionally, palynostratigraphic work can improve the understanding of the climate in the past, which is of especially importance for academics.

1.1 Aim of Study

This study is part of a broader palynostratigraphic research project dealing with the Middle to Upper Triassic succession of the Barents Sea area, currently being undertaken at the University of Bergen. The purpose of this larger project is to use palynology to improve the biostratigraphic resolution of the Upper Triassic Barents Shelf, and this thesis will be a contribution to this project.

The main aim for this study was to date the shallow stratigraphic core 7830/3-U-1 by using palynology. Core 7830/3-U-1 was drilled through the Snadd Formation, approximately 20 km east from Kong Karls Land in the Northern Barents Sea (Fig. 1), and is provided by the Norwegian Petroleum Directory (NPD) for this study. Kong Karls Land is an uplifted and exposed part of the Svalbard Archipelago.

An important part of the analysis was also to recognise any marine incursions to gain a better understanding of the paleoenvironments represented by the core, which helps to enhance the current understanding of the paleogeography of the Upper Triassic from the Barents Sea. Palynofacies analysis and a sedimentological log were carried out to contribute the understanding of the depositional environment.

Vigran et al. (2014) first published the palynology of this core and suggested that the lowermost 20 m of this 200 m long core was of Early Carnian age, while the upper part was suggested to be of Middle Carnian age. Vigran et al. (2014) refers to the presence of *Aulisporites astigmosus* and *Echinitosporites iliacoides*, and the overall abundance of *A. astigmosus.* However, Vigran et al. (2014) provided no quantitative data, palynofacies or sedimentological work. The present research will give a more detailed data set and verify the age. It was therefore critical to perform semi-quantitative analysis to verify or in the opposite case, redate this core.

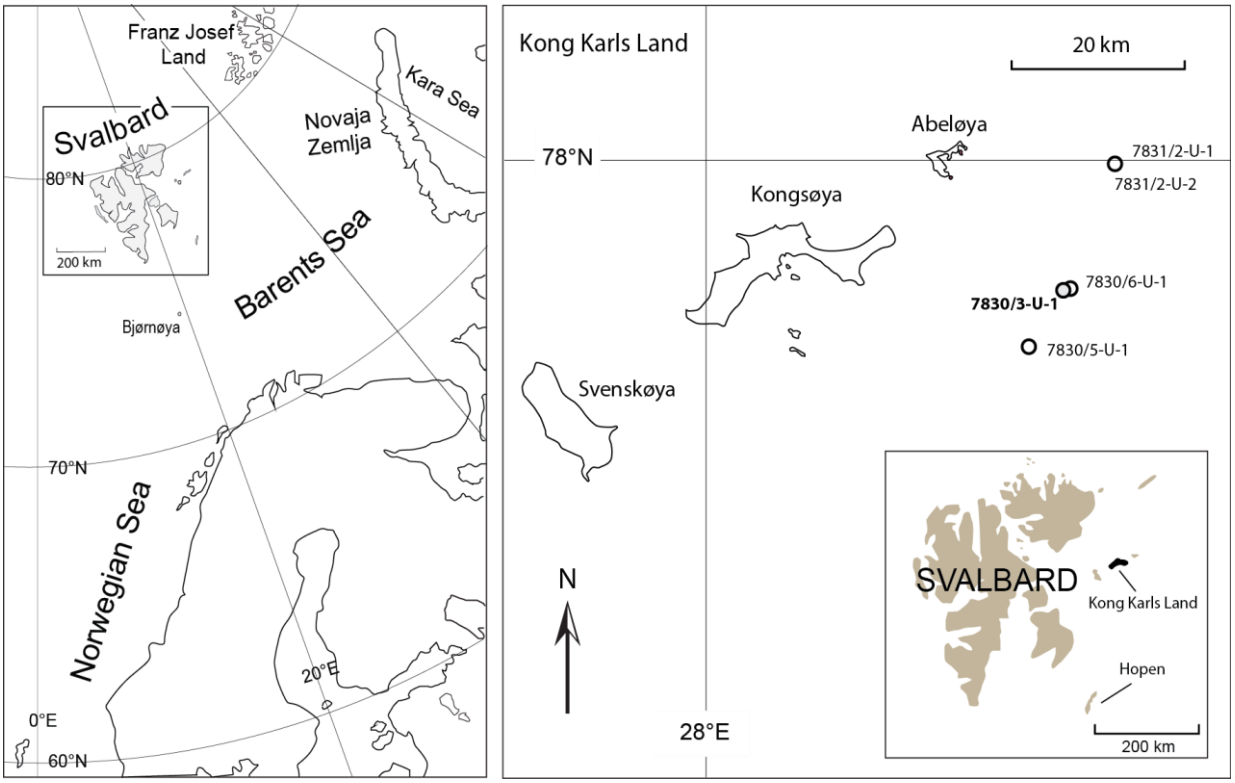

Figure 1: Overview map of the Barents Sea to the left. The close up map to the right shows the location of shallow stratigraphic core 7830/3-U-1, offshore Kong Karls Land, northern Barents Sea. (also showing location of the four nearby shallow boreholes) (Provided by Paterson, N.).

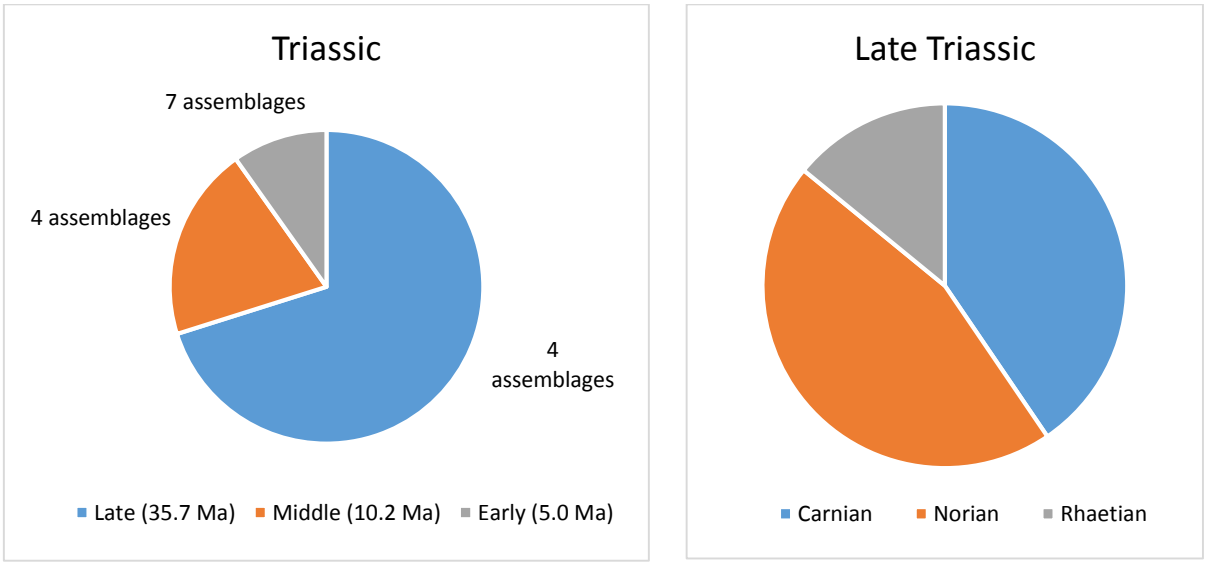

Figure 2: Timespan of the Triassic Period based on the ICS-chart v2015/01. The 15 Composite Assemblage zones in the left figure are based on Vigran et al. (2014) and correlates with Boreal ammonite zones.

1.2 Palynology

Palynology is the study of organic walled microfossils, and includes various microscopic organisms such as reproductive plant cells (e.g. pollen and spores) and whole organisms like algae (Traverse, 2007). These are collectively termed palynomorphs, and they include acritarchs, dinoflagellates, chitinozoans and scolecodonts as well. Their walls are composed of highly resistant organic materials, either sporopollenin (e.g. pollen, certain spores and acritarchs) or chitin, which make them resistant for maceration preparation using hydrochloric- (HCl) and hydrofluoric (HF) acid. The wall structure also makes palynomorphs relatively resistant during diagenesis and transportation. On the other hand, exposure to strong oxidation or highly alkaline environments will affect their preservation. They can be totally destroyed and useless for palynological research if they are too much affected by this (Traverse, 2007).

Due to the fact that palynomorphs are embedded within sedimentary rocks, are abundant, have a widespread distribution, rapid evolution and are easy to prepare for microscopic analysis they are very useful index fossils. Palynomorphs are also the only fossil group that can be used to correlate between terrestrial- and marine strata. In what extent the palynomorphs are present in sedimentary rocks are affected by the facies. Traverse (2007) reports silt samples containing 5 million dinoflagellates per gram liquid and samples containing 4 million pollen grains per gram liquid. That implies that one slide may contain 5000 specimens. Palynomorphs ranging in size between five and 500 micrometres (µm), where sizes from 20 - 90 µm occurs most. However, there are some exceptions, e.g. megaspores with a size above 200 µm (Traverse, 2007).

The most common palynomorphs in the Triassic of the Norwegian Arctic are acritarchs, spores and pollen. Acritarchs are single celled, organic microfossils of uncertain biological affinity. They range from the Precambrian (1.4 GA old) to the present, and are the oldest known palynomorphs (Fig. 4). They include a large range of presumable algal bodies, with a common size range between 15 – 80 µm (but have been observed from less than 10 µm to more than 1000 µm) (Traverse, 2007). Most of them are inferred to be of marine origin, but there are also several brackish-water or freshwater forms as well. Common morphological types include psilate, scabrate, spiny and reticulate (Fig. 3) (Traverse, 2007).

Spores range from Upper Ordovician to present (Fig. 4), and are typically characterized by a laesura. This is seen as a scar in the grains, either as a monolete or as a trilete mark resulting from the contact between a tetrad of spores produced by meiosis from a spore mother cell in the sporangium of the parent plant (Traverse, 2007). Their shape is often subtriangular to round, and they have different ornaments (e.g. psilate, verrucate, baculate) (Fig. 3). Bryophyta (mosses) and Pteridophyta (ferns) are examples of spores producing plants (Traverse, 2007).

Pollen grains appear later in the geological record and are recorded in sediments from the Upper Devonian to present. Gymnosperms (e.g. conifers), cycadophytes (cycads) and angiosperms (flowering plants) are land plants that produce pollen. Pollen grains are typically characterised by having a sulcus and/or saccus/saccae. The sulcus is like an opening in the pollen grain (Fig. 5). Saccate pollen are pollen grains with at least one saccus, and the sacci are often known as “vesicle”, “bladder”, “wing” or “bag”. The saccus makes it easier for a pollen grain to float over longer distances in water, and perhaps in the air as well, due to a reduction in total specific gravity. For this reason, it is possible for saccate pollen to be transported over longer distances than spores. However, it is now generally agreed that the primary purpose to the saccus is biological. Saccate pollen was very common in the Mesozoic, especially in the Late Triassic (Traverse, 2007).

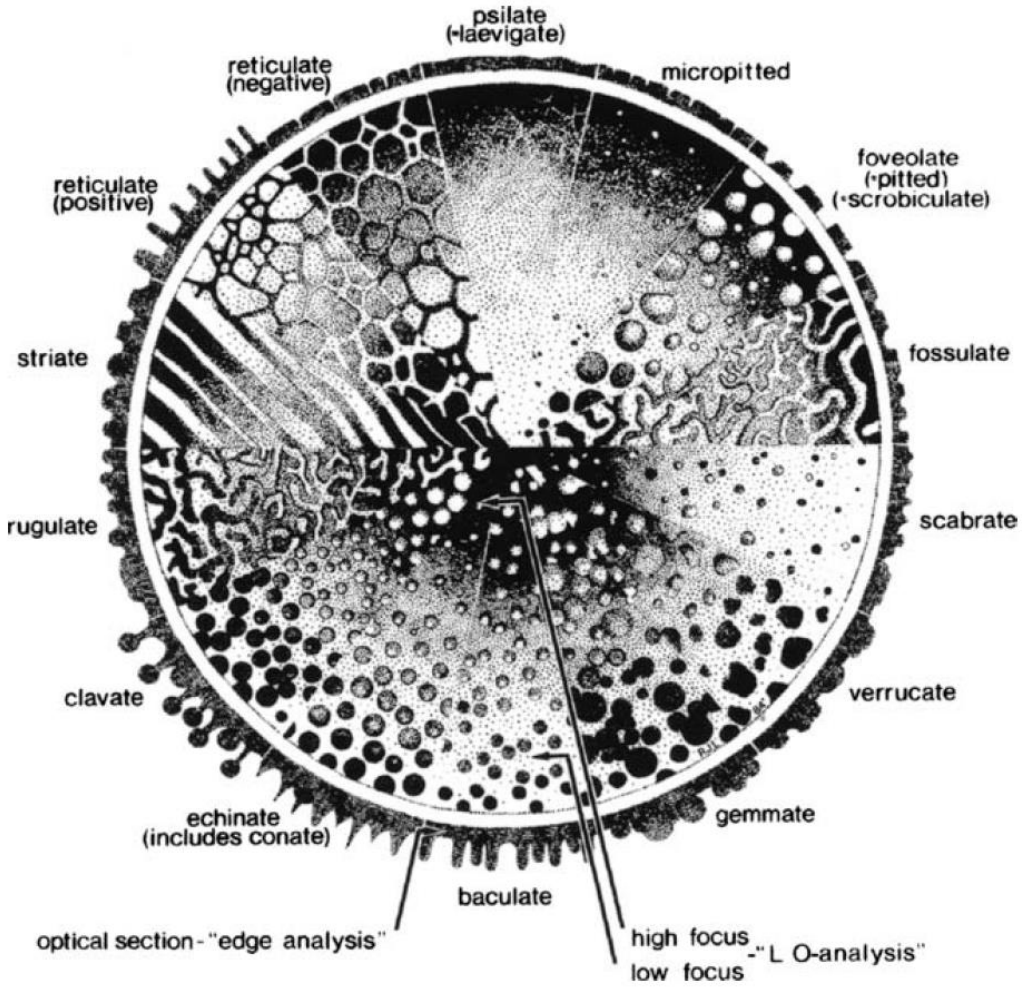

Figure 3: Sculpture types of palynomorphs, both edge-analysis and various levels of focus are shown. Low focus is shown towards the edge and high focus toward the centre. (From Traverse, 2007).

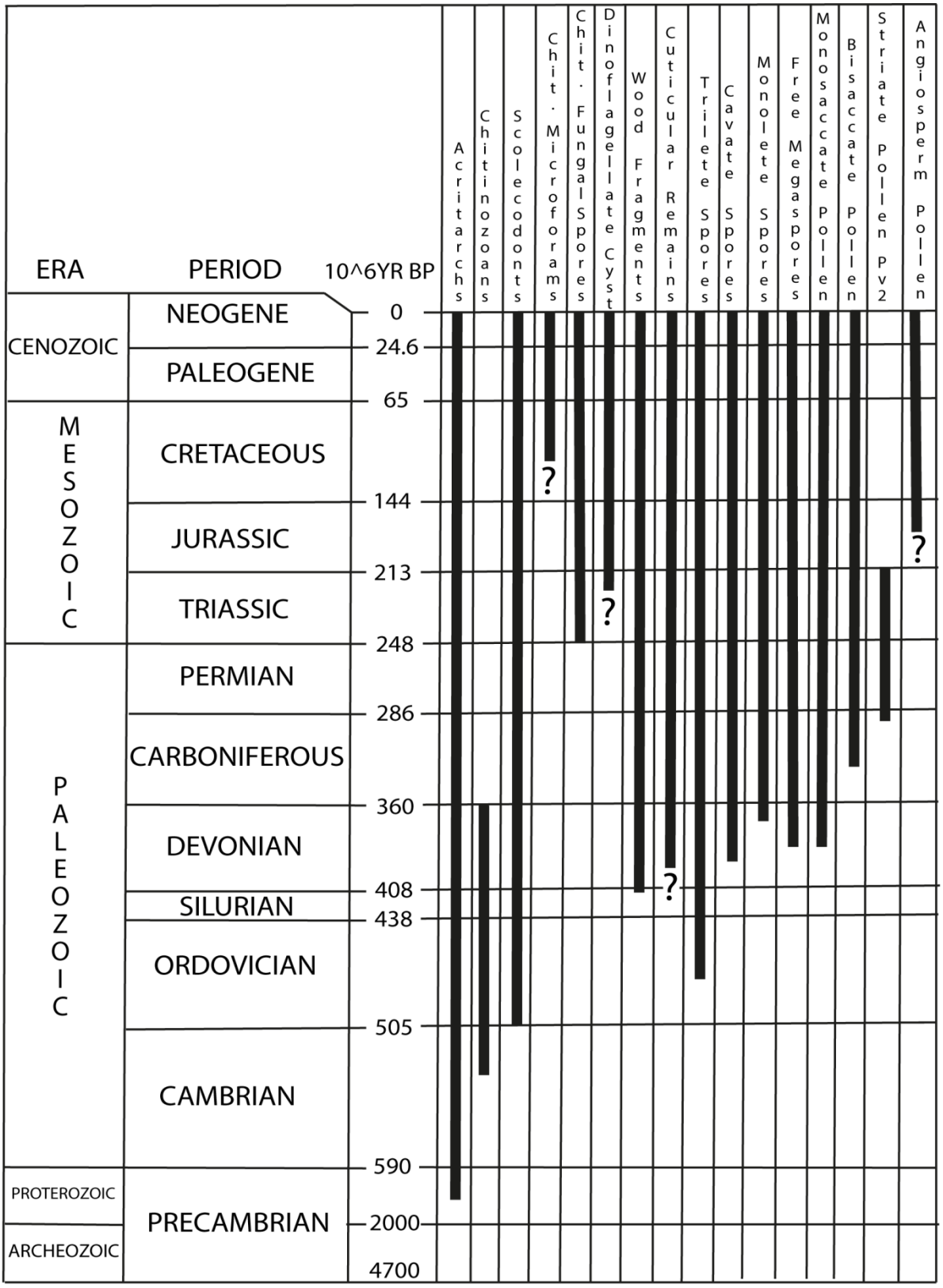

Figure 4: Range of occurrence in time of the most commonly used palynomorphs. E.g. striate pollen was present until the Triassic/Jurassic boundary and Dinoflagellate Cyst occurred in Late Triassic. (Modified from Traverse, 2007).

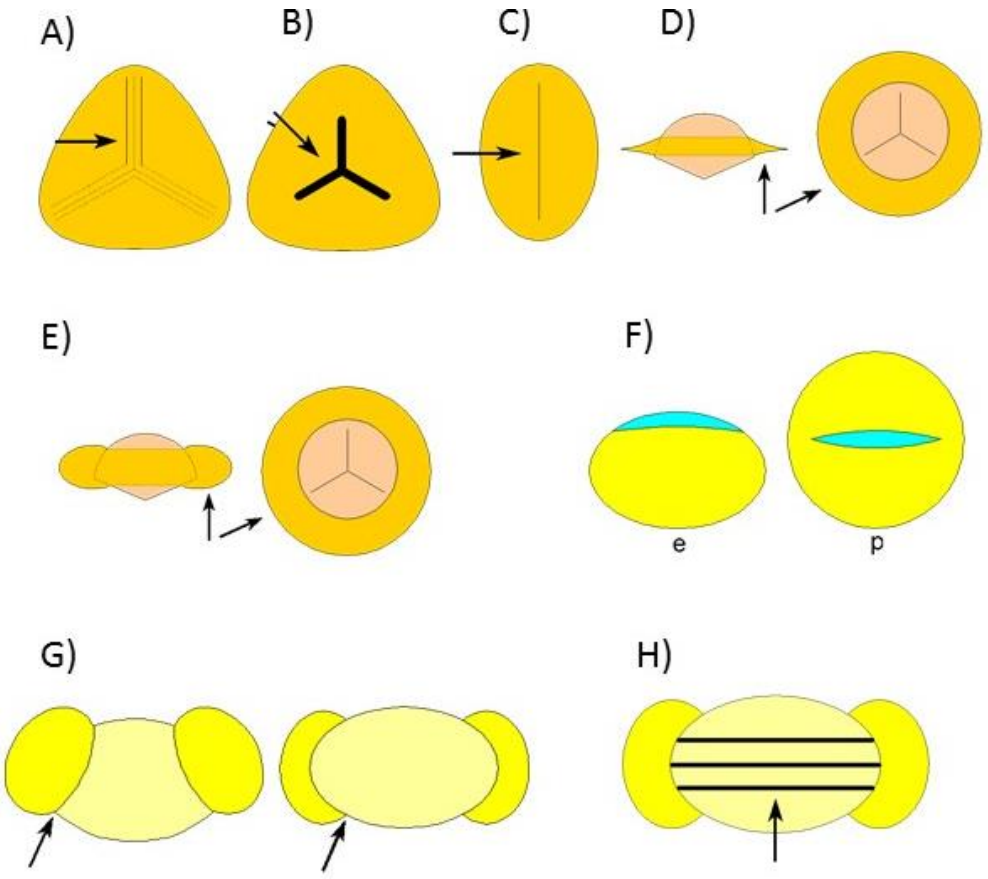

Figure 5:
A) Laesura (The arm of a proximal fissure or scar of a spore. A trilete spore has three laesura, while a monolete spore has one)
B) Shows the trilete mark (Y-mark) of a spore.
C) Shows a monolete mark, appear rarely on pollen grains.
D) Shows the zona which is a thin outer structure of a spore that projects at the equator, but does not extend over the distal face or proximal face.
E) Cingulum (A thick outer structure of a spore that projects at the equator, but does not extend over the distal or proximal face).
F) Shows the sulcus which is an elongated latitudinal ectoaperature situated at the distal or proximal pole of a pollen grain.
G) Bisaccate pollen grains in which the outline of the sacci in polar view is discontinuous with the outline of the corpus (body of Bisaccate pollen) so that the grains seem to consist of three distinct.
H) Taenia is shown as one or more strap-like structures, more or less parallel strips on the corpus (E.g. *Striatites*).
(Modified from Punt et al. 2007).

2. Geological Framework

2.1 Geological Setting of the Barents Sea area with focus on the Triassic Period

The Barents Sea Shelf covers a large area in the northern part of the Eurasian plate. The shelf extends from the Arctic Ocean to the coastline of Northern Norway and Russia, and from the Norwegian-Greenland Sea to the Russian island Novaya Zemlya (Fig. 1). The entire Barents Shelf covers an area of approximately 1.3 million km^2, whereas the Svalbard Archipelago in the northwestern corner are covering a land area of approximately 63 000 km^2, representing less than 5% of the entire Barents Sea (Worsley, 2008). The Svalbard Archipelago is an uplifted and exposed part of the Barents Sea and provides an exposed analogue of the offshore geology (Mørk et al., 1999). The map presented by Smith et al., (1976) shows the submarine contours nearby Kong Karls Land (Fig. 6), and the Barents Sea has an average depth of approximately 230 m (Sakshaug et al., 1994). The Barents Shelf is divided into two major geological provinces; the western province consisting of numerous basins and platforms, and an eastern region with its massive North and South Basin (Fig. 7) (Worsley, 2008).

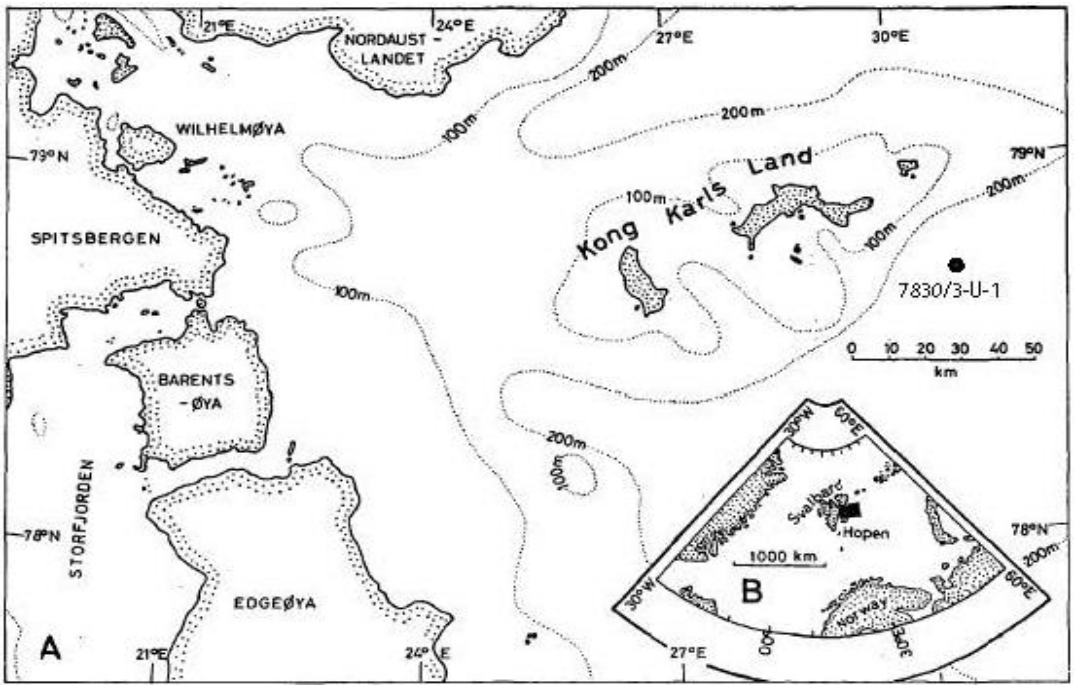

Figure 6: A) Kong Karls Land – geographical location showing 100 m submarine contours. The location where core 7830/3-U-1 is drilled is highlighted. B) Overview map of the Arctic region. (Modified from Smith et al., (1976)).

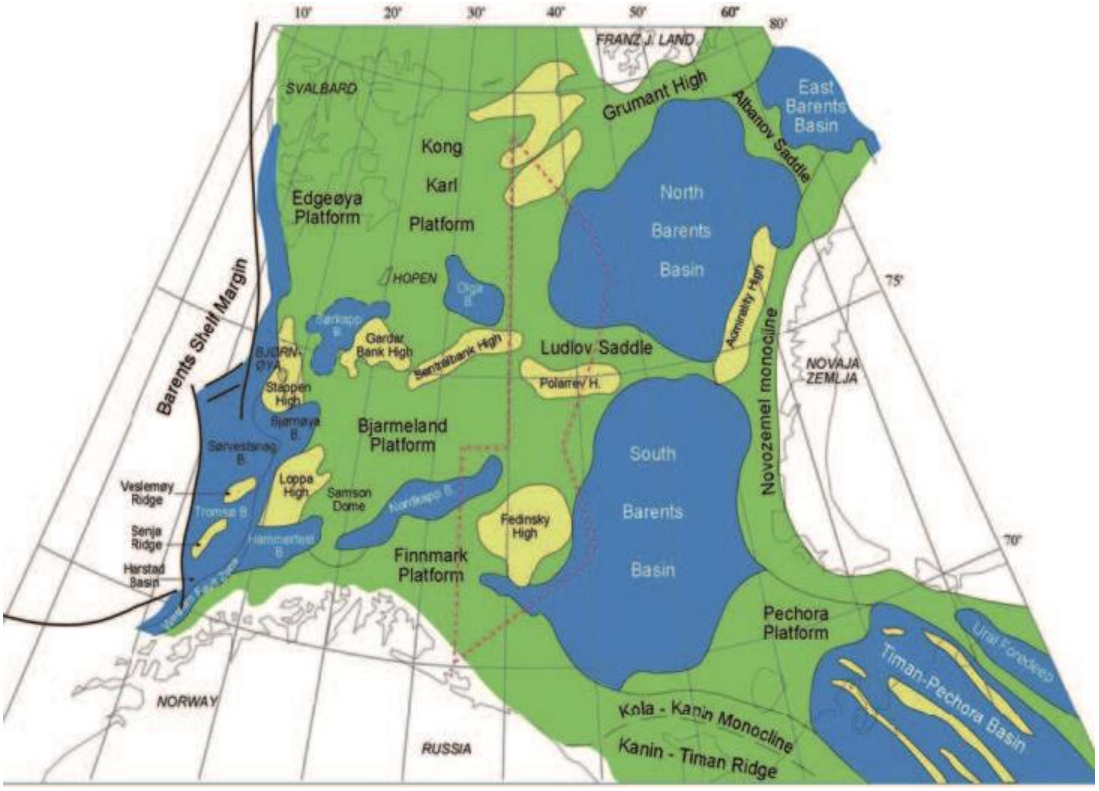

Figure 7: The two major geological provinces in the Barents Sea; the western province consisting of numerous basins and platforms, and an eastern region with its massive North and South Basin (From Worsley, 2008).

During the Triassic, the study area and rest of the Barents Sea area was located in the northern part of the supercontinent Pangea, at a palaeolatitude of approximately 50° north. The sedimentological succession of Svalbard and the Barents Sea records a lot of changes in the climate and the environment from their position at Triassic to where it is located today, at around 78°N 40°E. However, this project has the main focus on the development and depositional environment of the Triassic time.

By the end of the Palaeozoic Era the Barents Sea was situated in a large embayment in the northern part of Pangea, and made up a vast epicontinental sea (Fig. 8). The embayment was surrounded by mainland in west, south and east, and an opening directly to the Panthalassa Ocean in the north (Worsley, 2008; Torsvik and Cocks, 2005; Buiter and Torsvik, 2007; Glørstad-Clark et al., 2010). The continent Laurentia collided with Western Siberia during the Permian, and formed the Uralian Mountain chain. Erosion products from this mountain chain during

Late Permian/Early Triassic, together with erosion products from the previously formed Caledonian Orogeny, filled the Barents Sea basin in a northwesterly direction (Fig. 10).

During the Carnian Kong Karls Land was situated at the delta front (prodelta/delta) (Fig. 10) (Riis et al., 2008; Worsley, 2008; Glørstad-Clark et al., 2010). The infill of sediments from southeast is reflected in the prograding clinoforms seen in seismic data, a progradation that probably started by the latest Permian (e.g. Riis et al., 2008; Lundschien et al., 2014).

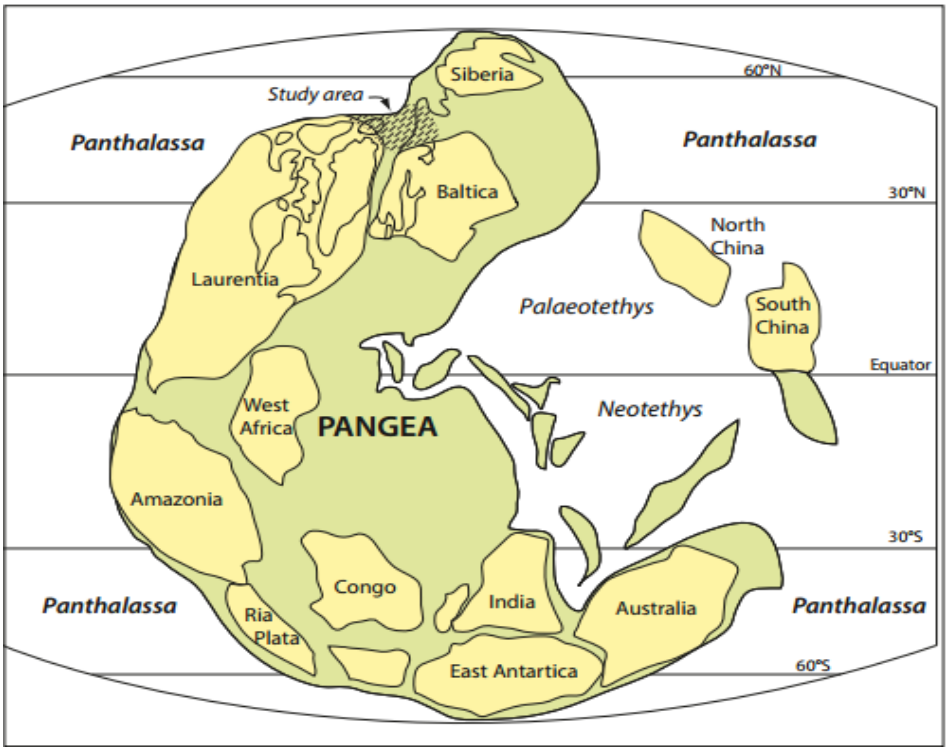

Figure 8: The Pangea supercontinent. Showing the study area in northern corner. (Based on Torsvik and Cocks, 2005)

During the Middle and Late Triassic, sediment sources along the margins of the Barents Sea in the eastern and southeastern parts gradually filled in the deeper shelf areas creating a paralic platform. During the Middle Carnian the paralic deposits continued into the Svalbard Archipelago. There are no indications of sediment sources north of Svalbard (Riis et al. 2008).

Five explorations wells (shallow cores) were drilled approximately 20 km east of Kong Karls Land (Figs.1 and 6). The area is located on a salt-cored structure, which has brought Triassic rocks to the sea floor (Fig. 9) (Riis et al., 2008). There are no commercial seismic data from northern Barents Sea. However, Riis et al. (2008) presented a section (Fig. 11) enabling a correlation between the drilled Triassic sections and the surrounding platform (Riis et al., 2008). Since Triassic strata crop out on the sea floor over large parts of the Barents Sea Shelf, or as some places right under Quaternary sediments, it is easier to drill and it is possible to detect hydrocarbons at quite shallow depths. An example of an area is southeast of Svalbard where exploration the last years has proven this (Lundschien et al., 2014).

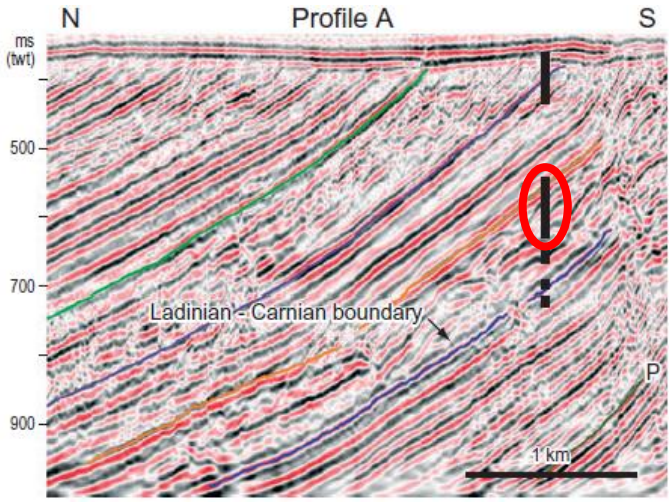

Figure 9: Showing seismic data from Kong Karls Land. The five exploration cores are projected into a single seismic line, and shows the approximate position where the cores were drilled. Core 7830/3-U-1 is the second line from the sea floor (framed in red circle). The blue reflector, between the two lowermost cores which were presented by Meltveit (2015) represents the Ladinian-Carnian boundary. The highest stratigraphically core 7830/5-U-1 was presented by Paterson et al. (2016) (Modified from Riis et al. (2008)).

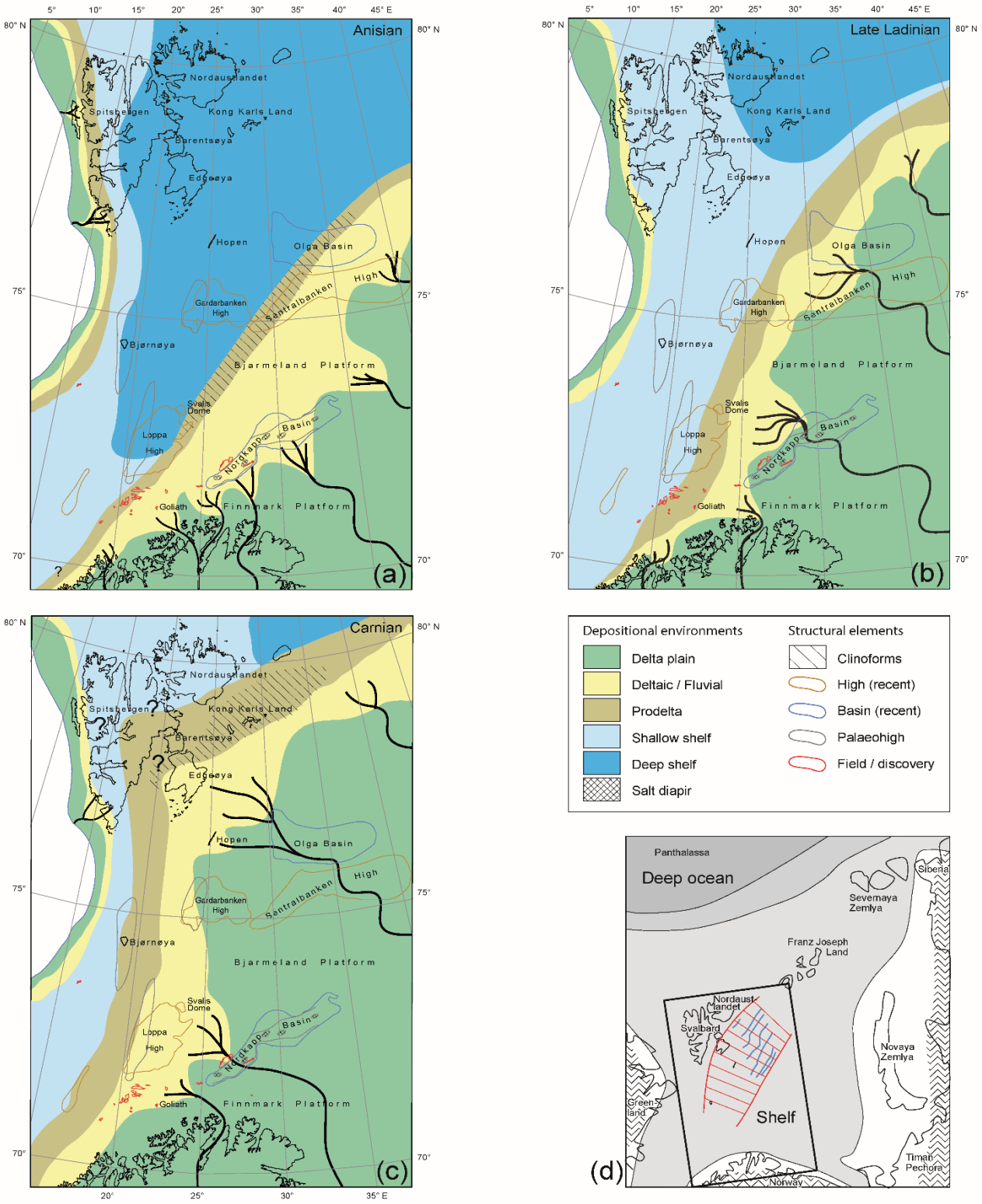

Figure 10: Paleographic maps showing the evolution of the Barents Shelf, from (a) Anisian to (b) Late Ladinian to (c) Carnian, illustrating an extensive progradation from south-east and the development of delta plain and prodelta environment over the entire Barents Shelf. (d) Overview map of the interpreted progradation in the current area, from Anisian (red line in east) to Carnian (red line in west) (from Riis et al. (2008)).

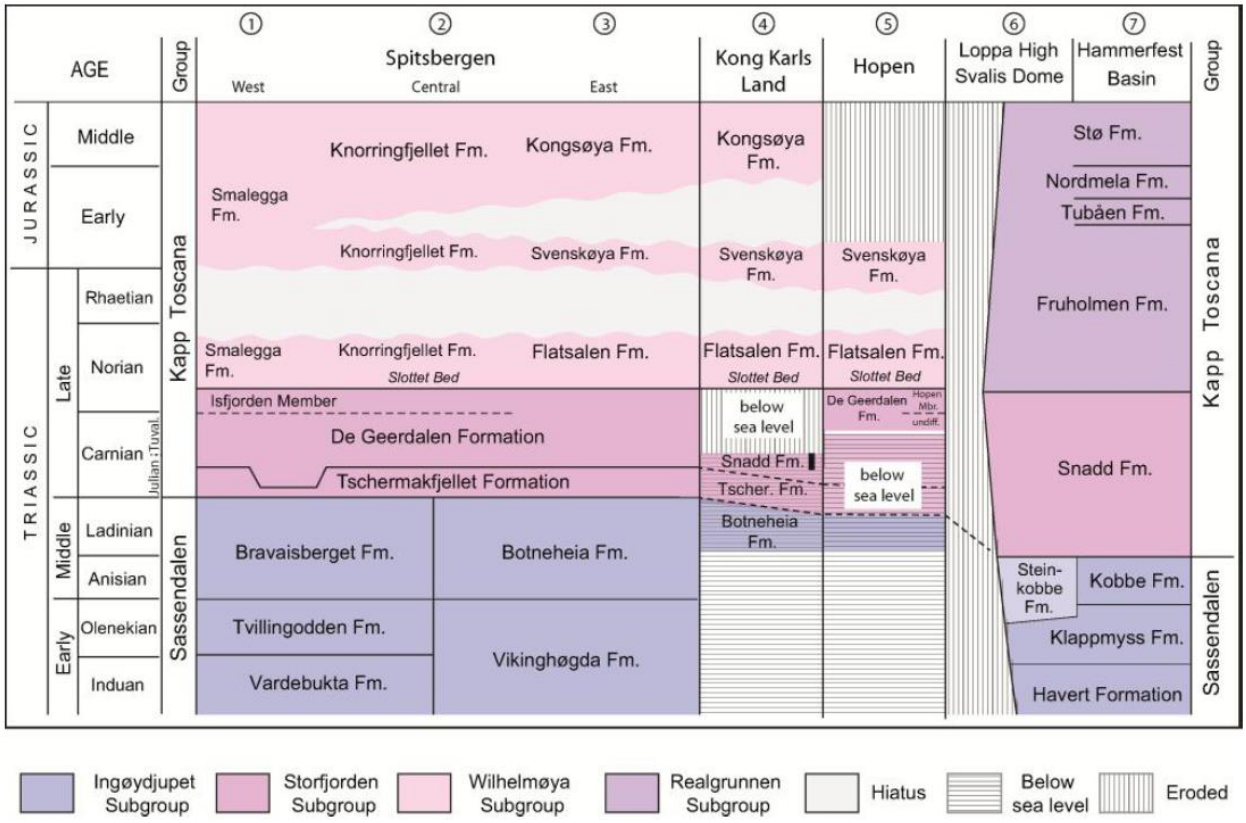

Figure 11: Lithostratigraphic subdivisions for the Triassic to Middle Jurassic successions of Svalbard and the Barents Shelf (modified from Mørk et al. (1999a) by Paterson et al. (2016)).

Mørk et al. (1999a) used data from non-commercial 2D seismic and from shallow cores to construct a common stratigraphy from the Mesozoic of Svalbard and the Barents Sea (Fig. 6) (Lundschien et al., 2014). The Triassic succession on Svalbard are divided into the Sassendalen and the Kapp Toscana Groups (Fig. 11). The Lower and Middle Triassic comprises The Sassendalen Group, and the Upper Triassic comprises The Kapp Toscana Group (Fig. 11).

Regional seismic data presented by Riis et al. (2008) shows a continuing Carnian progradation towards the north and the north-west in the Barents Sea. It also shows that the water level increases towards the area east of Svalbard, including Kong Karls Land (Fig. 10) (Riis et al., 2008). However, there is huge difference in the thickness from Carnian succession of the De Geerdalen and Tschermakfjellet formations in Svalbard compared to the area east of Kong Karls Land. The total thickness around the Kong Karls Land exceeds 1000 m (Riis et al., 2008). The thickness of the Tschermakfjellet Formation in the eastern part of Svalbard, combined with the prodeltaic lower part of De Geerdalen Formation, is typically in the order of 100 m. The same formations east of Kong Karls Land are approximately 400 m, based on seismic interpretation (Riis et al., 2008). This greater thickness close to Kong Karls Land implies a larger accommodation space, which could be related to a deeper shelf prior to the deltaic infilling. This interpretation is strengthened by a drilled core east of Kong Karls Land, where the uppermost Botneheia Formation is interpreted as deep water environment (Riis et al., 2008). The Botneheia Formation consist mainly of blackish shales and some upwards-coarsening interval where mudstone is grading to siltstone. The overlaying Tschermakfjellet Formation consist of shales, siltstones and sandstones (Mørk et al., 1999).

2.2 Previous Palynological Work

Numerous studies on the palynostratigraphy of the Triassic have been carried out worldwide, and the Upper Triassic succession are of worldwide interest since it is well enriched in palynomorphs. The Triassic palynology in the Alpine and Germanic realm has been well documented (e.g. Van der Eem, 1983; Blendinger, 1988; Hochuli and Frank, 2000; Bonis et al. 2009; Kürschner and Herngreen, 2010). Palynostratigraphic studies of the Late Triassic in the Svalbard region have also been conducted in the recent decades; (e.g. Riis et al., 2008; Vigran et al. 2014). Other studies of the Triassic have been carried out by Klaus (1960) (Germany), Lund (1977) (Danish North Sea), Fisher (1979) (Canadian Arctic) and Roghi (2004) (Italy). However, in general fewer studies have been done in the Barents Sea compared to the Alpine realm.

In southern Europe, Van der Eem (1983) did palynological investigations in the Ladinian and Lower Carnian of the western Dolomites, Italy. He recognized seven palynological phases from Upper Anisian to Middle Carnian (Julian Substage), which were calibrated with ammonite zonations. The palynostratigraphy of the Ladinian and Carnian were studied in the southeastern Dolomites by Blendinger (1988). In that study, a qualitative and quantitative of 50 palynological samples was carried out, and 60 pollen and spore taxa were identified. Five palynological phases were recognised and compared with the work done by Van der Eem (1983).

Roghi (2004) did palynological investigations in the Carnian of the Cave del Predil area (Southern Alps in northwestern Italy), and recognized three palynological assemblages which were calibrated with ammonites and conodonts. Later, Roghi et al. (2010) studied the Raibler Schicten (Austria) and the Lunz area. Four assemblages were defined, three of them were assigned a Carnian age. They also proposed a palynostratigraphic correlation between the Northern Calcareous Alps, the Germanic Basin and the Dolomites where they found the same palynological associations.

Several authors have conducted palynological studies of the Triassic stratigraphy in the Barents Sea area, e.g. Smith (1974); Smith et al. (1975); Bjærke (1977); Bjærke and Manum (1977); Hochuli et al. (1989); Vigran et al. (1998); Hochuli and Vigran (2010); Ask (2013); Vigran et al. (2014); Holen (2014); Paterson and Mangerud (2015); Landa (2015); Meltveit (2015); Mueller et al. (2016).

Bjærke and Manum (1977) studied Mesozoic sediments from Norwegian Arctic and proposed a relationship to Rhaetian assemblages from northwest Europe, Britain and Arctic Canada. The long distance correlation was done due to lack of palynological work in the Norwegian Arctic. However, their results were affected by differences in assemblage composition, species diversity, preservation and palynomorph production. Long distance correlation is often uncertain due to climatic and environment changes (e.g. plants), and the rest listed above (Bjærke and Manum, 1977). Smith (1982) changed the Rhaetian age set by Bjærke and Manum (1977) to a Norian age, due to finding of Norian age ammonites in the Flatsalen Formation in the area (Korčinskaya, 1980). The Rhaetian assemblages have also been partially revised by Paterson and Mangerud (2015).

Later on, Hochuli et al. (1989) established 16 palynological assemblage zones, which covered the Latest Permian and the entire Triassic. Their work is based on the study of material from outcrops in Spitsbergen and Bjørnøya and from boreholes in the Barents Sea. Hochuli et al. (1989) used the first down-hole occurrence and not the first stratigraphic occurrence of the recorded taxa, this is due to their use of cuttings. Vigran et al. (1998) established eight assemblage zones (Svalis-1 to Svalis-8) from Lower and Middle Triassic deposits near the Svalis Dome in the Barents Sea. Six of the assemblages are calibrated by ammonoids, and the work done by Hochuli et al. (1989) in the Barents Sea area was used for comparison. Svalis-8 represents deposits from the middle part of Snadd Formation (Ladinian age). The rest of the assemblages are from Anisian age and older (Contain Steinkobbe, Klappmyss and Havert formations), and therefore older than the scope of current study.

Climate variations from late Early Triassic (Late Smithian) to Late Triassic (Rhaetian) based on palynomorphs was studied by Hochuli and Vigran (2010). They attribute some assemblages to climatic changes, like in the middle Triassic the pollen assemblages are characterized by cycadophyta and *Araucariacites*. The changes in the dominance of specific floral elements observed by Hochuli and Vigran (2010) can probably be related to climatic changes. However, may also be related to paleoenvironmental control (Paterson et al., 2015 online).

Nagy et al. (2011) studied deposits from offshore marine to paralic conditions from the Upper Triassic to Lower Jurassic Kapp Toscana Group of Spitsbergen. The study is based on microfossil-based biofacies feature mainly from foraminifera, but the study also includes palynomorphs.

Vigran et al. (2014) presented a review of the palynology and the geology of the Triassic succession of Svalbard and the Barents Sea from previous work that includes shallow stratigraphic cores and explorations well, and samples from Svalbard as well. Vigran et al. (2014) established 15 new palynological composite assemblage zones from Changhsingian (Late Perm) to Rhaetian (Late Triassic). The Late Triassic has a timespan of approximately 36 million years; however, is it represented by only four composite assemblage zones (Fig. 2). This is a relative poor resolution regarding the rest of Triassic.

Paterson and Mangerud (2015) analysed 154 palynological samples from eight outcrop localities on the island Hopen, Svalbard Archipelago, spanning the De Geerdalen, Flatsalen and Svenskøya formations (Kapp Toscana Group). Six palynological assemblages were recognised using relative abundance and first stratigraphic appearance data, and they range from late Carnian to Rhaetian age.

The arid conditions interrupted by a humid phase that is characterizing the climate in the Late Triassic is well documented in the Tethyan realm, but the documentation for a climate like this in the Boreal realm is scarce (Mueller et al., 2016). Mueller et al. (2016) present evidence from quantitative palynology for the Carnian Pluvial Event (CPE) from the Kapp Toscana Group from Spitsbergen. They also integrated their results with organic carbon isotope data linked to the geomagnetic polarity time scale. Analysis indicate wetter conditions from the Julian-2 onwards, and the paleotemperature indicates a cooler climate during the early Julian-1 followed by a warming during the late Julian-1 (Mueller et al., 2016).

Paterson et al. (2015 online) conducted a multidisciplinary biofacies characterisation of the Kapp Toscana Group on the island Hopen in the Norwegian Arctic, providing an enhanced paleoenvironmental interpretation for the Upper Triassic. Paterson et al. (2015 online) used a combination of palynological, palynofacies and micropalaeontological analyses to define different biofacies. Two of them were lower undifferentiated De Geerdalen Formation and upper De Geerdalen Formation (Hopen Member). The lower De Geerdalen Formation had a dominance of fern spores, and was interpreted to reflect deltaic deposition environment during maximum marine regression. The Upper De Geerdalen Formation were rich in bisaccate gymnosperm pollen and the freshwater algae *Plaesiodictyon mosellanum*, which implies a brackish marginal marine setting (Paterson et al., 2015 online).

Paterson et al. (2016) presented palynostratigraphic and palynofacies data from the shallow stratigraphic core 7830/5-U-1 drilled offshore Kong Karls Land. The 127m long core yielded well-preserved palynomorphs and the core was assigned an earliest Late Triassic (Carnian) age (Snadd Formation). Observations of palynofacies indicated an increasingly proximal pro-deltaic setting during deposition, and variations of terrestrial organic matter, amorphous organic matter and the occurrence of acritarchs and algae were interpreted to be episodic fluctuations along a nearshore-offshore environment.

Holen (2014) presented a master thesis in palynology from core 7533/3-U-7 drilled through the Snadd Formation on the Sentralbanken High, northern Barents Sea. Holen (2014) recognized four assemblages (A1-A4) spanning from a middle to late Carnian age. Additional, eight samples from Blåfjellet (Hopen), collected from the De Geerdalen Formation, were analysed and they were also interpreted to range in age from the middle to late Carnian. The depositional environment from the Sentralbanken High was interpreted to represent a delta plain, due to sedimentological analysis and a high dominance of wood particles in the palynofacies analysis. The most easily distinguishable result from core 7533/3-U-7 are the acmes of *Leschikisporis aduncus* in the upper part of the core, interpreted as late Carnian.

Palynology of the shallow stratigraphic core 7534/4-U-1 from Sentralbanken High were studied by Landa (2015), and were assigned a late Ladinian to late Carnian age. A palynomorph assemblage zone which was dominated by *Leschikisporis aduncus* in the very top of the core is the most prominent feature; similar assemblage has previous been observed from late Carnian in the Norwegian Arctic (Landa, 2015). Delta/coastal plain swamp depositional environment is suggested based on the dominance of terrestrial matter in the samples and the interpretation of a sedimentological log. The sporadic presence of marine taxa was also observed throughout the core and interpreted to indicate episodic marine influence (Landa, 2015).

Meltveit (2015) studied the shallow cores 7831/2-U-2 (Botneheia Formation) and 7831/2-U-1 (Tschermakfjellet Formation), offshore Kong Karls Land, by applying palynology and palynofacies analysis. These two cores are inferred to span the late Ladinian to early Carnian on the basis of Re-Os dating previously conducted by Xu et al. (2014). The Re-Os dates provide relatively good constraints on the position of the Ladinian-Carnian boundary, which was inferred by Xu et al. (2014) to be located within the uppermost part of core 7831/2-U-2. The palynofacies data presented by Meltveit (2015) showed a total dominance of amorphous organic matter in the oldest core (7831/2-U-2), which was inferred to indicate deposition in an anoxic environment. The youngest core (7831/2-U-1) contained an increasing influx of terrestrial organic matter and were interpreted to be prograding towards a delta.

2.3 Absolute Datings

Xu et al. (2014) presented new Re-Os ages for shale sections from Middle to Upper Triassic series in the Norwegian Arctic, including several datings from offshore Kong Karls Land. For example, they have dated the top of Ladinian and placed the beginning of the Late Triassic about 12 million years earlier than previously estimated. Their work has provided excellent age constraints for the Kong Karls Land cores, which gives independent age control for the palynological assemblages from the cores. Xu et al. (2014) have also made an example on an absolute time scale for the Anisian-Ladinian-Carnian boundaries based on Re-Os datings. The Ladinian-Carnian boundary was dated to be in core 7831/2-U-2, which is the stratigraphic lowermost core drilled offshore Kong Karls Land by NPD.

3. Material and Methods

3.1 Collection of Material

The NPD have carried out seismic data collection in the Northern Barents Sea since 1973. No commercial seismic acquisition or drilling has been conducted in the area; however, the distance between the seismic lines that the NPD have carried out varies from five to ten kilometres, which is sufficient for regional mapping. Exploration companies have conducted exploratory drilling in the Norwegian Arctic during the last decade (Riis et al., 2008), but commercial exploration north of Bjørnøya is banned.

SINTEF Petroleum Research, with the Norwegian Petroleum Directorate (NPD) as the contractor, drilled the shallow stratigraphic core 7830/3-U-1 approximately 20 km east of Kong Karls Land in 2005 (Riis et al., 2008, Figs. 1 and 6). The core number 7830 refers to the latitudinal position (78°N) and the longitudinal position (30°E). Core 7830/3-U-1 penetrated 196.23 m into the sea floor (3.37 – 199.60 m), and is one of five shallow stratigraphic cores drilled in the Kong Karls Land east area by the NPD (Figs. 1 and 9). The five boreholes in this area comprise 450 m of core in a 700 m thick section, ranging in age from Late Ladinian to Carnian. The original purpose of the cores was to find the Permian-Triassic boundary; however, upon inspection the cores were determined to be Triassic age, which is considerably younger than first thought. One reason is that the cores are drilled in an area where salt movement have brought the Middle and Upper Triassic successions upwards, as earlier mentioned (Riis et al., 2008, Fig. 9). Another reason was caused by the poor age control on the seismic reflectors before the cores were drilled, because of the low data coverage in this vast region. Thirty-one samples were collected from the core for palynological analysis, providing an average sampling density of approximately one sample per 6 m (Table 2). Sixteen rock samples were collected and processed by SINTEF Petroleum Research, and fifteen more samples were added at NPD during the core logging in 2013. The additional samples were processed by Palynological Laboratory Services, UK. Approximately 20 g of rock per sample was collected for processing. Sample depths relative to the core are shown in the core log (Fig.

23). Both sets of the palynological slides were of relatively good quality, with well-preserved palynomorphs. None of the slides were barren, but some contained significant amounts of pyrite (Figs. 15 and 18C, D). Semi-quantitative palynological analysis were conducted for all slides, and palynofacies was done for the samples collected at NPD. Vigran et al. (2014) presented quantitative analysis of 18 samples from the current core, semi-quantitative analysis.

Two duplicates of oxidized slides were provided for each of the 31 samples, and 15 single non-oxidized slides were available throughout the core (Figs. 17 and 23). About half of the oxidized slides were processed in 2013, and the rest are from pre-2013. All kerogen slides were processed in 2013 (Table 2). The two duplicates of oxidized slides seemed to be of comparable quality, regarding the preservation and the size of the palynomorphs. However, the set processed in 2013 contained a bit more AOM than the pre-2013 one. The studied core is stored in a core storage at the NPD in Stavanger, Norway.

3.2 Preparation of Slides

The prepared slides from core 7830/3-U-1 were processed following standard palynological preparation techniques (Fig. 14). The purpose with this process is to separate palynomorphs from the minerals (Traverse, 2007). The slides were prepared at APT (the first set sampled by SINTEF Petroleum Research) and by the Palynological Laboratory Services Ltd. (PLS), Gwalchmai, United Kingdom (the second set sampled at NPD). No significant qualitatively or semi-quantitatively differences were observed between the two batches during this study.

The rock samples in this study were first crushed in order to speed up the following process in the standard palynological preparation technique. Approximately 10-20 g of rock sample material was used. After the rock sample was crushed it was washed and cleaned, and then the next step was to add 10% hydrochloric acid (HCl) to remove carbonates from the sample. Methanol is often added in this phase to reduce gas production during the reaction (dissolution), and it was also used during the washing of the samples to avoid foaming when soap was used. To avoid any impact of HCl-acid in the following procedure, the samples were neutralized after the carbonate was dissolved. If there still are calcium ions in the sample these will make a reaction with the hydrofluoric acid (HF), and calcium fluoride (CaF_2) will be formed (Riding and Kyffin-Hughes, 2004). The next step was to remove all silicates from the sample, which was done by adding HF-acid. When all the silicates were dissolved, the sample was neutralized again. This is done because HF-acid is a hazardous and corrosive chemical solution (even in low concentration). HF-acid will penetrate the skin rapidly, and it will attack calcium (tissues and bones) (Riding and Kyffin-Hughes, 2004).

The samples were put into an ultrasonic bath after they were neutralized again, which makes sieving easier as the organic matter will not clog the sieve. A centrifuge was also used before the finally mount residue was finished and ready to be placed on a glass plate (Figs. 12 and 13). The purpose with centrifuging is to get rid of undesirable heavy minerals, like rutile and tourmaline. Some heavy minerals are according Riding and Kyffin-Hughes (2004) resistant against HF (e.g. rutile). Two set of samples were provided, one with oxidized material and one with non-oxidized material. Nitric acid (HNO_3) (oxidation) was added to the samples to remove

undesired organic matter, which leads to cleaner slides for palynological analysis. Non-oxidized slides were provided for palynofacies analysis. The size of the palynomorphs processed for this study varied between 20 and 90 µm, which is in general a common size for them.

To prevent loss of data/palynomorphs the remains of the aqueous residue (mount residue) can be stored as a liquid in test tubes (sample tubes) (Fig. 13). Drops of diluted HCl or phenol (C_6H_6O) are added to prevent fungal to grown (Elsik, 1966).

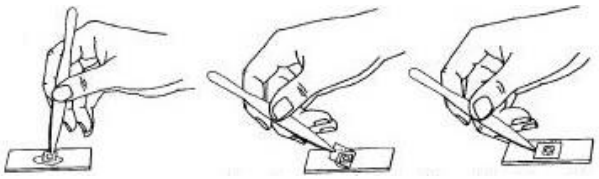

A B C

Figure 12: Shows the steps of creating palynological slides. A) Add a drop of mount residue to a slide. B) Place the edge of a coverslip on the slide so that it touches the edge of the mount residue. C) Lower the coverslip carefully over the glue and the mount residue to prevent forming and trapping air bubble. (Modified from http://users.rowan.edu/~wagnerf/oldwebs/EFGBold/microscope/coverslip.jpeg).

Figure 13: Showing two prepared palynological slides and a sample tube with final aqueous residue (mount residue). Processed during "preparation of slide" course at Applied Petroleum Technology, Lillestrøm.

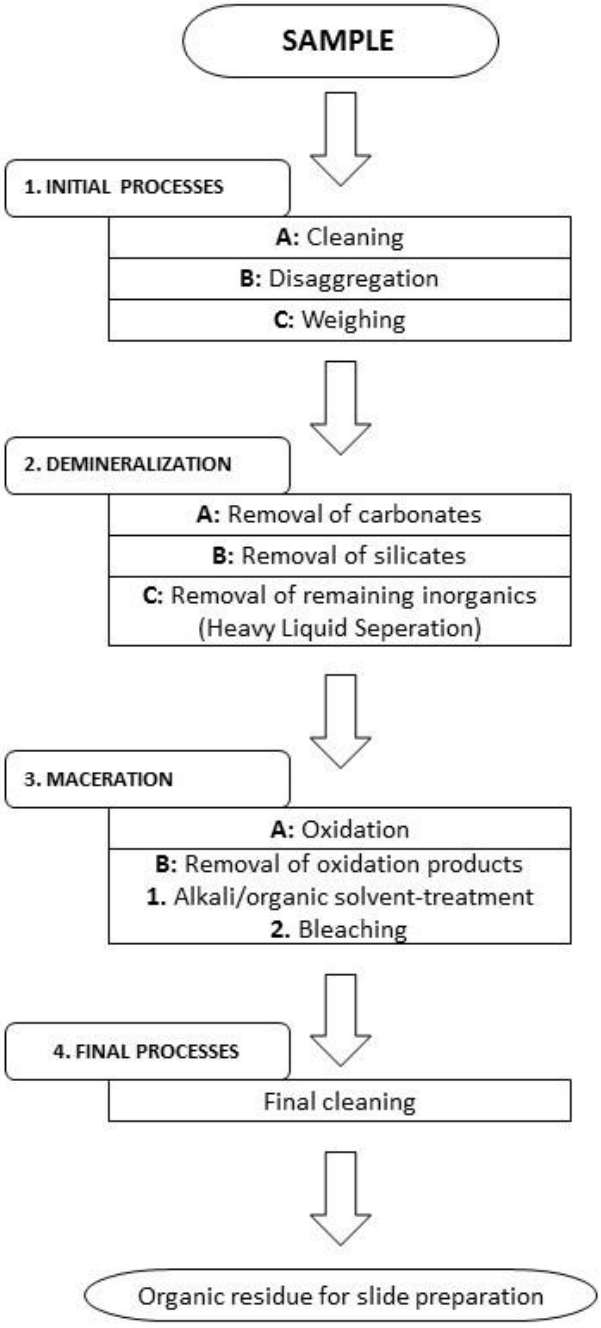

Figure 14: Showing systematically how to extract palynomorphs from rock samples using Standard palynological preparation technique. (Simplified and modified from Traverse (2007) and Wood et al. (1996).

3.3 Microscopy and Quantitative Palynology

The palynological and palynofacies slides were analysed using a Zeiss Axioplan transmitted light microscope. A Zeiss Axio imager.A2 with AxioCam ERc 5s camera was used to obtain pictures of the selected palynomorphs (Appendix IV). A 40x objective (which gave 400x magnification) was used for the pictures, if there are any exceptions this is noted. The counting and identification of taxa were an extensive work in this study, where 200 specimens were counted and identified in a delimited area for each of the 31 slides (Appendix II). Thus was semi-quantitative abundances determined. The counts include spores, pollen, acritarchs and algae. The slides were also scanned outside the counting area, and if there were any new species identified within a slide these are marked with a "+"-sign in the range chart (Appendix II). Scanning is important regarding detection of less dominant/rare species or species that are pale and difficult to observe (e.g. certain acritarchs). All analyses were conducted at the University of Bergen. The software StrataBugs was used to create the range chart.

During the microscope work awareness about potential sources of error caused by sampling, processing and analysis is important to keep in mind. This can include for example reworking of sediments or contamination in the processing laboratory (Riding and Kyffin-Hughes, 2004).

The structure and ornamentations of palynomorphs will change when the focus on the microscopes changes (Fig. 3). The term LO-analysis (L=lux, O=obscurus) is used for comparing the levels between low- and high focus (Traverse, 2007). Features appear lux (bright) or obscuritas (dark) in different levels of focusing (Hesse et al., 2009). Edge analysis provides verification on the LO-analysis, that is done by using moderate focus on the surface of the exine at the outer edge of the grain (Traverse, 2007, Fig. 3).

All palynological results have been plotted into a range chart using StrataBugs (program software) (Appendix II).

3.4 Use of literature for taxa identification

Several papers with original descriptions were used to identify different taxa, including papers like Klaus (1960) and Scheuring (1970), which also provide good quality illustrations of important taxa. “Mesozoic Palynology of Svalbard” by Bjærke and Manum (1977) and the paper by Vigran et al. (2014) and Paterson and Mangerud (2015) were particularly useful due to geographic relevance of this study. Jansonius and Hills (1976) provided a good summary of original generic descriptions of various Triassic pollen and spore taxa and was of particular importance. The genus *Triadispora* was extensively illustrated by Scheuring (1978), and this paper was especially important for the identification of this group.

3.5 Palynofacies

The French geologist Combaz (1964) introduced the term palynofacies as the study of sedimentary organic matter (SOM) found in palynological preparations along with palynomorphs, also organic matter (OM) that are not consisting any extent of sporopollenin or chitin (Batten, 1996). SOM is often referred to as palynodebris, and includes all visible organic particles in the palynological size range (roughly 2-250 µm) (Traverse, 2007). Palynofacies is an important field within (paleo-) palynology that is useful to provide the interpretation of depositional environments, as well as the source potential for hydrocarbons in given sediments. Slides that are enriched in amorphous organic matter are also often enriched in pyrite and acritarchs. Such samples indicate high potential for liquid hydrocarbons within the host rock and are of special importance when exploration drilling is the purpose. The dominance of phytoclasts in slides is an indicator for natural gas production. Cuticles found in the slides are originating from leafs, it is a layer of wax that is supposed to protects the leaf against water loss. These are easy to break down, and is therefore an evidence that the deposition occurred close to the source (short transportation) (Traverse, 2007; oral communication; Paterson, 2015). The use of palynofacies has increased from the 1980s and has become a standard technique in academic and industrial studies. The preservation of the organic matter may also contribute to determining transport distances, regarding the shape of the material (size/sorting/roundness etc.) (Traverse, 2007).

Fifteen un-oxidized slides were used for palynofacies analysis of core 7830/-3-U-1. These samples are from same depth as the palynological slides that were processed in 2013, and they are spread throughout the core (Figs. 17, 23 and Table 2). They were processed using the previously mentioned standard palynological processing techniques that contains HCl- and HF-acid, except that these are non-oxidized slides. The microscope work was conducted by estimating the ratio between particulate organic matter (POM) in ten “microscope-view” fields, and thereafter an average of the ten fields was done. All counts were done in the middle parts of the slides to get similar results for all slides, considering the density of POM.

A simplified version of the scheme made by Tyson (1995) was used for palynofacies analysis in this study (Table 1). The particles were separated into four main categories. The structured are zooclasts, palynomorphs and phytoclasts, and the structureless is amorphous organic matter (AOM). Both the phytoclasts- and the zooclast groups are structured fragmentary particles (clast) with angular broken outline. While the zooclast group includes diagnostic animalian features, like spines, slits, hair, joints etc. While the phytoclasts group contain no diagnostic animalian features (Tyson, 1995). The phytoclasts group includes translucent particles (at least at the edge of them) and particles that are opaque up to the edge and non-fluorescent (Tyson, 1995). The third group of structured particle is the palynomorph group, including spores, pollen etc.

If phytoclast particles are abundant in a shale it is generally an indicator on a lagoonal or deltaic environment. Alternatively, shales that are very abundant in cuticular fragments are usually typical of lacustrine or fluvio-lacustrine deposition. If degraded algae and plant tissues are found in a slide that can be an indicator of a marine deposition (Traverse, 2007).

Time, climate, tectonics, changes in sea level and the amount of oxygen all affect the rate of preservation of SOM on a global scale. On a regional scale the amount of sediment, the rate of accumulation, vegetation and the chemical composition of the water are important factors. Grain size and oxidation are two other factors that affect the preservation of organic matter. If the grain sizes of the particulate detritus are very fine they are often winnowed from coarser sediments or they can be damaged by abrasion (Batten, 1996).

Table 1: The palynofacies scheme made by Tyson (1995) which was used for the classification in this study.

Category		Source		Constituent
Structured	Zooclasts	Zooplankton Zoobenthos		Graptolite debris Arthropod debris
	Palynomorphs	Zoomorphs		Scolecodonts Tectin foraminiferal linings Chitinozoa
		Organic-walled phytoplankton (including meroplankton)		Prasinophyte phycomata
				Chronococcale cyanobacteria
				Botryococcales Hydrodictyales
				Dinocysts Acritarchs Rhodophyte spores
		Sporomorphs		Miospores: microspores pollen Megaspores
	Phytoclasts	Macrophyte plant debris		Cuticle/epidermal tissue
				Cortex tissues
				Secondary xylem (wood)
				Charcoal Biochemically oxidized wood
		Fungal debris		Hyphae
Structureless	Amorphous	Higher plant secretions		Resins
		Higher plant decomposition products		Humic cell-filling precipitates Humic extracellular precipitates
		("AOM")	Flocs	Organic aggregates Facal pellets
			Phytoplankton	
			Bacteria	Cyanobacteria/Thiobacteria

4. Results for shallow stratigraphic core 7830/3-U-1

4.1 Palynological Results

A total of 31 slides were analysed from core 7830/3-U-1 for palynostratigraphy. Two sets of slides were available for each depth, and the set with the best preserved palynomorphs was used for the semi-quantitative analysis. The other set was scanned for rare palynomorphs not recorded in the main set. A complete list of all samples with depth, lithology and preservation is included in Table 2. The preservation of the palynomorphs were of a generally high quality (Table 2, Fig. 15), and all slides were used for analysis. However, some exceptions made the identification of palynomorph taxa a bit difficult. Some of the slides contained an abundance pyrite (Fig. 15A), which was often observed together with amorphous organic matter and marine algae. Some other slides contained a significant number of palynomorphs that were broken into unidentifiable pieces (Fig.15B). The identifications in cases like this were normally done to generic levels, or ignored if they were too much damaged. Each slide contained about 25 to 50 different identified taxa. In average, it was about 40% dominance of pollen and 60% dominance of spores along the core (Fig. 16). Most of the slides that were dominated by spores were collected in sand- and siltstone (Figs. 17 and 23, Appendix II). For example, sample number four at 188.13 m was collected from claystone and it contains more pollen than spores. In the lowermost part of the core, there were two slides (number 3 and 5, respectively at 188.13 and 175.50 m depth) with a significant number of microplankton.

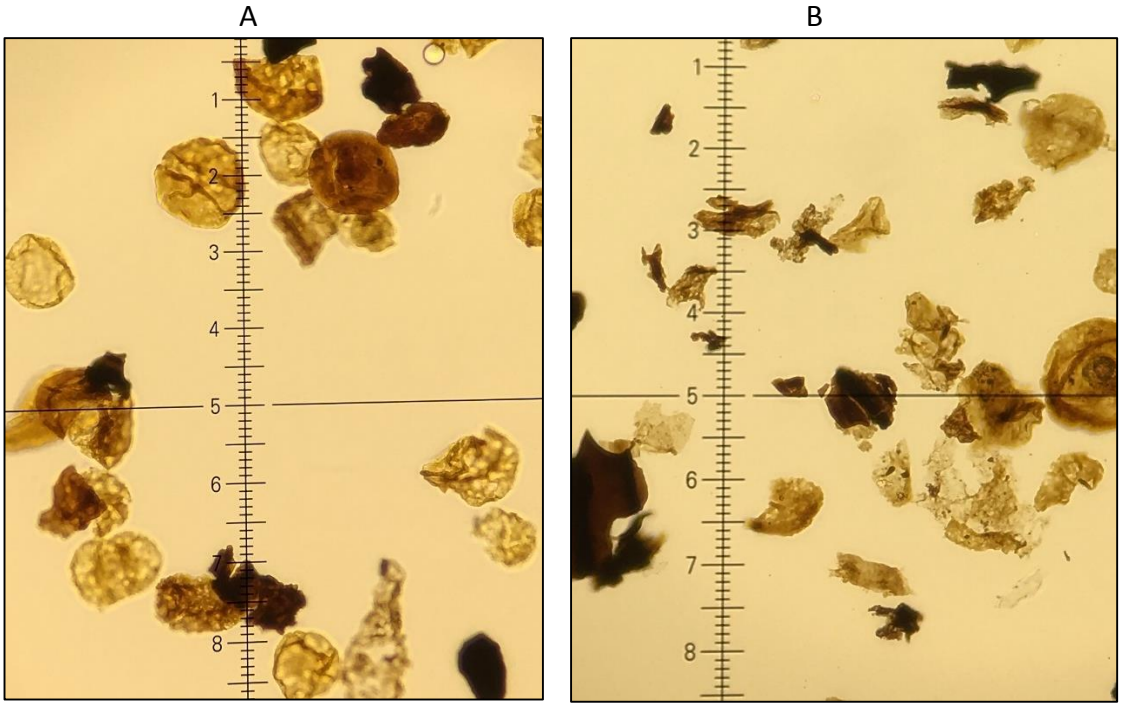

Figure 15: Example of preservation quality. A) is showing good preserved palynomorphs enriched in pyrite. B) is showing moderate preserved palynomorphs. Scale not included.

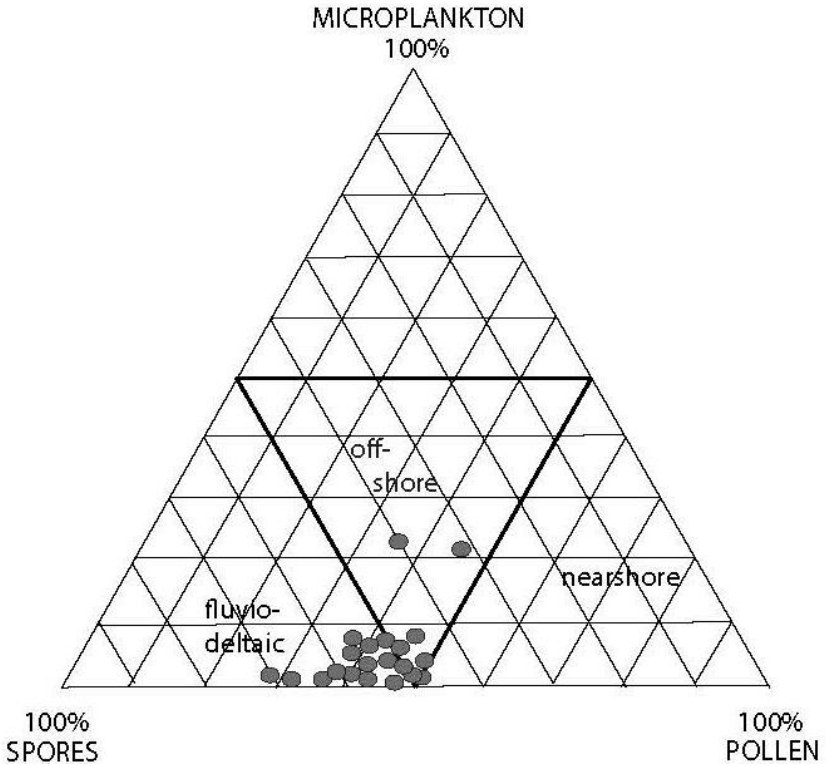

Figure 16: Spore-pollen-microplankton (SPM) ternary plot for core 7830/3-U-1, showing a more or less even distribution of spores and pollen in all palynological slides. Most of the slides are placed in a fluvio-deltaic- and offshore environment, and a couple of slides are placed on the boundary to a nearshore environment. Some of the points are overlapping. (After Federova 1977; Traverse 1988, p. 32; Duringer and Doubinger 1985, p. 27).

Table 2: Complete list of sampling information of core 7830/3-U-1.

Formation	Sample No.	Sample depth (m)	Kerogen slide	Year processed	Lithology	Preservation and recovery
Snadd Formation	31	4.75	K1	2013	Claystone with siltstone interbeds	Moderate preservation and recovery. AOM dominated.
	30	14.99	K2	2013	Mixture of claystone and sandstone	Moderate preservation and recovery. Phytoclast dominated.
	29	31.46	K3	2013	Claystone with siltstone interbeds	Good preservation and moderate recovery. Phytoclast dominated.
	28	36.48		Pre-2013	Claystone	Relatively good preservation and recovery.
	27	47.56		Pre-2013	Siltstone with traces of sandstone	Good preservation and moderate recovery.
	26	53.63	K4	2013	Silty claystone	Moderate preservation and poor recovery. Phytoclast dominated.
	25	58.74		Pre-2013	Silty claystone	Good preservation and recovery. Pyrite.
	24	61.90	K5	2013	Claystone	Moderate good preservation and good recovery. Phytoclast dominated.
	23	67.36		Pre-2013	Claystone interbedded with sandstone	Poor preservation and recovery. Phytoclast dominated.
	22	78.75		Pre-2013	Claystone	Moderate preservation and good recovery.
	21	82.82	K6	2013	Silty claystone	Relatively poor preservation and recovery. Phytoclast dominated.
	20	87.82		Pre-2013	Siltstone	Moderate good preservation and recovery.
	19	93.23	K7	2013	Claystone	Relatively good preservation and recovery. AOM dominated.
	18	95.66	K8	2013	Claystone	Relatively poor preservation and recovery. AOM dominated.
	17	99.52		Pre-2013	Claystone	Good preservation and recovery.
	16	102.77	K9	2013	Silty claystone	Relatively poor preservation and recovery. Phytoclast dominated.
	15	107.46		Pre-2013	Claystone with traces of sandstone	Moderate poor preservation and recovery. Affected by pyrite.
	14	107.51	K10	2013	Claystone with traces of sandstone	Moderate poor preservation and recovery. Affected by pyrite. Phytoclast dominated.
	13	121.61		Pre-2013	Muddy sandstone	Moderate good preservation and recovery.
	12	132.72		Pre-2013	Sandy mudstone	Moderate good preservation and recovery. Pyrite.
	11	139.80	K11	2013	Sandy mudstone	Poor preservation and recovery. Phytoclast dominated.
	10	144.91		Pre-2013	Sandy mudstone	Moderate good preservation and recovery.
	9	154.88		Pre-2013	Sandy mudstone	Moderate good preservation and recovery. Pyrite.
	8	166.03		Pre-2013	Sandy mudstone	Good preservation and recovery.
	7	170.37	K12	2013	Claystone	Moderate good preservation and poor recovery.
	6	173.36		Pre-2013	Sandstone	Good preservation and moderate recovery.
	5	175.50	K13	2013	Sandy Claystone	Moderate preservation and poor recovery. phytoclast dominated. Enriched in pyrite.
	4	183.38	K14	Pre-2013	Claystone	Moderate poor preservation and good recovery. AOM dominated. Enriched in pyrite.
	3	188.13		2013	Claystone	Moderate preservation and good recovery.
	2	194.30	K15	2013	Claystone	Moderate good preservation and recovery. AOM dominated. Enriched in pyrite.
	1	199.49		Pre-2013	Sandstone	Good preservation and recovery.

In this thesis, a semi-quantitative palynological count of 200 specimens was conducted for each of the 31 slides in the 200 m long core; which yielded several long ranging taxa (Appendix II). Some variations in the taxonomic composition of the assemblage was observed, but these seem to reflect changes in paleoenvironment and are not of biostratigraphic significance. Because of the long ranging taxa and changes in the environment it is difficult to set first appearance datums (FADs) and last appearance datums (LADs) in the semi-quantitative analysis. The assemblages recovered from core 7830/3-U-1 consist of pteridophyta and lycopodiophyta spores, and coniferopsida and cycadophyta pollen.

Spore taxa recorded include *Aratrisporites laevigatus*, *Baculatisporites* spp., *Calamospora tener*, *Camarozonosporites laevigatus*, *Camarozonosporites rudis*, *Conbaculatisporites* spp., *Cyathidites* spp., *Deltoidospora* spp., *Dictyophyllidites* spp., *Kraeuselisporites cooksonae*, *Kyrtomisporis* spp., *Leschikisporis aduncus*, *Raistrickia* spp., *Striatella parva*, *Striatella seebergensis, Todisporites minor*, *Velosporites cavatus*.

Pollen taxa recorded include *Alisporites* spp., *Araucariacites australis*, *Chasmatosporites apertus*, *Chasmatosporites hians*, *Cycadopites* spp., *Granasporites magnus*, *Illinites chitinoides*, *Lunatisporites* spp., *Ovalipollis ovalis*, *Podosporites amicus*, *Protodiploxypinus* spp., *Schizaeoisporites worsleyi*, *Striatoabieites* spp., *Triadispora* spp., *Vitreisporites pallidus*.

Large quantities of bisaccate pollen were observed as dominant in all samples. Most of them are identified as *Alisporites* spp. in this study. This genus varies between 10 and 53 specimens in each slide and was the most commonly occurring pollen. Rest of the bisaccate pollen are grouped as “Bisaccate” spp. in the range chart (Appendices II and IV).

The pteridophyte spore *Deltoidospora minor* was recorded as dominant in all samples for the current core (9-43 specimens of 200 in each slide) (Appendix II). Similarly, the monolete spore *Leschikisporis aduncus* (pteridophyta) was present in all slides and varies from common to dominant through the entire core. The lycopodiophyte spore *Kraeuselisporites cooksonae* and the pteridophyte spore *Baculatisporites* spp. were two other species and genus that were recorded as common to dominant in this study.

The conifer pollen *Alisporites* spp. and *Triadispora* spp. were recorded through the entire core, where *Alisporites* spp. was the most common bisaccate pollen recorded in this study. The monosulcate cycad pollen *Chasmatosporites hians* was observed in all sample along the entire core, and the conifer pollen *Araucariacites australis* was common. The fern spores *Baculatisporites* spp., *Deltoidospora* spp., *Dictyophyllidites mortonii* and *Leschikisporis aduncus* were common throughout the core. Also the lycopsid spore *Kraeuselisporites cooksonae* was present in high quantities. These specimens were the palynomorphs with the highest abundance and were recorded through the entire core (Appendices II and IV).

Marine palynomorphs recorded includes *Baltisphaeridium* spp., the freshwater algae *Botryococcus*, the green algae *Crassosphaera* spp., the prasinophyte *Leiosphaeridium* spp., the acritarch *Micrhystridium* spp., the acritarch *Veryhachium* spp. and the fresh water algae *Plaesiodictyon mosellanum*. The green algae *Tasmanites* spp. was also observed in small quantities. All the marine palynomorphs were relative rare, with the exception of *Crassosphaera* spp. which was recorded in almost every slides in quantities between one and 15 from bottom to top of the core. A peak of 15 specimens where recorded in the sample at 58.74 m. The remainder of marine palynomorph taxa were recorded sporadically through the entire core. In the lowermost part of the core acmes of the acritarch *Micrhystridium* spp. was recorded, and represented one of the dominant palynomorphs in the total count comprising about 20% of the assemblage in sample five and four. Note the almost total absence of marine palynomorphs between 47.56 m and 4.75 m (Appendix II). No dinoflagellate cysts were observed in core 7830/3-U-1.

The cycad pollen grain *Aulisporites astigmosus*, which has previously been recorded as abundant in Carnian assemblages in the Norwegian Arctic, was not observed in any of the slides. Vigran et al. (2014) recorded *A*. *astigmosus* as abundant in several of the slides from core 7830/3-U-1. Neither was the pollen *Echinitosporites iliacoides*, which has its youngest occurrence in Carnian, observed in this research.

Stratigraphical intervals that were enriched in AOM (as described in section 4.3), e.g. at 95.66 m had a higher diversity of several palynomorphs, e.g. *Alisporites* spp., *Araucariacites australis*, *Baculatisporites* spp., *Calamospora tener*, *Deltoidospora* spp., *Dictyophyllidites mortonii* and *Leschikisporis aduncus*. Intervals with less AOM have a more even distribution of palynomorphs and *Conbaculatisporites* spp. seems to occur more (Appendices II and III).

4.2 Core Description

The core 7830/3-U-1 was studied and logged during a week at the NPD in Stavanger, the logging is an important part of the thesis for the understanding of the depositional environment. The sedimentology of core 7830/3-U-1 has been discussed in earlier papers (e.g. Riis et al., 2008), despite that the core is not published for the general public by the NPD yet. However, a detailed log with the most identifiable features of the almost 200 m long core was drawn (Fig. 23). A simplified log is included in the range chart (Appendix II). The grain size varies from clay to medium/coarse sand. As shown in the log there are several asymmetrical upwards coarsening sedimentary packages, where the lithology varies from claystone/mudstone to sandstone. The core is divided into different facies, from delta front to offshore environment (Table 3, Figs. 17/24). The facies are distinguished from each other by grain size, colour, sedimentary structures like ripples, bioturbation, etc.

The current core is divided into seven intervals (A-G), based upon the lithology, grain size and sedimentary structures. The interpreted depositional environments for these intervals are discussed in full in section 5.2. Within each interval there are several facies, some of the facies are also located in more than one interval. The core is in general characterized by repeated asymmetrical, upwards coarsening sedimentary packages (Figs. 17 and 23), grading from claystone/mudstone to sandstone. Mica was observed throughout the entire core, and framboids of pyrite were observed sporadically within mudstone intervals (Fig. 18C, D). Bivalves were observed in the lowermost part of the core, where they were present sporadically between 135 and 195 meter. Bioturbation was observed in different intensities through the core but was generally restricted to finer grained lithologies. No age diagnostic ammonites that could have been used for independent dating were recorded.

Figure 17: A slightly simplified log of core 7830/3-U-1 showing the facies associations and Intervals A-G. Legend below the core log shows the features.

Interval A comprises an approximately 3.5 m thick (199.60-196.0 m) section in the lowermost part of the core and consists of medium sandstone with some thin layers of coarse sand. The sandstone was interbedded with claystone in the top of the interval. The few meters of sandstone were affected by bioturbation and ripples.

Interval B comprises the lower part of the core, between 196.0 m - 170.0 m depth. The interval starts at 196.0 m with 13 m of almost pure dark grey claystone (Fig. 18A, B and C), deposited at the top of the sandstone (Interval A) (Fig. 18 E), and reaching up to 182 m. The claystone was laminated and uniform, and it contains of abundant number of bivalves. Also framboids of pyrite was occasional observed. Seven meters (182-175 m) of dark grey claystone interbedded with thin layers of silt- and sandstone were deposited above the pure (uncontaminated) claystone. Within these seven meters no bivalves were recognized; however, bioturbation and ripples were observed. At 175.0 m an erosive surface was observed and was a distinction between the shale layers below and new layers that changes between of medium and coarse sand. A medium degree of bioturbation was observed in the sandstone, and it was also possible to see the porosity of the rock with a hand lens. The sandstone zone from 175 to 170 m was oil stained (Fig. 22).

A)

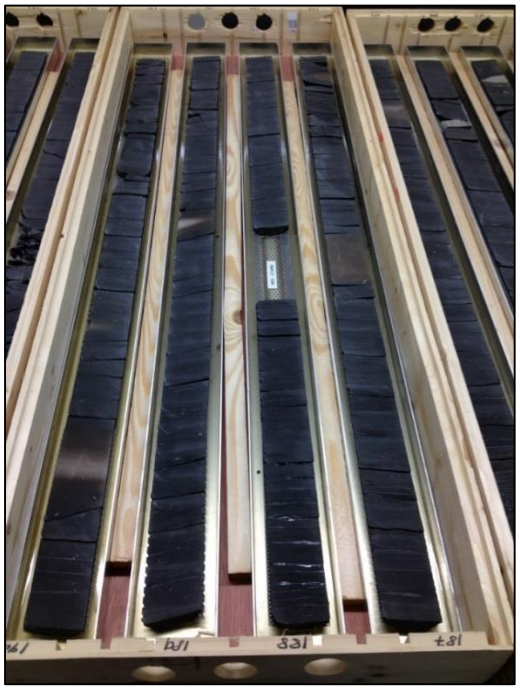

B)

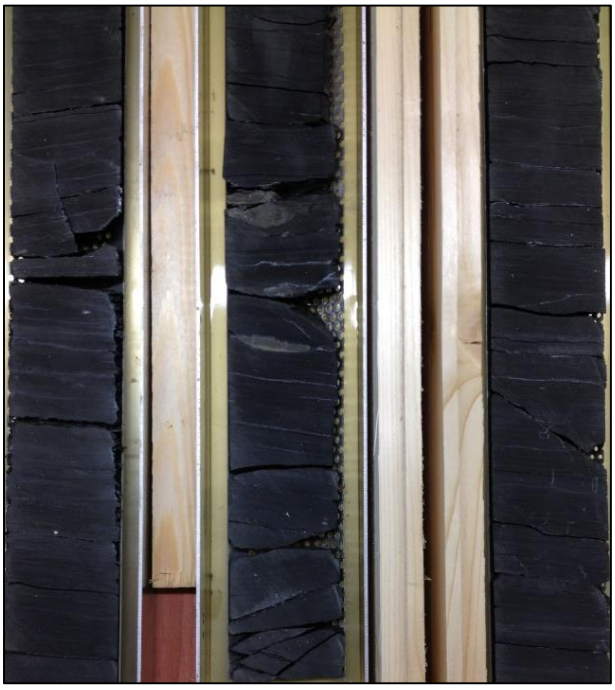

C)

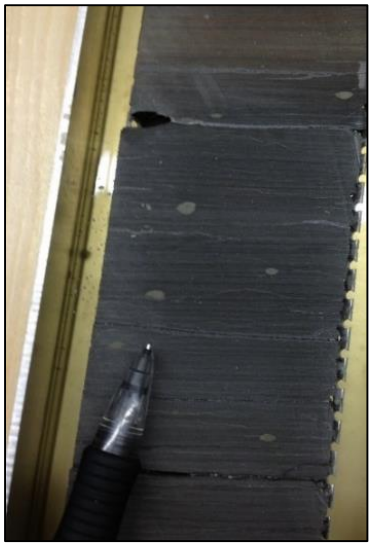

D)

E)

Figure 18:

A) Overview of the laminated dark grey claystone in the lower part of Interval B, which is characteristic for the Snadd Formation in the Norwegian Arctic. The core is divided into intervals of one meter in length.

B) Close-up of the same claystone as A). Covers about 25 cm.

C) Showing framboids of pyrite in dark grey mudstone from the lowermost part of the core.

D) Close-up of a 2 mm wide pyrite clast. Framboids of pyrite were spread throughout the entire core in different degree.

E) Showing medium grained sandstone from top of the parasequence in Interval A). Similar sandstone was observed in the top of all interval. Covers about 10 cm.

Interval C was recorded between 170 and 106 m (Figs. 17 and 23) and sits directly above the sandstone layers at the top of Interval B. The basal layers of Interval C consist of almost pure dark grey, laminated claystone (between 170 and 167 m), similar to those at the base of Interval B. From 167 to 166 m there was a sequence with slightly upwards coarsening grain-size, grading from claystone to muddy siltstone. The laminated muddy siltstone sequence has layers of sandstone that continues to 127 m, 40 m in total (Fig. 19). Ripples were observed in the sandstone along the entire interval (Fig. 20D), and a few micro faults were observed (Fig. 23). Mica and some pyrite clasts were found throughout the muddy siltstone part, and bivalves were also observed, approximately 2 meters apart from each other from the bottom to the top. Above the top of the muddy siltstone at 127 m a gradation to sandstone was noted, which in some places was intercalated with claystone or siltstone (Intervals between 122-116 m and 111-109 m) (Fig. 20A, B and 23). The sandstone was fine grained, and has a dark yellowish to brownish colour (oil stained) (Fig. 22). The sandstone section consists mainly of ripples as sedimentological structures, and some mud flakes (Fig. 20C). However, some laminated fine sandstone layers were present in the lower part of the sand section as well (Figs. 17 and 23).

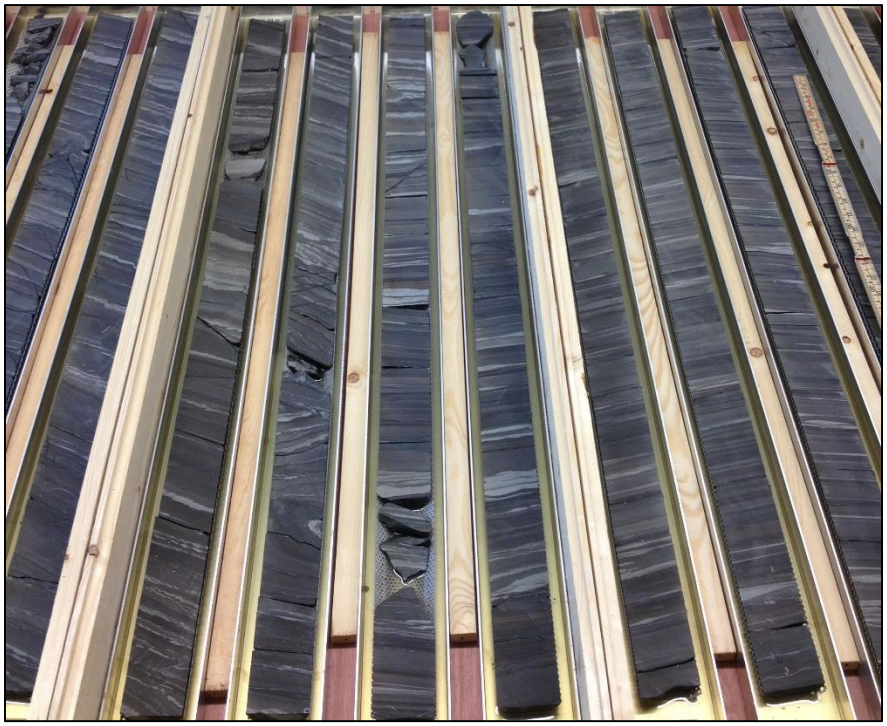

Figure 19: Muddy siltstone that characterizing Interval C. The core is divided into intervals of one meter in length.

A)

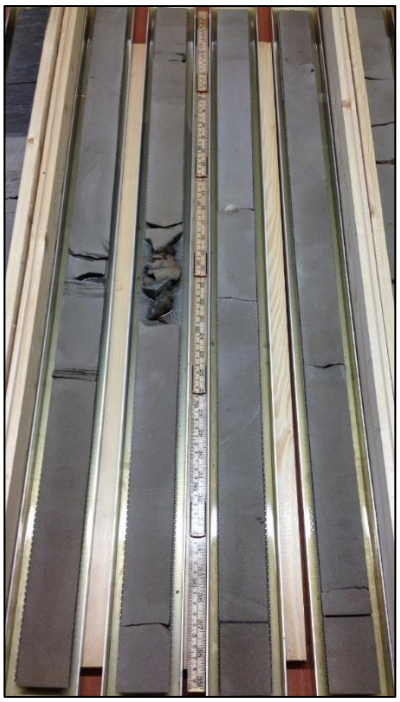

B)

C)

D)

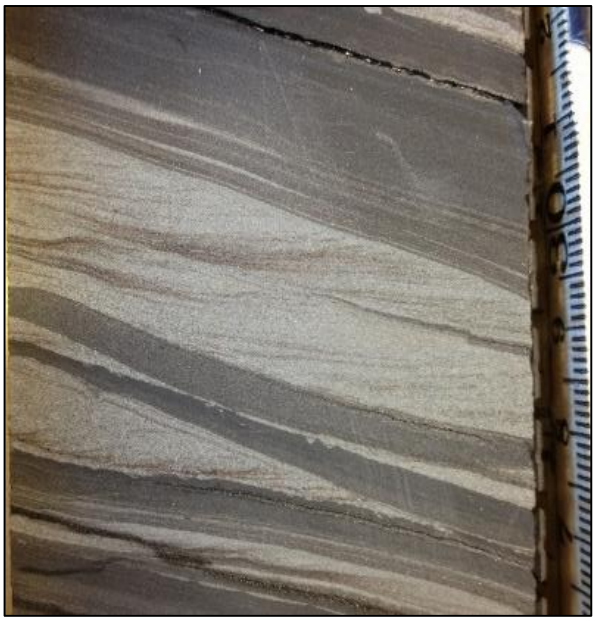

Figure 20:
A) Showing several meters of a medium sandstone section in top of Interval C. The core is divided into intervals of one meter in length.
B) Showing the transition from Interval C to D. Sandstone in Interval C and claystone in Interval D. The core is divided into intervals of one meter in length.
C) Mud flakes in top of Interval C. Covers about 20 cm of the core at 109 m.
D) Lamina in claystone and ripples in siltstone. Covers 11 cm of the core at 119 m.

Interval D was recorded between 106 and 64 m and was in general characterized by an upward coarsening sequence, grading from claystone at the base to fine sandstone at the top. In between there were some small intervals where it changes to siltstone and then back to claystone again (Figs. 17 and 23). The uncontaminated laminated claystone in Interval D was characterized by framboids of pyrite, different degree of bioturbation and occasionally ripples (Fig. 21C and D, Figs. 17 and 23). The short intervals with siltstone were characterized by ripples, pyrite and low degree of soft sedimentary deformation. Erosive surfaces were observed at 78 m, 73 m and at the top of the interval where it changes from sandstone and directly to claystone in Interval E (64 m).

Interval E consists of an upwards coarsening sequence between 64 and 37 m (Figs. 17 and 23). It changes from claystone to fine sandstone, and the interval terminates with an erosive surface at 37 m. This interval was quite heavily bioturbated making it difficult to determine any sedimentological structures. However, some ripples and soft sedimentary deformation were observed (Fig. 21). Interval E was also the only interval where traces of roots were observed. These were seen in the fine sandstone at the top of the interval (Figs. 17 and 23).

Interval F was recorded between 37 and 15 m, and was quite similar to Interval E with an upwards coarsening sequence changing from claystone to fine sandstone (Figs. 17 and 23). Bioturbation was not observed in this interval, so it makes it possible to detect lamina and some few ripples in the claystone. The sandstone does not have any recognisable structures, except some occasionally ripples. An erosive surface was observed on the top of the claystone at 27 m and another one at 24 m.

Interval G, recorded from 15 m to the top of the core (3.37), consist of laminated claystone that some places were interbedded with minor sandstone beds (Figs. 17 and 23). Ripples were observed in the interval where the sandstone was observed. Other features observed were some occasional framboids of pyrite, and mud flakes in the lower part of Interval G.

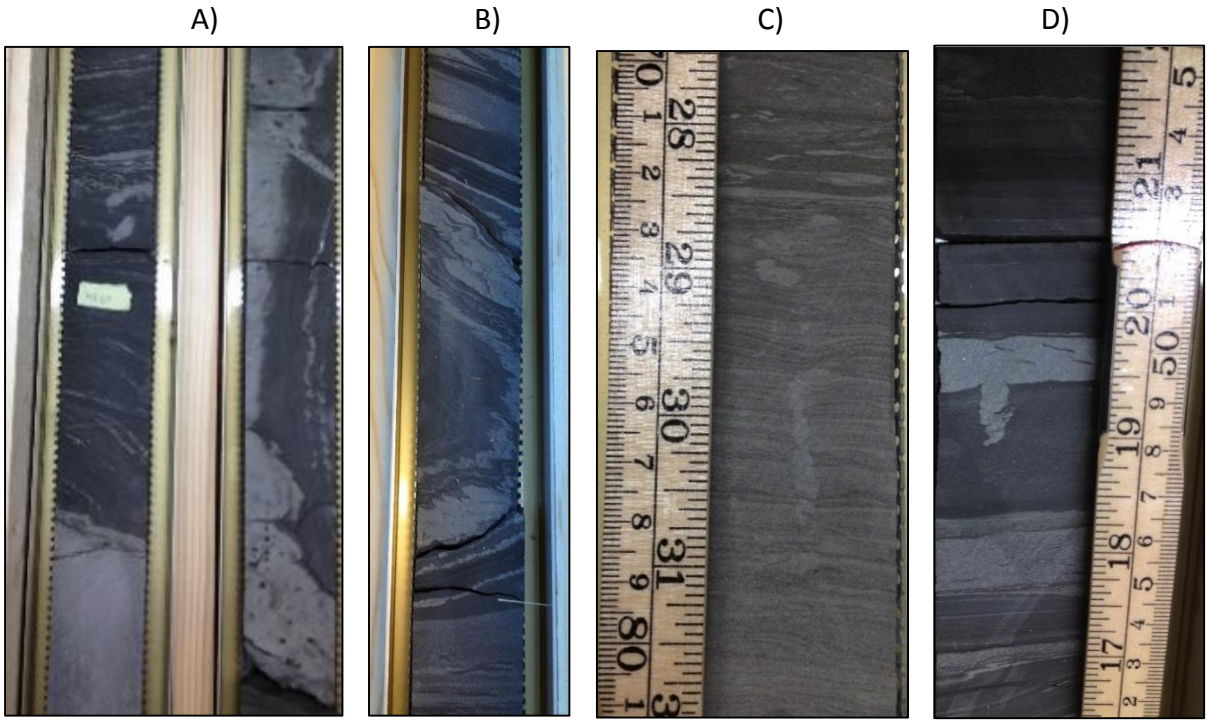

Figure 21:
A) and B) Showing soft sedimentary deformation which were observed several places in the upper third of the core. Covers about 40 cm in height.
C) Bioturbation and burrows in siltstone.
D) Burrow of trace fossil in silty claystone.

Figure 22: Photo of oil stained sandstone within the core. Covers about 20 cm.

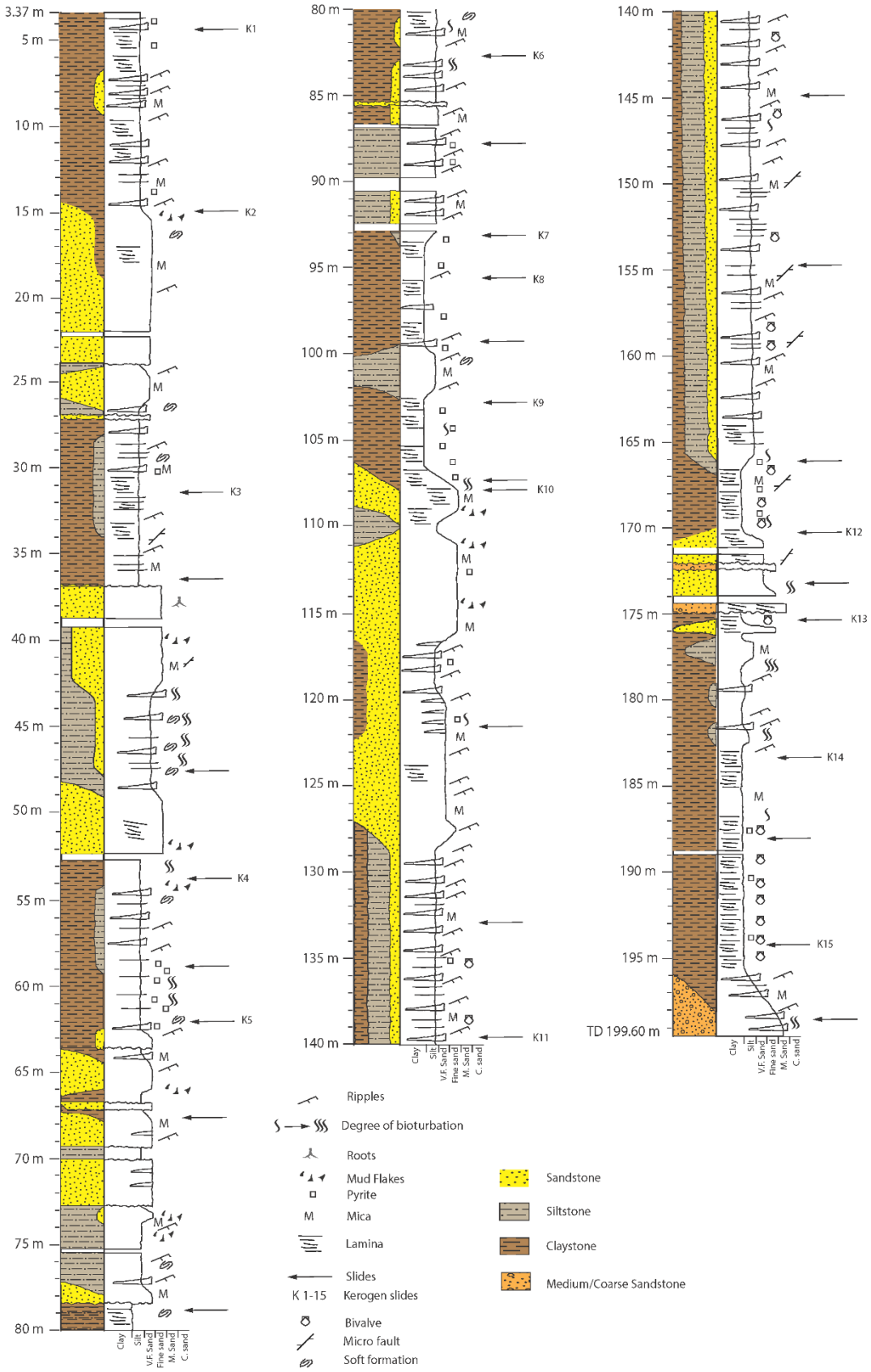

Figure 23: Detailed log of core 7830/3-U-1, representing the Snadd Formation offshore Kong Karls Land east area. Legend below the core log shows the features.

Table 3: Facies of core 7830/3-U-1, arranged in decreasing energetic conditions.

Facies	Intervals (Depth in m)	Description	Interpretation of environment
1	199.6 – 195.5 175.0 – 170.5 43.0 – 37.0 27.0 – 15.0	Medium to coarse sandstone with oil stain.	Delta front
2	183.0 – 175.0	Dark grey claystone with thin sandstone and siltstone beds. Some ripples and heavy bioturbation.	Distal delta front
3	77.5 – 64.0 49.0 – 43.0 37.0 – 27.0	Siltstone grading to claystone with thin beds of sandstone.	Pro-delta
4	117.0 – 106.0 52.5 – 49.0	Sandstones with interbedded claystone. Mud flakes and framboids of pyrite were included.	Shoreface
5	128.0 – 117.0 102.0 – 77.5 64.0 – 52.5	Mix of silty claystone with sandstone interbeds, sandstone layers and siltstone layers with claystone clasts.	Lower shoreface
6	166.0 – 128.0 106.0 – 102.0 15.0 – 3.3	Laminated muddy siltstone with thin rippled sandstone beds. Occasionally bivalves.	Shallow shelf
7	195.5 – 183.0 170.5 – 166.0	Dark grey to blackish grey laminated claystone with abundant bivalves. Micro pyrite and minor bioturbation.	Offshore

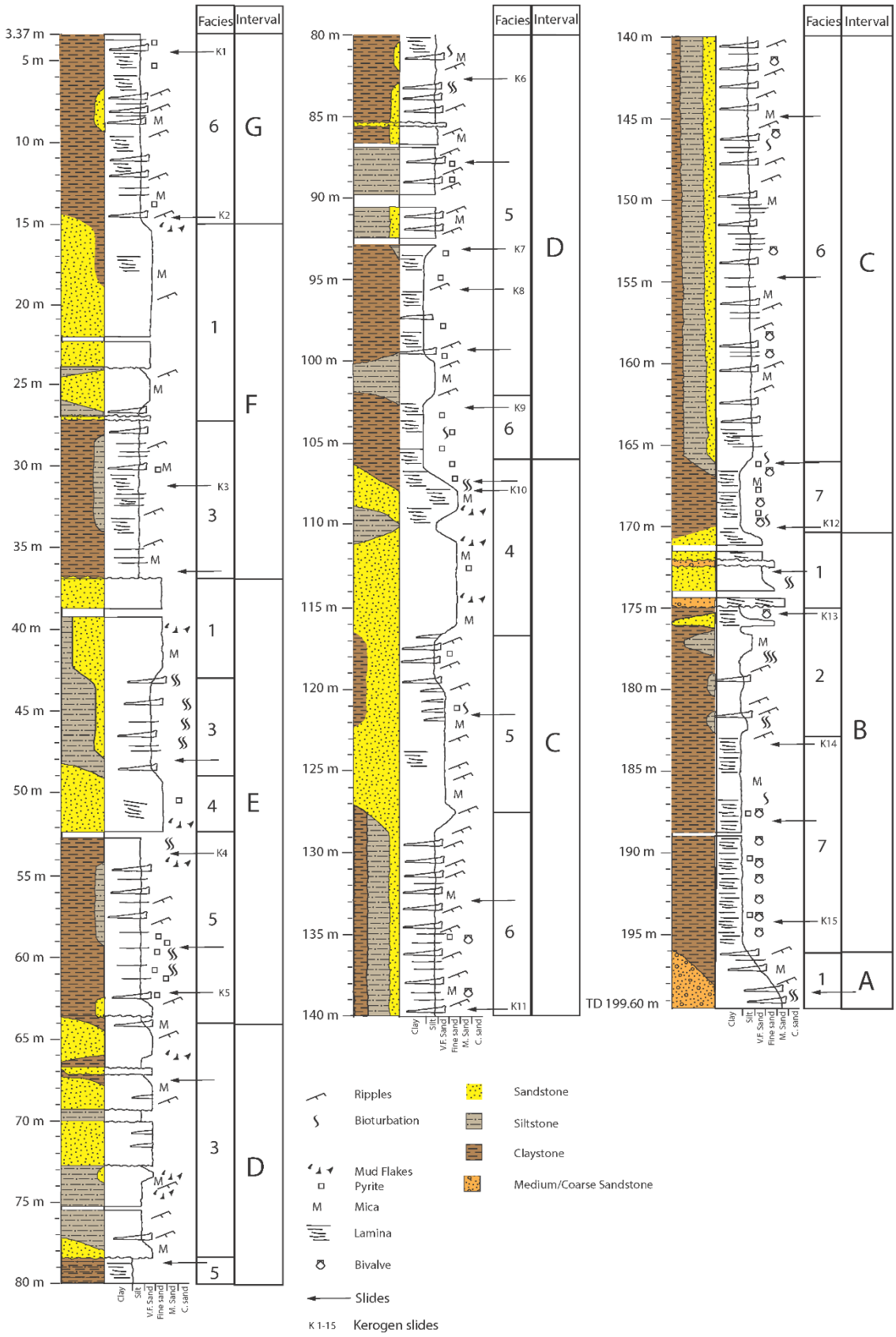

Figure 24: A slightly simplified log of core 7830/3-U-1 showing the facies associations. Legend below the core log shows the features.

4.3 Palynofacies Results

The palynofacies analysis was conducted by estimating the ratio between amorphous organic matter, palynomorphs and phytoclasts in the kerogen slides. The palynofacies results from core 7830/3-U-1 are included in a range chart together with a simplified core log (Appendix III). One range chart for the palynofacies only, and one combined range chart with all palynological results. The palynofacies results are also plotted into a ternary plot after Tyson (1985, 1989, 1993) showing the ratio between amorphous organic matter (AOM), palynomorphs and phytoclasts (APP-diagram) (Fig. 26). All points in the diagram have a number (1-15) representing a specific sample depth, the corresponding sample number can be found in the detailed log where the lithology is shown for each sample (Figs. 23 and 24). There is a "K" in the front of the numbers (K1-K15) in the core log which are representing the kerogen slides. AOM, palynomorphs and phytoclasts were the palynofacies groups that were observed, no zooclasts were observed. The APP-diagram can be useful for interpretation of the deposition environment (Tyson, 1995).

The ternary plot (APP-diagram) shows that AOM and phytoclasts were the two most commonly represented groups. Examples of slides dominated by AOM or phytoclast are shown in Figure 25. The ternary plot (Fig. 26) indicates that the samples alternate between being enriched in AOM to being enriched in phytoclasts several times throughout the core. The samples dominated by AOM were taken in clay- and mudstone intervals.

In the range chart (Appendix III) there are three main intervals that are dominated by AOM, the intervening intervals are dominated by phytoclasts. The two lowermost samples (194.30 m and 183.38 m) in the core were dominated by AOM. Approximately 90% AOM in both of them. The samples were also containing traces of acritarchs. These are plotted in the ternary plots as number 14 and 15 (Fig. 26).

The sample from 175.50 m indicate significant decrease in the relative abundance of AOM, from 87% to 5%. Phytoclasts increases from approximately 10% to 70%. The palynomorphs increases from 4% to 25%. This is shown as point 13 in the ternary plot (Fig. 26). It is shown in the log that the samples were collected from a zone where it varies between claystone to medium sandstone.

A change in the palynofacies was recorded in sample 170.37 m, with a decrease in the relative abundance of phytoclast from 70% down to approximately 40%, and the amorphous organic matter increased from 5% to almost 50%. This is plotted in the APP-diagram as point 12, and according to the diagram the deposited environment has been a distal dysoxic-anoxic shelf. This sample was collected from a transition between sandstone and claystone (Figs. 23 and 24).

Above the sample at 170.37 m follows three samples dominated by phytoclasts. These samples constitute 139.80, 107.51 and 102.77 m. As shown in the core log (Figs. 23 and 24) this zone consist of a mixture of clay-, silt-, and sandstone.

There were two samples above 102.77 m that consisted mostly of AOM (95.66 and 93.23 m). Shown as number seven and eight in the APP-diagram (Fig. 26). These samples were collected from a claystone (Figs. 23 and 24).

Above this again it follows five samples that were dominated by phytoclasts. These samples are 82.82, 61.90, 53.63, 31.46 and 14.99 m. They are plotted from two to six in the APP-diagram (Fig. 26). The samples were collected in silty claystone or siltstone (Figs. 23 and 24).

The uppermost sample 4.75 m (K1) consist of 69% AOM and 23% of phytoclasts (Fig. 26). This sample is plotted as number 1 in the APP-diagram (Fig. 26). The sample is from a claystone layer, shown in the core log (Figs. 23 and 24).

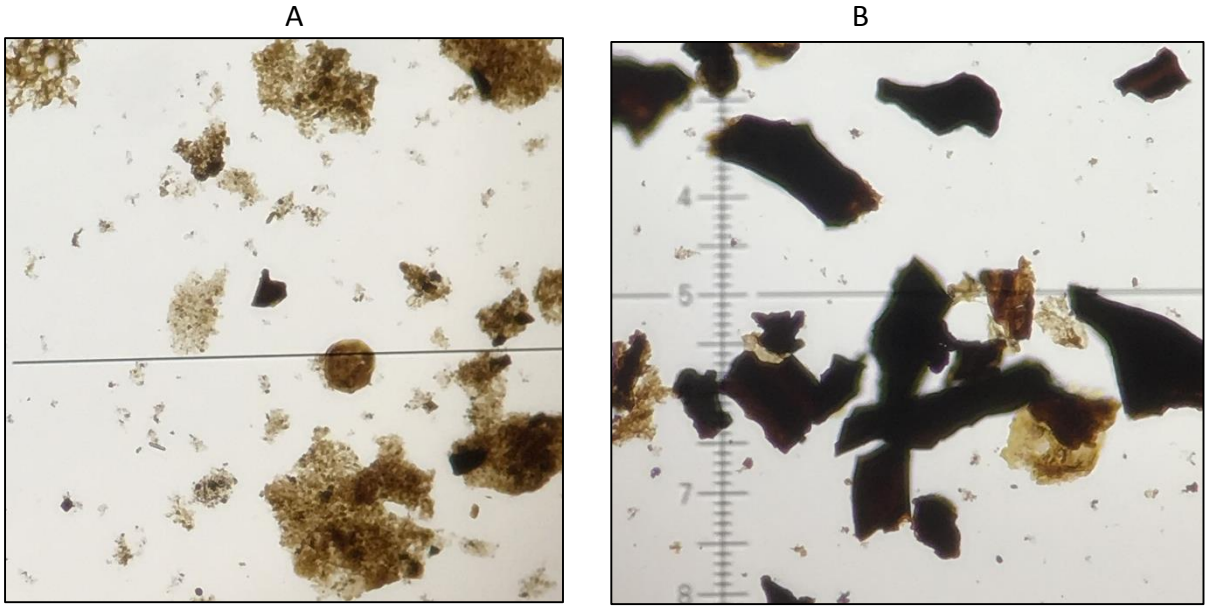

Figure 25: Examples on palynofacies. A) Sample dominated by AOM. B) Sample dominated by phytoclast. Scale not included.

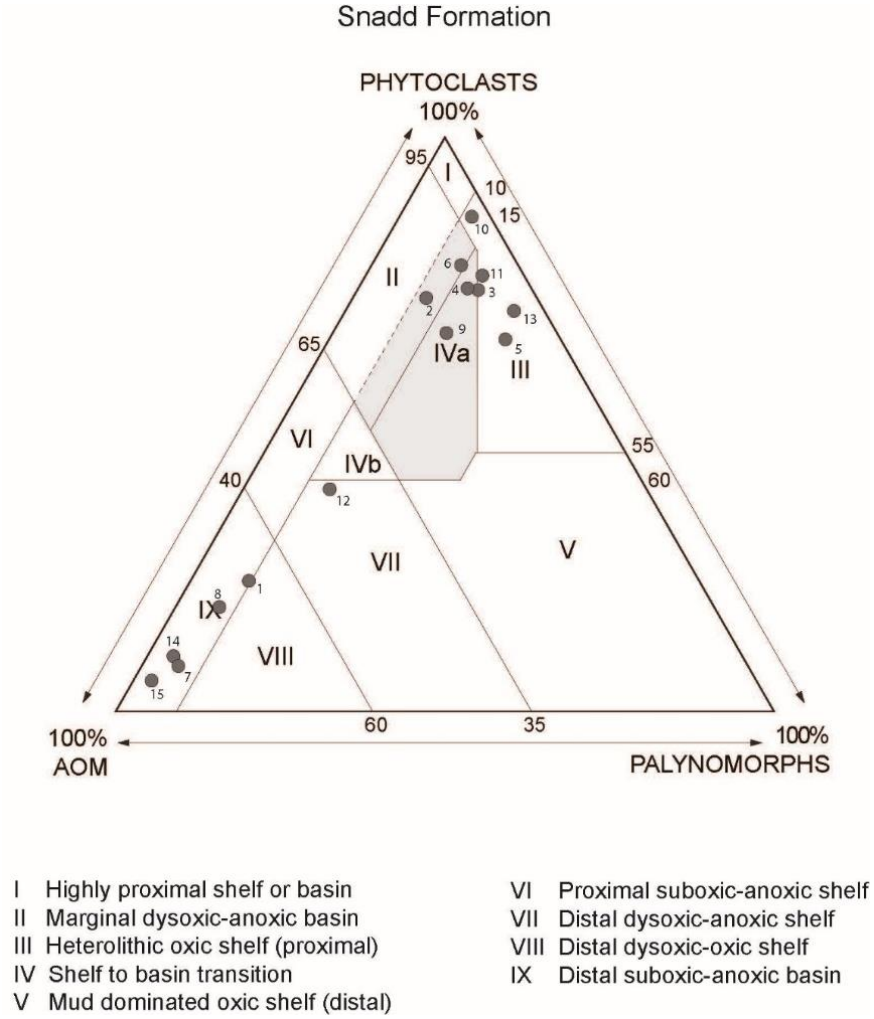

Figure 26: "AOM" – Palynomorph – Phytoclast (APP) ternary plots for core 7830/3-U-1 (after Tyson 1985, 1989,1993). Shows fluctuation between AOM and phytoclast enrichment in the slides (K1-K15).

5. Discussion

5.1 Biostratigraphic correlation and age determination

The palynomorphs in core 7830/3-U-1 are considered to represent one single assemblage based on the results from the semi-quantitative analysis, which were dominated by long ranging palynomorphs. No obvious division was observed in the range chart (Appendix II). The recorded assemblage is most closely comparable with previously described zones; "Assemblage F" of Hochuli et al. (1989) and the informal palynozone termed the *Podosporites* cf. *amicus* assemblage of Paterson et al. (2016). The recorded assemblage includes the bisaccate pollen *Alisporites* spp., the coastal conifer pollen *Araucariacites australis*, the sulcate pollen *Chasmatosporites apertus* and *C. hians,* the spore *Baculatisporites* spp., the trilete spore *Deltoidospora* spp., the laevigate spore *Dictyophyllidites* spp., the cavate trilete spore *Kraeuselisporites cooksonae* and the monolete spore *Leschikisporis aduncus*.

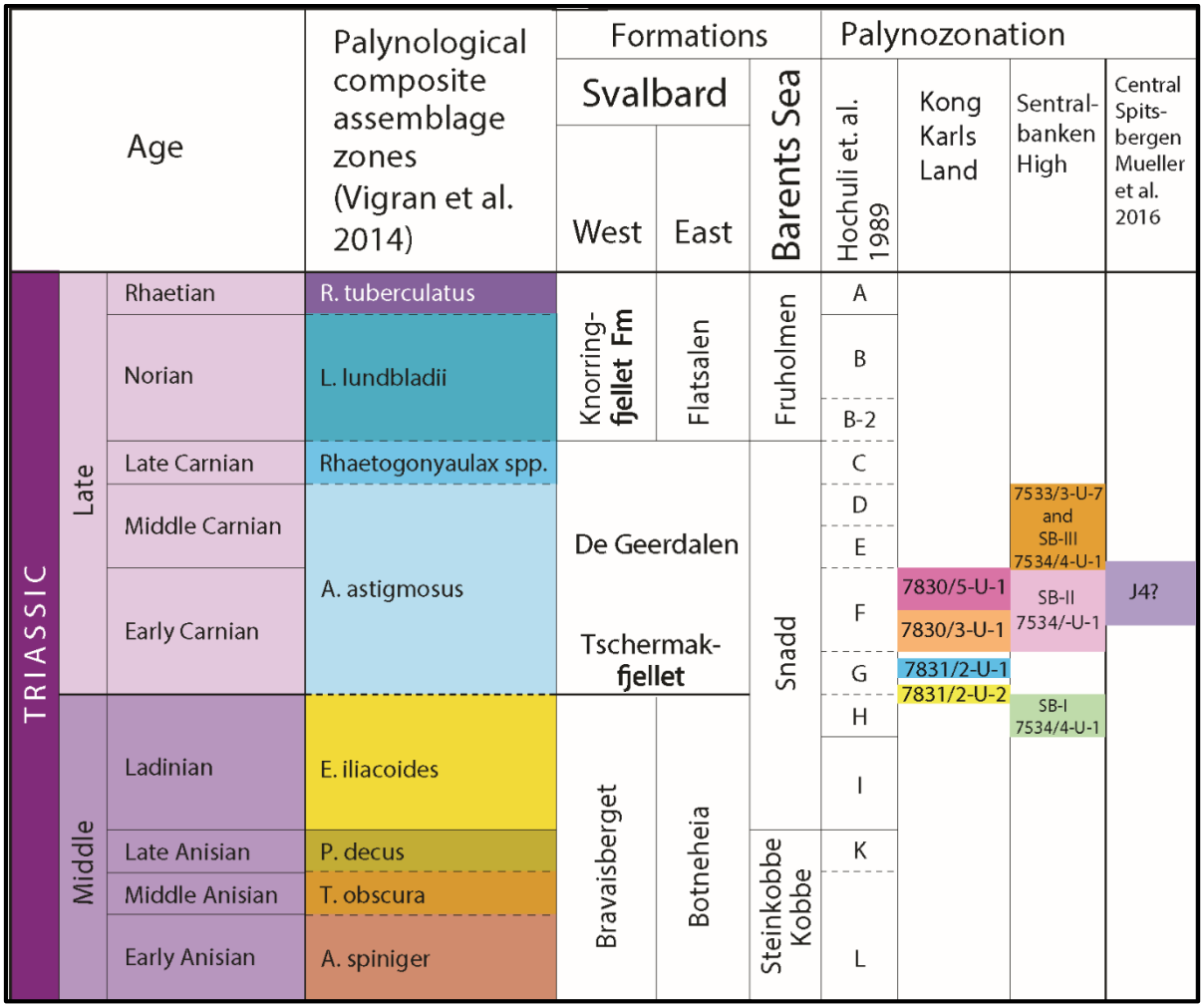

Figure 27: Palynological correlation of the present study (core 7830/3-U-1, pale orange outline) with the palynological assemblage zones of Vigran et al. (2014), Hochuli et al. (1989), Paterson et al. (2016) (7830/5-U-1), Meltveit (2015) (7831/2-U-1 and U-2), Holen (2014) (7533/3-U-7), Landa (2015) (7534/4-U-1) and Mueller et al. (2016). The stratigraphic thickness of the cores from Kong Karls Land, Sentralbanken High and central Spitsbergen are not to scale. (Modified from Vigran et al., 2014).

The two shallow stratigraphic cores 7831/2-U-2 and U-1, drilled in the Kong Karls Lands east area (Figs. 1 and 9), have previously been dated by Xu et al. (2014) based on Re-Os geochemistry. Xu et al. (2014) suggested the Ladinian-Carnian boundary to be located in the stratigraphic lowermost core 7831/2-U-2, and consequently assigned an earliest Carnian age for the stratigraphic uppermost core 7831/2-U-1 due to the datings results. Since core 7830/3-U-1 is stratigraphically above cores 7831/2-U-2 and 2-U-1 (Fig. 9) the age control from the cores dated by Xu et al. (2014) suggest that the current core is of early Carnian age or younger.

Hochuli et al. (1989) described 5 assemblages (C-G) from the Tschermakfjellet and the lower De Geerdalen formations on Spitsbergen, and assigned a Carnian age to these (Fig. 27), suggesting a late Carnian age for Assemblage C, Assemblages D and E as informal middle Carnian and Assemblages F and G as early Carnian. The palynomorph assemblage recorded in this study of core 7830/3-U-1 resembles the early Carnian age assemblage F from Hochuli et al. (1989) (Fig. 27). The age of assignment of assemblage F is based on an independently ammonite dated section from the lower part of the Tschermakfjellet Formation (Hochuli et al., 1989). A typical feature was that bisaccate pollen such as *Lunatisporites* and *Striatoabieites* spp. were more abundant in assemblage F than in the younger assemblages. *Striatoabieites* spp. was relative common throughout core 7830/3-U-1 and *Lunatisporites* was also present. *Podosporites amicus* and *Angustisulcites klausii*, both present in core 7830/3-U-1, had their last appearances in assemblage F. Note however that *Podosporites amicus* was recorded as relatively common throughout the core; whereas, *A. klausii* was only observed in the lowermost part of the core (sample number 3 at 188.13 m). The overlying assemblage D and E in Hochuli et al. (1989) were characterised by a dominance (acmes) of *Leschikisporis aduncus*. No acmes of *L. aduncus* were observed in core 7830/3-U-1, further strengthening the correlation with assemblage F.

Previously, Vigran et al. (2014) published a qualitative palynological study based on 18 samples from core 7830/2-U-1 and assigned it to the *A*. *astigmosus* Zone based on abundance of *Aulisporites astigmosus* and high diversity of bisaccate pollen and spores, including the *Aratrisporites* group. They identified 49 spore taxa, 38 pollen taxa and nine marine species (plankton and varia), recorded as dominant, abundant, common or present. Vigran et al. (2014) proposed an early Carnian age for the three lowermost samples (199.49 - 173.36 m) from core 7830/3-U-1, and an informal middle Carnian age for the rest of the core (166.08 - 8.73 m). The early Carnian age (199.49 - 173.36 m) was assigned based on the presence of the pollen grain *Echinitosporites iliacoides* together with *A*. *astigmosus*. There were not records of *E*. *iliacoides* in the interval between 166.08 and 8.73 m and the association was therefore assigned by Vigran et al. (2014) to the upper part of the *A*. *astigmosus* Composite Assemblage Zone (informal middle Carnian). Considering the Carnian timespan of approximately 7 million years, the temporal resolution of the *A*. *astigmosus* zone by Vigran et al. (2014) is relatively low. Vigran et al. (2014) also defined a *Rhaetogonyaulax* zone based on the first appearance datum of *Rhaetogonyaulax* spp., and assigned it a late Carnian age. *Rhaetogonyaulax* spp. was not recorded in core 7830/-U-1 and provided further evidence that the core is of an age older than late Carnian.

Many of the same species that were identified by Vigran et al. (2014) were also observed in this study. For example, Vigran et al. (2014) recorded *Deltoidospora minor* as abundant to dominant through the entire core. Similar results of *Deltoidospora minor* were found in this study, where *D. minor* is common in all samples (9-43 specimens of 200 in each slide) (Appendix II). The same applies for *Leschikisporis aduncus*. Vigran et al. (2014) have found *L*. *aduncus* abundant to common in more than 50% of their samples, and in this current study the species is common throughout the entire core, without any acmes. *Kraeuselisporites cooksonae* and *Baculatisporites* spp., and bisaccate pollen grains were also recorded as common to dominant in both studies. However, in this study most of the bisaccate pollen are identified as *Alisporites* spp., these most likely correspond with the “Bisaccate pollen” recorded by Vigran et al. (2014) (Appendices II and IV).

Many of the taxa recorded by Vigran et al. (2014) from all five cores from the Kong Karls Land east area (Figs. 1 and 9) have been recorded during this study for core 7830/3-U-1. This indicates that the majority of the palynomorphs recorded in the present study have a relatively long stratigraphic range. The most common spores reported by Vigran et al. (2014) from all cores includes *Deltoidospora minor, Leschikisporis aduncus*, *Conbaculatisporites* spp. and *Kraeuselisporites* cooksonae. Common pollen taxa recorded in the five cores were *Podosporites amicus*, *Protodiploxypinus* spp., *Triadispora* spp. All species above are also common throughout the current core 7830/3-U-1 (Appendices II and IV). Species with their first occurrence in the early Carnian observed in the current study, include *Camarozonosporites rudis* and *Uvaesporites argentaeformis*. These were also recorded by Vigran et al. (2014). The stratigraphically younger core 7830/5-U-1 studied by Paterson et al. (2016) documented many of the same taxa, and also strengthens long ranging palynomorphs.

Vigran et al. (2014) recorded an increase in the abundance and diversity of gymnosperm pollen compared with Ladinian assemblages, these includes *Araucariacites*, *Ovalipollis* and the *Protodiploxypinus* groups. *Araucariacites* and *Chasmatosporites* are two of the most common taxa recorded in this study, while *Protodiploxypinus* and *Ovalipollis* are abundant throughout the entire core. Also Meltveit (2015) noted an increase of *Araucariacites* spp. in the early Carnian by Xu et al. (2014) compared to Ladinian successions. This strengthens the indication that the current core 7830/3-U-1 contains the same assemblage as the early Carnian age core studied by Meltveit (2015). This implies core 7830/3-U-1 has an early Carnian age or younger.

Similarly, palynological assemblage from core 7830/5-U-1 presented by Paterson et al. (2016) contained and were dominated by several of the same palynomorphs recorded in the current core 7830/3-U-1. This includes *Densosporites* spp., *Kraeuselisporites* spp. and *Araucariacites australis*. Also many other of the palynomorphs were observed in the two cores, which makes the current core 7830/3-U-1 (Appendix II) closely comparable to the stratigraphic higher core 7830/5-U-1. Paterson et al. (2016) proposed a new subdivision of the *Aulisporites astigmosus* CAz of Vigran et al. (2014) and refer to the new subdivision as the *Podosporites* cf. *amicus* assemblage. *Podosporites*. cf. *amicus* assemblage by Paterson et al. (2016) is younger than the *Echinitosporites iliacoides* CAz of Vigran et al. (2014) and older than the *Leschikisporis aduncus* assemblage of Paterson and Mangerud (2015). *Podosporites* cf. *amicus* assemblage seems to

fit for core 7830/3-U-1 as well, regarding quantity of many similar palynomorphs. *Podosporites* cf. *amicus* recorded by Paterson et al. (2016) is recorded as *Podosporites amicus* in this study.

Hochuli and Vigran (2010) documented several 'floral phases' (Fig. 28) based on quantitative data and the ratio of hygrophyte and xerophyte palynomorphs from Triassic age exploration wells in the southern Barents Sea. The composition of palynomorphs assemblages in the studied core 7830/3-U-1 closely correlate with phase 11 dated by Hochuli and Vigran (2010) as early Carnian. This comparison is based particularly on the high abundance of bisaccate pollen together with the common occurrence of the *Araucariacites* group observed in the current core. A dominance of monolete spores, including *Leschikisporis aduncus*, was noted in floral phase 12 (Fig. 28). Similar acmes of *L*. *aduncus* have been recorded by several authors in the Barents Sea area, who have likewise assigned an informal middle Carnian - Carnian age. These include Holen (2014) and Landa (2015). Based on comparison with those studies, the age of the current core is considered to be older than that of floral phase 12, based on fundamental differences in the composition of the palynomorph assemblages, such as a high abundance of bisaccate pollen and the absence of the *L*. *aduncus* acme in floral phase 11.

The present core 7830/3-U-1 is comparable with the *Concavisporites-Semiretisporites* assemblage (J4) which is dated as early Carnian (Julian) age by Mueller et al. (2016). Assemblage J4 was described in samples collected from the lower De Geerdalen Formation on Spitsbergen. Mueller et al. (2016) recorded the laevigate deltoid spore *Deltoidospora* and the rugulate spore *Striatella* spp. as abundant in their samples, together with high abundance of the lycopsid spore *Kraeuselisporites cooksonae*. *Chasmatosporites* spp. is designated as one of the main pollen taxa for this assemblage (J4) by Mueller et al. (2016). Similar results are recorded in this study (Appendix II).

The gymnosperm pollen *Aulisporites astigmosus* has it earliest occurrence in assemblage F (early Carnian) of Hochuli et al. (1989), and in the *Aulisporites astigmosus* CAz of Vigran et al. (2014). *Aulisporites astigmosus* was common to dominant in 15 of 18 samples the study by Vigran et al. (2014) of the current core 7830/3-U-1. No specimens were observed during the current study; however, similar palynomorphs that may be confused with *A. astigmosus* were observed. These include *Leschikisporis aduncus*, *Podosporites amicus* and *Crassosphaera* sp. and were recorded as common throughout the studied core. Paterson et al. (2016) studied core 7830/5-U-1, which is stratigraphically above the current core 7830/3-U-1, and *A. astigmosus* were observed in 18 of 47 slides; however, the relative abundance of the taxon was recorded as relatively low. They also suggested that the new form, *P*. cf. *amicus*, had been previously misidentified as *A*. *astigmosus*. The cores 7831/2-U-2 and 7831/2-U-1, which are stratigraphic below the present core, have been studied for palynology by Meltveit (2015) who recorded *A. astigmosus* sporadically in these two cores. However, Meltveit's observations are uncertain since the diagnostic trilete mark to *A*. *astigmosus* was not observed. This species therefore seems to be relatively rare in the Snadd Formation in the Kong Karls Land area (Paterson et al. 2016; Meltveit 2015). Mueller et al. (2016) observed that *A*. *astigmosus* was restricted to the Tschermakfjellet Formation and that the taxon is rare in the Snadd Formation. Mueller et al. (2016) also accentuates that the *A*. *astigmosus* zone was located in the lower parts of the Tschermakfjellet Formation in the Boreal region and is older in this region than in the Tethyan region. These observations indicate that *A*. *astigmosus* is a somewhat unreliable marker for the Carnian. Since it seems to be much less common than reported by Vigran et al. (2014), and since the characteristic trilete mark is often "hidden" and difficult to spot. *Aulisporites astigmosus* has also been previously recorded in sediments from Ladinian (e.g. Hankel, 1993; Geleta and Wille, 1998; Kürschner and Herngreen, 2010). Considering these criteria above, *A*. *astigmosus* is a potentially unreliable marker for early Carnian in the Snadd Formation, especially around the Kong Karls Land area in the Norwegian Arctic.

Vigran et al. (2014) recorded the presence of the pollen taxon *Echinitosporites iliacoides,* which has its last occurrence in early Carnian, in the samples at 199.49 and 173.36 m (bottom of the core). An early Carnian age below 173.36 m of the core was therefore suggested. Assemblage G of Hochuli et al. (1989) is defined by the latest occurrences of *E. iliacoides*. This taxon was originally set as a zonal marker and thought to be restricted to the Ladinian in the Germanic and Alpine realms by Visscher and Brugman (1981). The taxon was initially thought to have the same range in the Barents Sea region (e.g. Hochuli et al. 1989). However, Mørk et al. (1990) recorded this species on Bjørnøya and it was then dated as early Carnian based on ammonites and *Halobia* bivalves. More samples were included in the present study, but the pollen *E. iliacoides* was not observed in any of the slides. However, a specimen similar to *E. iliacoides* was recorded in the lowermost samples from the core. E.g. specimens of the spore *Conbaculatisporites* spp. which were observed in the lowermost part of the current core could easily be interpreted as *E. iliacoides*. This spore had a triangle shape and was thick, and it also had the characteristic baculate morphology. In addition, it was twisted and its corners appeared as dark “folds”.

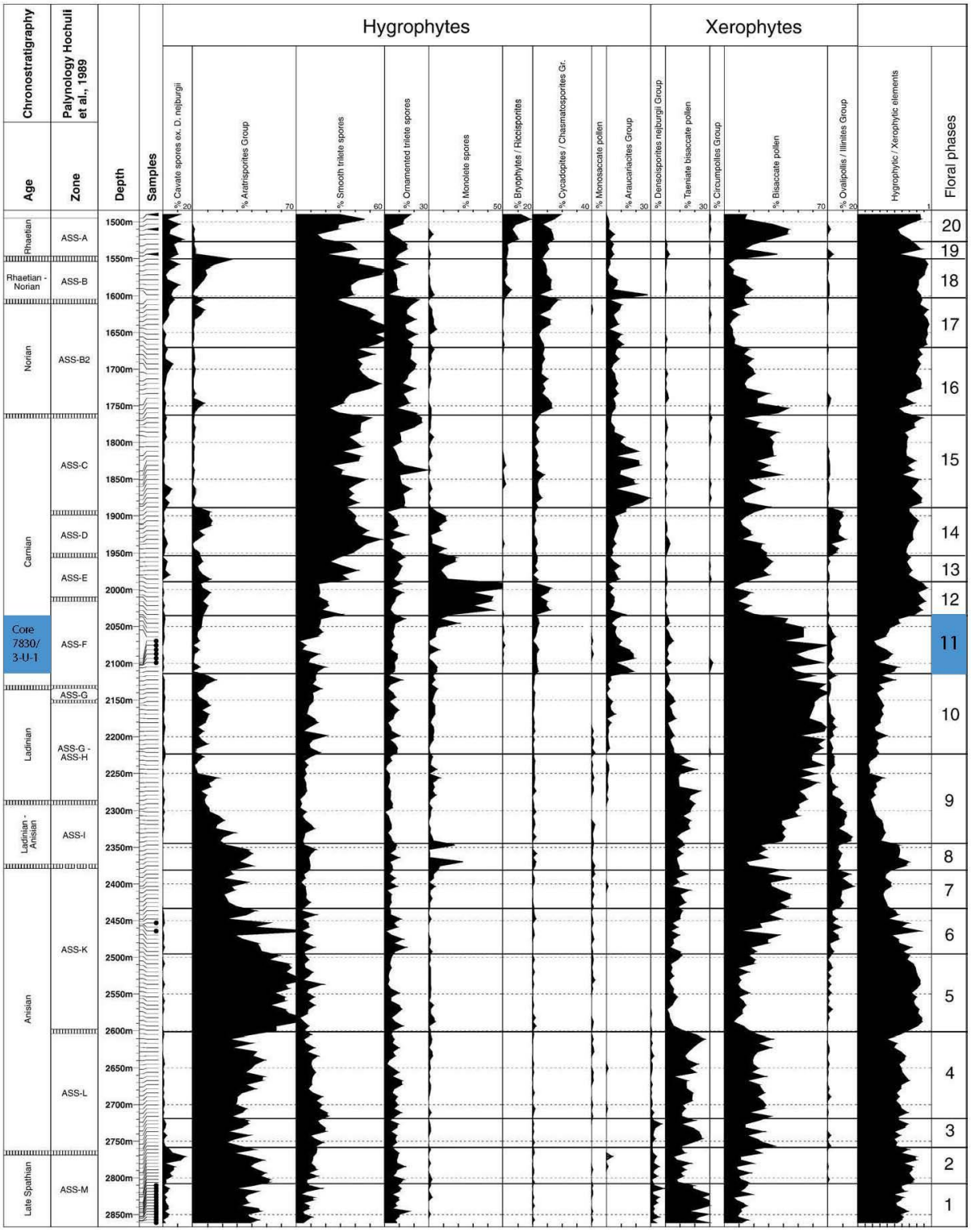

Figure 28: Showing quantitative distribution of main floral elements of well 7228/7-1A from the Nordkapp Basin recognized by Hochuli and Vigran (2010). Twenty floral phases that are correlated with the established palynology work done by Hochuli et al., (1989) are identified. E.g. floral phase 11 is characterised with a large volume of Bisaccate pollen, which has also been observed in the current core 7830/3-U-1. The present core has been correlated with floral phase 11 which by Hochuli and Vigran (2010) is correlated to Assemblage F (early Carnian) of Hochuli et al. (1989). Core 7830/3-U-1 is highlighted with a blue colour (from Hochuli and Vigran, 2010).

Dinoflagellate cysts were not observed from core 7830/3-U-1 in this thesis or by Vigran et al. (2014). Dinoflagellates should have been observed if they were present, since they are widely recorded in the Barents Sea (e.g. Hochuli et al., 1989). The absence of dinoflagellates supports the interpretation that the studied core is older than late Carnian, since there have not been published any recorded dinoflagellate cyst older than late Carnian in the Barents Sea (oral communication; Paterson, 2015). Bujak and Fisher (1976) supported that the earliest occurrence of dinoflagellate cysts from the late Carnian of Northern Canada. Evidence presented by Paterson and Mangerud (2015) indicate that the earliest occurrence of dinoflagellate cysts in the Norwegian Arctic is of late Carnian age; however, they do not seem to be common before Norian. Dinoflagellates cysts have their youngest occurrence in Assemblage C (late Carnian) in the palynological zonation of Svalbard by Hochuli et al. (1989).

Palynomorphs with the last occurrence in the middle Carnian according Vigran et al. (2014) include *Triadispora verrucata,* and *Podosporites amicus* and *Staurosaccites quadrifidus* had their last occurrence in late Carnian. These species are recorded in the current study and strengthens an age older than or a middle Carnian.

5.2 Depositional Environment and Paleoenvironment

The depositional environment of core 7830/3-U-1 has previously been interpreted to represent variations between open shelf to delta front and shoreface conditions (Lundschien et al. 2014). Lundschien et al. (2014) observed several marine bivalves of the *Daonella*/*Halobia* group. They also observed mud flake conglomerates in sandstone beds which were interpreted to represent delta front deposits. The sequences from Late Triassic in the northern Barents Sea are interpreted to represent prograding lobes within a delta system, which means the sequences are stacked laterally (Høy and Lundschien, 2011; Lundschien et al., 2014). Alternatively, the repeated upward coarsening stacking pattern that characterises the Upper Triassic succession in the region may be interpreted to reflect progradational parasequences.

The core was divided into seven intervals (A-G) based upon upward-coarsening sedimentary packages, grading from claystone to sandstone (Figs. 23, 29 and 30). Each of the intervals will be discussed further. The "AOM" – Palynomorph – Phytoclast (APP) ternary plot (Fig. 26) for core 7830/3-U-1 shows several cycles where the samples vary between dominance of either amorphous organic matter or phytoclasts. Amorphous organic matter is an indicator of an offshore environment, while phytoclasts are normally observed in delta-front environments (Tyson, 1995). Intervals mainly consisting of claystone were observed to be enriched in AOM, while sandstone and siltstone interbedded with claystone intervals were dominated by phytoclasts. These observations (Figs. 23, 24, 25 and 26) indicate several cycles where the depositional environment ranges between offshore- and delta front environment. According to Tyson (1995), the datapoints on the ternary plot indicate a fluctuation between distal suboxic-anoxic basin to marginal dysoxic-anoxic basinal environments. Also, the core contains significant amounts of bisaccate pollen which can be related to a long transportation by the "Neves Effect".

The sedimentary succession in core 7830/3-U-1 is interpreted to represent a series of progradational parasequences, grading from clay- to sandstone (Fig. 29). A parasequence is defined by Van Wagoner et al. (1990) as a relatively conformable, genetically related succession of beds or bedsets bounded by marine-flooding surfaces or their correlative

surfaces. Progradational parasequences form when the rate of deposition is larger than the rate of accommodation resulting in a seaward progradation of the sedimentary package. Individual parasequences are bounded by marine flooding surfaces, across which there is evidence of an abrupt increase in water depth and therefore accommodation space (Van Wagoner et al., 1990). An abrupt increase in water depth is seen above almost every major sandstone layer in the current core, where it changes directly from sand- to claystone. A huge delta front system that is prograding in a northwest direction on the Barents Sea Shelf is also earlier suggested by Riis et al. (2008) and Høy and Lundschien (2011).

The mud flakes that were observed, most often in the sandstone at the top of a parasequence, is an indicator of a proximal environment. Mud flakes are normally made in fluvial channel complexes (Lundschien et al., 2014; oral communication; Lundschien 2013). Since no large quantities of mud flakes were observed, and no other indications of a channel depositional environment on the sedimentological log, e.g. upwards-fining sandstone beds, it is concluded that the mud flakes are transported from fluvial channels to a delta front environment where the flakes were deposited.

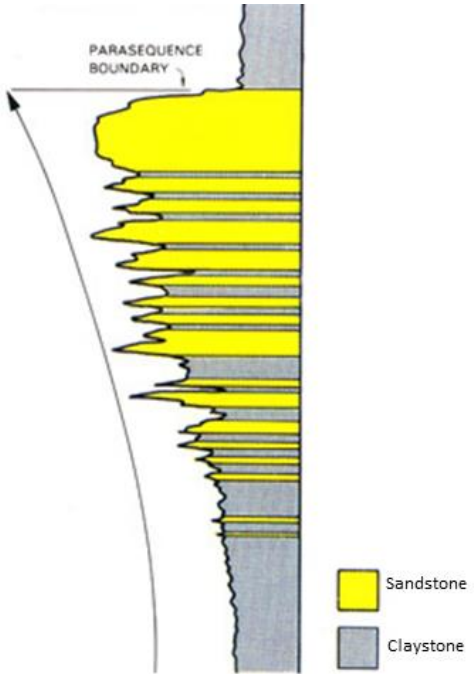

Figure 29: Shows idealised prograding parasequence deposition environment, such as is inferred to characterise core 7830/3-U-1. The depositional environment is interpreted to consist of several stacked prograding parasequences where the grain size increases towards the top of the package (Based on Van Wagoner et al., 1990).

The spore-pollen-microplankton (SPM) ternary plot (Fig. 16) shows a more or less even distribution of spores and pollen in all palynological slides. This can be a mixing of local spores and pollen transported from the hinterland. Another reason for this may be because of the majority of palynological samples studied were collected in silt rich claystone, due to palynomorphs are better preserved in this type of sediment. However, sample number four at 188.13 m was collected from the laminated uncontaminated dark grey claystone and found to contain more pollen than spores. This is an indicator of an offshore depositional environment, regarding the claystone and the pollen content (Tyson, 1995).

Other indicators for a marine depositional environment is the observation of pyrite. Some of the palynological slides were enriched of pyrite and were typically observed together with amorphous organic matter and marine algae. The best environment to form pyrite is in marine to brackish peats swamp environments. Pyrite occurs when H_2S reacts with iron. H_2S is a product of sulphate reduction in the uppermost part of a deposition area. This occurs especially during slow deposition of sediments in an anoxic environment (Batten, 1996). Also the marine bivalves observed in the core are an indicator of marine deposition. Other indicators on an offshore depositional environment is the laminated claystone, which indicate that the sea floor must have been below storm wave base in order for the laminations to be preserved. Also, the preservation of the lamina indicates slow deposition. Lamina are only preserved when there is no bioturbation, which have been observed in the current core (Figs. 23 and 30). Often offshore marine environments are anoxic, this prevents the colonisation of the sediment by infauna, therefore no bioturbation.

Samples enriched in hinterland pollen types, e.g. bisaccate pollen, in association with AOM can be explained by the “Neves Effect” of Chaloner and Muir (1968) forwarded by Traverse (2007). The “Neves Effect” is based on how different taxa are transported. For example, sediments deposited at considerable distance from the shore contain greater amounts of bisaccate pollen since they are more buoyant, making it easier for them to be transported over longer distances by air and water. Samples in this study that are enriched with small peaks of bisaccate pollen are also often enriched by AOM. This is easily recognized in palynological samples number 2 and 3 collected at 194.30 and 183, 38 m depth, respectively. The palynological sample number 3 contain about 25% bisaccate pollen and the kerogen slide

(K15) from the same interval contain around 80 – 85% AOM (Appendix II and III, Fig. 26). These indicators together with relatively bivalve-rich laminated claystone without bioturbation in the sampling interval strengthens the evidence for a distal marine depositional environment; an offshore setting. Further evidence for a distal depositional environment is that it seems to be a trend with an increase of bisaccate pollen where the uncontaminated claystone is observed (remember; no samples are collected in sandstone) (Appendix II).

Marine acritarchs were also observed in several slides, where they had their peaks in the claystone intervals. Specimens assigned to *Micrhystridium* spp. were especially common in the claystone in the lower part of the core. However, acritarchs were also observed in the muddy siltstone in Interval C (Appendix II, Fig. 30). Other slides contained a significant number of palynomorphs that were broken into unidentifiable pieces, which is often related to transport over longer distances. However, it is difficult to interpret something about the exactly length of transportation based on only this observation (Traverse, 2007).

High frequency of *Araucariacites* is, in general, correlated with a temperate and humid climate (Abbink et al., 2004). *Araucariacites* australis was common along the entire core, which strengthened a warm and humid climate in Late Triassic. *Vitreisporites pallidus*, which was recorded in in the core, belongs to the Caytoniales (seed plants) that are considered to have grown in a deltaic environment during a warm and rather wet environment (Abbink et al., 2004).

Table 3: Facies of core 7830/3-U-1, arranged in decreasing energetic conditions.

Facies	Intervals (Depth in m)	Description	Interpretation of environment
1	199.6 – 195.5 175.0 – 170.5 43.0 – 37.0 27.0 – 15.0	Medium to coarse sandstone with oil stain.	Delta front
2	183.0 – 175.0	Dark grey claystone with thin sandstone and siltstone beds. Some ripples and heavy bioturbation.	Distal delta front
3	77.5 – 64.0 49.0 – 43.0 37.0 – 27.0	Siltstone grading to claystone with thin beds of sandstone.	Pro-delta
4	117.0 – 106.0 52.5 – 49.0	Fine sandstone with interbedded claystone. Mud flakes and framboids of pyrite were included.	Shoreface
5	128.0 – 117.0 102.0 – 77.5 64.0 – 52.5	Mix of silty claystone with sandstone interbeds, sandstone layers and siltstone layers with claystone clasts.	Lower shoreface
6	166.0 – 128.0 106.0 – 102.0 15.0 – 3.3	Laminated muddy siltstone with thin rippled sandstone beds. Occasionally bivalves.	Shallow shelf
7	195.5 – 183.0 170.5 – 166.0	Dark grey to blackish grey laminated claystone with abundant bivalves. Micro pyrite and minor bioturbation.	Offshore

Figure 30: A slightly simplified log of core 7830/3-U-1 showing the facies associations (interpreted in Table 3), and intervals A-G. Seven prograding parasequences have been recognized throughout the core. Legend below the core log shows the features.

Interval A

Interval A comprises approximately 3.5 m of medium to coarse sandstone in the lowermost part of the core (Figs. 23 and 30). This interval is interpreted to be deposited in a delta front environment (Facies 1). Also, it is interpreted to be deposited in the top of a progradational parasequence, considering the huge difference from the laminated claystone observed above the sandstone and the other parasequences throughout the core. Other features, except the coarse sand, that indicates a proximal environment are ripples and bioturbation. Which means that the sediments were deposited in an environment in movement above wave basis; however, not deposited too proximal based on the medium degree of bioturbation observed.

Interval B

Interval B was recorded in the lower part of the core from 196.0 to 170.0 m and contained mostly dark grey laminated claystone which is interpreted to represent deposits in a quiet offshore environment (Facies 7) (Fig. 30). The claystone gradually grades into a medium sandstone with coarse sandstone interbeds, which is interpreted as a delta front environment (Facies 1). The offshore environment is strengthened with occurrence of bivalves and high abundance of marine acritarchs (mainly *Micrhystridium* spp.) (Figs. 23 and 30, Appendix II). The acritarch *Micrhystridium* spp. is very abundant (21.5%) at 173.36 m and they may signify a marine flooding surface marking the base of the next parasequence, as interpreted (Fig. 30). The interval with laminated claystone lacks bioturbation, which also strengthened an offshore environment. Bioturbation is an indicator of oxygenation and generally conditions favourable to life. Therefore lack of bioturbation is an indicator of anoxia. Above the offshore depositions it is an interval of grey claystone with thin silt- and sandstone beds interpreted as distal delta front (Facies 2). This interpretation is strengthened with bioturbation and ripples. On the top of the interpreted distal delta front there is an interval between 175.0 and 170.0 m containing medium to coarse sandstone with medium degree of bioturbation, which is interpreted to be deposited at a delta front (Facies 1). Considering these observations and interpretations this interval is interpreted to be one progradational parasequence grading from claystone to sandstone, starting and ending with a flooding surface.

The lowermost kerogen sample from 194 m, taken in the laminated dark grey claystone (Figs. 23, 30 and 26), is the sample that have the highest AOM content of all samples, almost 100% AOM. That is after Tyson (1995) a quite good indicator of a distal marine depositional environment. There is a change in the presence of palynomorphs in the suggested delta front (Facies 1) (Fig. 30). It has a higher content of spores, which strengthen the depositional environment to be at a delta front (Appendix II) (Traverse, 2007).

Interval C

Interval C is interpreted to be a progradational parasequence. There is an upwards increase in the grain size, which mean an upwards increase in energy. However, it differs some from Interval B in the way it is deposited. In the lowermost part there is a 3 m thick claystone (between 170 and 167 m) with the same features as in the bottom of Interval B, and is therefore interpreted to be deposited in an offshore environment (Facies 7).

Higher in Interval C there is a 40 m long interval of laminated muddy siltstone with thin rippled sandstone beds, from 167 to 127 m (Figs. 23 and 30). This interval is interpreted to be deposited at the shallow shelf (Facies 6) on the basis of the laminated muddy siltstone with some occasionally bivalves. The present of ripples is an indicator of more wave energy and shallower water depth, compared with the claystone interpreted as offshore deposits in Interval B. The APP-ternary plot (Fig. 26) shows that the muddy siltstone in Interval C (Fig. 30) is enriched in phytoclasts, based on the model presented by Tyson (1985, 1989,1993) this is consistent with a heterolithic oxic shelf depositional environment. The algae *Crassosphaera* spp. is present in the entire interval and is an indicator of a marine environment. Also acritarchs like *Micrhystridium* spp. and *Leiosphaeridia* sp. are present and strengthen the suggestion of a marine depositional environment.

Above the muddy siltstone there is an interval spanning between 127 and 106 m which consist mainly of fine yellowish to brownish sandstone with dark grey claystone interbeds and are interpreted to be deposited from lower shoreface (Facies 5) to shoreface (Facies 4) (Fig. 30). The lower part of this interval have a higher content of siltstone with some lamina, and are interpreted to be deposited at the lower shoreface (Facies 5). The upper part of this sandstone interval is interpreted to be deposited at a the shoreface (close to a delta front) (Facies 4), this

is based on the presence of mud flakes (originating from channels) and the presence of pyrite (indicating an anoxic environment). These interpretations are made on the basis of the underlying muddy siltstone which were interpreted to a shallow shelf environment. Few samples for palynology were collected in this interval and only two kerogen slides are available. One kerogen slide is collected in the very top of Interval C and shows a dominance of phytoclasts (Fig. 26) which indicate an environment closer towards shore (delta front).

Interval D

Interval D is interpreted as another parasequence grading from the laminated claystone (Facies 6) at 106 m to the top of the sandstone layer (Facies 3) at 64 m. Mud flakes were observed at the top of the interval which is therefore interpreted as a pro-delta (same conclusion as previous) (Facies 3). Algae (*Crassosphaera* spp.) with marine origin are recorded mainly in the lower part of this interval, which is an indicator of a marine environment. The high relative abundance of AOM in samples containing algae and acritarchs further strengthens the argument for a marine depositional environment.

Interval E

Interval E is a new parasequence spanning the interval from 64 m to 37 m. A mix of silty claystone with sandstone interbeds (Facies 5) in the lower part is grading to sandstone (Facies 1) in the upper part, there is an increase in the wave energy. Traces of mud flakes at the top of the parasequence together with fine sandstone indicate a delta front deposition (Facies 1). Also the traces of roots that were observed at 38 m (Fig. 30) strengthened a depositional environment relatively close to shore above sea level. The interval contained less framboids of pyrite than the other intervals, which is an indicator of deposition in a more oxic environment (Batten, 1996).

Interval F

Interval F (37 – 15 m) has the same features as the previous intervals, and is thereby also interpreted as a single parasequence. A mix of claystone and siltstone (Facies 3) at the bottom of the interval (on top of an erosional surface) grading to sandstone with traces of mud flakes, which indicate a delta front (Facies 1). This interval contained much less framboids of pyrite than the intervals A - D, which is an indicator of deposition in a more oxic environment (Batten, 1996).

Interval G

Interval G, spanning from 15 m to 3.37 m (Fig. 30), is the uppermost interval and consist mainly of claystone with some layers of silt- and sandstone interbeds. The sedimentological structures changes between lamina and ripples, and indicate an environment close to the wave base. It is thereby interpreted to be deposited at a shallow shelf (Facies 6) and to be the lower part of a parasequence.

6. Conclusion

Palynostratigraphy

The 200 m long shallow stratigraphical core 7830/3-U-1, which comprises mainly long ranging and well-preserved palynomorphs, is assigned an early Carnian age based on palynology, constrained by the available absolute and relative age constraints. The core has a relative high amount of *Araucariacites australis* which is common in early Carnian.

Concluding remarks:

- Re-Os datings by Xu et al. (2014) indicates that the two oldest stratigraphic cores in Kong Karls Land east area (7831/2-U-2 and 7831/2-U-1) are dated to the Ladinian-Carnian boundary, therefore constraining the age of core 7830/3-U-1 to the early Carnian age or younger.
- The presence of *Triadispora* supports a Norian age or older, and the absence of dinoflagellate cysts indicates a pre-Norian age for the current core.
- The assemblage correlates with the palynomorphs in "Assemblage F" of Hochuli et al. (1989) which has been ammonite dated to the early Carnian.
- The palynomorphs in the current core resembles with "*Aulisporites Astigmosus* Zone" of Vigran et al. (2014), even though the pollen grain *Aulisporites astigmosus* was not observed during this study.
- The current core also resembles with the *Podosporites* cf. *amicus* assemblage from the stratigraphic higher core 7830/5-U-1 in Kong Karls Land east area of Paterson et al. (2016), which is confidently assigned an early Carnian age.
- Core 7830/3-U-1 is comparable with the *Concavisporites-Semiretisporites* (J4) of Mueller et al. (2016) dated to the Julian (early Carnian).
- Floral phase 11 of Vigran and Hochuli (2010) is assigned an early Carnian age, and is closely comparable with core 7830/3-U-1.
- Future work within palynology of the Late Triassic in the Norwegian Arctic should be a more detailed taxonomic study (especially on *Aulisporites astigmosus* in early Carnian), and greater integration with other wells in the region, especially at Sentralbanken and exploration wells in the southern Barents Sea. A higher biostratigraphic resolution for Carnian is recommended.

Paleoenvironment

A paralic depositional environment is suggested for the core based on the sedimentological analysis which indicates the presence of several asymmetrical sedimentary packages from offshore to delta front environment.

- A marine depositional environment is suggested based on marine influx throughout the core, such as acritarchs.
- Presence of bivalves and some places strong bioturbation strengthen the conclusion of a marine environment.
- Prograding parasequences are suggested on the basis of the core log, specifically the asymmetrical upwards coarsening sedimentary packages grading from claystone/mudstone to sandstone in seven repetitions.
- Palynofacies results are consistent with a depositional setting ranging from a delta front to offshore environment, based on the fluctuation in the marine/terrestrial organic matter ratio.
- The abundance of fern and lycopsid spores could indicate temperate and humid conditions.

References

Abbink, O. A., Van Konijnenburg-Van Cittert, J. H. A., and Visscher, H., 2004, A sporomorph ecogroup model for the Northwest European Jurassic-Lower Cretaceousi: concepts and framework: *Netherlands Journal of Geosciences-Geologie en Mijnbouw*, v. 83, no. 1, p. 17-31.

Ask, M., 2013. Palynological dating of the upper part of the De Geerdalen Formation on central parts of Spitsbergen and Hopen (MSc. thesis), University of Bergen, Norway, 1-79.

Batten, D. J., 1996, Palynofacies and palaeoenvironmental interpretation: *Palynology: principles and applications*, v. 3, p. 1011-1064.

Bjærke, T., and Manum, S. B., 1977. Mesozoic palynology of Svalbard. I, The Rhaetian of Hopen, with a preliminary report on the Rhaetian and Jurassic of Kong Karls Land. *Norsk Polarinstitutt, no. Skrifter nr. 135, 1-48.*

Bjærke, T., 1977. Mesozoic palynology of Svalbard II. Palynomorphs from the Mesozoic sequence of Kong Karls Land. *Norsk Polarinstitutt Årbok 1976*, 83-120.

Blendinger, E., 1988. Palynostratigraphy of the late Ladinian and Carnian in the southeastern Dolomites. *Review of palaeobotany and palynology, 53*, 329-348.

Bonis, N., Kürschner, W., and Krystyn, L. (2009). A detailed palynological study of the Triassic-Jurassic transition in key sections of the Eiberg Basin (Northern Calcareous Alps, Austria). *Review of Palaeobotany and Palynology, 156*(3), 376-400.

Buiter, S. J., and Torsvik, T. H. (2007). Horizontal movements in the eastern Barents Sea constrained by numerical models and plate reconstructions. *Geophysical Journal International, 171*(3), 1376-1389.

Bujak, J. P., and Fisher, M. J. (1976). Dinoflagellate cysts from the Upper Triassic of Arctic Canada. *Micropaleontology*, 44-70.

Combaz, A. (1964). Les palynofacies. *Revue de Micropaléontologie*, 7(3), 205-218.

Chaloner, W. G., and Muir, M., 1968, Spores and floras, in: *Coal and Coal-bearing Strata* (D.G. Murchison and T. S. Westall, eds.), Edinburgh, Oliver and Boyd, pp. 127-146.

Duringer, P., Doubinger, J., 1985. La palynology: un outil de characterisation des facies marins et continentaux a la limite Muschelkalk Supérieur – Lattenkohle. *Science Géologie Bulletin, Strasbourg 38*, 19-34.

Elsik, W. C., 1966. Biologic Degradation of Fossil Pollen Grains and Spores. *Micropaleontology*, 12(4), 515-518.

Federova, V.A., 1977. The significance of the combined use of microphytoplankton, spores, and pollen for differentiation of multi-facies sediments. In: Samoilovich, S.R., Timoshina, N.A., (Eds.), Questions of Phytostratigraphy. *Trudy Neftyanoi nauchno-issledovatelskii geologorazcedochnyi Institut* (VNIGRI), Leninggrad 398, 70-88. (in Russian).

Fisher, M. J., 1979, The Triassic palynofloral succession in the Canadian Arctic Archipelago. *American Association of Stratigraphic Palynologists Contribution Series 5B*, p. 83-100.

Geleta, W., and Wille, W. (1998). Middle Triassic Palynomorphs from the Fincha-a River valley section, Horo Guduru, Western Central Ethiopia. (With 5 figures and 1 table). *Neues Jahrbuch fur Geologie und Palaontologie-Monatshefte*, (5), 257-268.

Glørstad-Clark, E., Faleide, J. I., Lundschien, B. A., and Nystuen, J. P., 2010. Triassic seismic sequence stratigraphy and paleogeography of the western Barents Sea area. *Marine and Petroleum Geology*, 27(7), 1448-1475.

Hankel, O. (1993). Early Triassic plant microfossils from Sakamena sediments of the Majunga Basin, Madagascar. *Review of palaeobotany and palynology, 77*(3), 213-233.

Hesse, M., Halbritter, H., Weber, M., Buchner, R., Frosch-Radivo, A., and Ulrich, S., 2009. *Pollen terminology: an illustrated handbook*. Springer Science and Business Media.

Hochuli, P. A., and Frank, S. M., 2000. Palynology (dinoflagellate cysts, spore-pollen) and stratigraphy of the Lower Carnian Raibl Group in the Eastern Swiss Alps. *Eclogae Geologicae Helvetiae*, 93(3), 429-443.

Hochuli, P. A., and Vigran, J. O., 2010, Climate variations in the Boreal Triassic — Inferred from palynological records from the Barents Sea: *Palaeogeography, Palaeoclimatology, Palaeoecology*, v. 290, no. 1–4, p. 20-42.

Hochuli, P. A., Colin, J. P., and Vigran, J. O., 1989. Triassic biostratigraphy of the Barents Sea area. In: Collinson, J. (Ed.), *Correlations in Hydrocarbon Exploration,* Graham and Trotman, London, pp. 131–153.

Holen, L. H., 2014. Late Triassic (Carnian) Palynology of the Northern Barents Sea (Sentralbanken High). (MSc. thesis), University of Bergen, Norway, 1-96.

Høy, T., and Lundschien, B. A., 2011. Triassic deltaic sequences in the northern Barents Sea. *Geological Society, London, Memoirs, 35*(1), 249-260.

Jansonius, J., and Hills, L. V., 1976, Genera File of Fossil Pollen and Spores: Special publication, University of Calgary, Calgary, Alta, v. 3286.

Klaus, W., 1960. Sporen der karnischen Stufe der ostalpinen Trias, *Jahrb. Geol. Bundesanst,* 107–183.

Korčinskaya, M. V., 1980, Rannenoriskaja fauna Arhipelaga Svalbard: Early Norian fauna of the Svalbard Archipelago.) In DV Semevskij (ed.): *Geologija osadocnogo cehla arhipelaga Sval'bard*. (Geology of the sedimentary cover of Svalbard.) Pp, p. 30-43.

Kürschner, W. M., and Herngreen, G. W., 2010. Triassic palynology of central and northwestern Europe: a review of palynofloral diversity patterns and biostratigraphic subdivisions. *Geological Society, London, Special Publications*, *334*(1), 263-283.

Landa, J., 2015. Middle to Late Triassic (late Ladinian – late Carnian) palynology of the shallow stratigraphic core 7534/4-U-1, Sentralbanken High, Northern Barents Sea. (MSc. thesis), University of Bergen, Norway, 1-91.

Lund, J. J., 1977, Rhaetic to Lower Liassic palynology of the onshore south-eastern North Sea Basin: *Geological Survey of Denmark* v. II, no. Series No. 109.

Lundschien, B. A., Høy, T., and Mørk, A., 2014. Triassic hydrocarbon potential in the Northern Barents Sea; integrating Svalbard and stratigraphic core data. *Norwegian Petroleum Directorate Bulletin*, *11*, 3-20.

Meltveit, A. R., 2015. Middle to Late Triassic (Ladinian to Carnian) palynology of shallow stratigraphic cores 7831/2-U-2 and 7831/2-U-1, offshore Kong Karls Land, Norwegian Arctic. (MSc. thesis), University of Bergen, Norway, 1-89.

Mueller, S., Hounslow, M. W., and Kürschner W. M., 2016, Integrated stratigraphy and palaeoclimate history of the Carnian Pluvial Event in the Boreal realm; new data from the Upper Triassic Kapp Toscana Group in central Spitsbergen (Norway) *Journal of the Geological Society*, V. 173, p. 186-202.

Mørk, A., Dallmann, W. K., Dypvik, H., Johannessen, E. P., Larssen, G. B., Nagy, J., Nøttvedt, A., Olaussen, S., Pchelina, T. M., and Worsley, D., 1999. Mesozoic lithostratigraphy: Lithostratigraphic lexicon of Svalbard. Upper Palaeozoic to Quaternary bedrock. *Review and recommendations for nomenclature use*, p. 127-214.

Nagy, J., Hess, S., Dypvik, H., and Bjærke, T., 2011, Marine shelf to paralic biofacies of Upper Triassic to Lower Jurassic deposits in Spitsbergen: *Palaeogeography, Palaeoclimatology, Palaeoecology*, v. 300, no. 1, p. 138-151.

Ogg, J. G., 2012, The Triassic Period. In F. M. Gradstein, G. Ogg, and M. Schmitz (Eds.), *The Geologic Time Scale 2012 2-Volume Set, Volume 2*. Elsevier, UK.

Paterson, N. W., and Mangerud, G., 2015. Late Triassic (Carnian-Rhaetian) palynology of Hopen, Svalbard. *Review of Palaeobotany and Palynology*.

Paterson, N. W., Mangerud, G., Cetean, C. G., Mørk, A., Lord, G. S., Klausen, T. G., and Mørkved, P. T., 2015. A multidisciplinary biofacies characterisation of the Late Triassic (late Carnian–Rhaetian) Kapp Toscana Group on Hopen, Arctic Norway. *Palaeogeography, Palaeoclimatology, Palaeoecology*. (online).

Paterson, N. W., Mangerud, G., B. A., Lundschien and Mørk, A., (2016). Late Triassic (early Carnian) palynology of shallow stratigraphic core 7830/5-U-1, offshore Kong Karls Land, Norwegian Arctic, DOI: 10.1080/01916122.2016.1163295.

Punt, W., Hoen, P. P., Blackmore, S., Nilsson, S., and Le Thomas, A., 2007. Glossary of pollen and spore terminology. *Review of Palaeobotany and Palynology, 143*(1), 1-81.

Riding, J. B., and Kyffin-Hughes, J. E., 2004. A review of the laboratory preparation of palynomorphs with a description of an effective non-acid technique. *Revista Brasileira de Paleontologia*, *7*(1), 13-44.

Riis, F., Lundschien, B. A., Høy, T., Mørk, A., and Mørk, M. B., 2008, Evolution of the Triassic shelf in the northern Barents Sea region: *Polar Research*, v. 27, no. 3, pp. 318-338.

Roghi, G., 2004, Palynological investigations in the Carnian of the Cave del Predil area (Julian Alps, NE Italy): *Review of Palaeobotany and Palynology*, v. 132, no. 1, p. 1-35.

Roghi, G., Gianolla, P., Minarelli, L., Pilati, C., and Preto, N., 2010, Palynological correlation of Carnian humid pulses throughout western Tethys: *Palaeogeography, Palaeoclimatology, Palaeoecology,* v. 290, no. 1, p. 89-106.

Sakshaug, E., Bjørge, A., Gulliksen, B., Loeng, H., and Mehlum, F., 1994. Structure, biomass distribution, and energetics of the pelagic ecosystem in the Barents Sea: a synopsis. *Polar Biology*, *14*(6), p. 405.

Scheuring, B. W., 1970, Palynologische und palynostratigraphische Untersuchungen des Keupers im Bölchentunnel (Solothurner Jura). Schweiz. *Palaeontol. Abh*. 88, 1-119.

Scheuring, B. W., 1978, Mikrofloren aus den Meridekalken des Mte. San Giorgio (Kanton Tessin), Birkhäuser. *Schweizerische paläontologische abhandlungen*

Smith, D. G., 1974. Late Triassic pollen and spores from the Kapp Toscana Formation, Hopen, Svalbard – a preliminary account. *Review of palaeobotany and palynology*, 17(1), 175-178

Smith, D. G., Harland, W. B., and Hughes, N. F., 1975. Geology of Hopen, Svalbard. *Geological Magazine*, *112*(01), 1-23.

Smith, D. G., Harland, W. B., Hughes, N. F., and Pickton C. A. G., 1976. The geology of Kong Karls Land, Svalbard. *Geological Magazine*, 113, pp 193-232.

Smith, D. G., 1982. Stratigraphic significance of a palynofloral from ammonoid-bearing Early Norian strata in Svalbard. *Newsletters on Stratigraphy, 11*(3), 154-161.

Torsvik, T.H. and Cocks, L.R.M. 2005: Norway in space and time: A Centennial Cavalcade. *Norwegian Journal of Geology, 85*, 73-86.

Traverse, A., 1988. *Paleopalynology*, 1st edition, Unwin Hyman, Boston, 600 pp.

Traverse, A., 2007. *Paleopalynology*. 2nd edition. Springer, Dordrecht, Netherlands, pp. 1-813.

Tyson, R. V., 1985. *Palynofacies and sedimentology of some Late Triassic sediments from the British Isles and northern North Sea* (PhD thesis) The open University, Milton Keynes (623 pp.).

Tyson, R. V., 1989. Late Jurassic palynofacies trends, Piper and Kimmeridge Clay Formations, UK onshore and offshore, In: Batten, D.J., Keen, M.C. (Eds.), Northwest European Micropalaeontology and Palynology. *British Micropalaeontological Society Series. Ellis Horwood, Chichester*, pp. 135-172.

Tyson, R. V., 1993. Palynofacies analysis. In: Jenkis, D.J. (Ed.), *Applied Micropalaeontology*. Kluwer, Dordrecht, pp. 153-191.

Tyson, R. V., 1995. *Sedimentary organic matter: organic facies and palynofacies*, Springer, 615 p.

Van der Eem, J. G. L. A., 1983. Aspects of Middle and Late Triassic palynology. 6. Palynological investigations in the Ladinian and Lower Karnian of the western Dolomites, Italy. *Review of Palaeobotany and Palynology*, *39*(3), 189-300.

Van Wagoner, J. C., Mitchum, R. M., Campion, K. M., and Rahmanian, V. D. (1990). Siliciclastic sequence stratigraphy in well logs, cores, and outcrops: concepts for high-resolution correlation of time and facies. *AAPG Methods in Exploration Series*. 7 pp. 1-55.

Vigran, J. O., Mangerud, G., Mørk, A., Bugge, T., and Weitschat, W., 1998. Biostratigraphy and sequence stratigraphy of the Lower and Middle Triassic deposits from the Svalis Dome, central Barents Sea, Norway. *Palynology, 22*, 89-141.

Vigran, J. O., Mangerud, G., Mørk, A., Worsley, D., and Hochuli, P. A., 2014, Palynology and geology of the Triassic succession of Svalbard and the Barents Sea, *Geological Survey of Norway Special Publication*, 14, 247 pp.

Visscher, H., and Brugman, W. A., 1981. Ranges of selected palynomorphs in the Alpine Triassic of Europe. *Review of Palaeobotany and Palynology*, 34(1), 115-128.

Wood, G. D., Gabriel, A. M., and Lawson, J. C., 1996, Palynological techniques—processing and microscopy: *Palynology: principles and applications*, v. 1, p. 29-50.

Worsley, D., 2008, The post-Caledonian development of Svalbard and the western Barents Sea. *Polar Research, 27*(3), 298-317.

Xu, G., Hannah, J. L., Stein, H. J., Mørk, A., Vigran, J. O., Bingen, B., Schutt, D. L., Lundschien, B. A., 2014. Cause of Upper Triassic climate crisis revealed by Re-Os geochemistry of Boreal black shales. *Palaeogeography, Palaeoclimatology, Palaeoecology,* 395, 222-232.

Appendices

Appendix I: List of palynomorph taxa

Appendix II: Range chart of core 7830/3-U-1

Appendix III: Range chart, including palynofacies estimates

Appendix IV: Plates

Appendix I: List of palynomorph taxa

Spores

Anapiculatisporites spiniger	(Leschik 1955) Reinhardt 1962
Annulispora folliculosa	(Rogalska 1954) de Jersey 1959
Aratrisporites laevigatus	Bjærke and Manum 1977
Aratrisporites paenulatus	Playford and Dettmann 1965
Aratrisporites scabratus	Klaus 1960
Aratrisporites spp.	
Baculatisporites spp.	
Calamospora tener	(Leschik, 1955) Mädler 1964
Camarozonosporites laevigatus	Schulz 1967
Camarozonosporites rudis	(Leschik, 1955) Klaus 1960
Cingulizonates rhaeticus	(Reinhardt 1962) Schulz 1967
Clathroidites papulosus	Bai 1983
Clathroidites spp.	
Conbaculatisporites hopensis	Bjærke and Manum 1977
Conbaculatisporites sp. A	Sensu Paterson and Mangerud 2015
Conbaculatisporites spp.	
Converrucosisporites spp.	
Deltoidospora spp.	
Densoisporites spp.	
Dictyophyllidites mortonii	(de Jersey, 1959) Playford and Dettmann, 1965
Kraeuselisporites cooksonae	(Klaus 1962) Dettmann 1963
Kraeuselisporites spp.	
Kyrtomisporis laevigatus	Mädler 1964
Kyrtomisporis spp.	
Leptolepidites spp.	
Leschikisporis aduncus	(Leschik 1955) Potonié 1958
Lycopodiacidites rugulatus	(Couper 1958) Schulz 1967
Lycopodiumsporites semimuris	(Danze-Corsin and Laveine 1963) Mc Kellar 1974

Punctatisporites fungosus	Balme 1963
Punctatisporites spp.	
Raistrickia spp.	Schopf, Wilson and Bentall, 1944
Reticulatisporites spp.	
Retusotriletes spp.	
Semiretisporis sp. A	Sensu Paterson and Mangerud 2015
Striatella parva	(Li and Shang) Filatoff and Price 1988
Striatella seebergensis	Mädler 1964
Todisporites minor	Couper 1958
Uvaesporites cf. argentaeformis	(Bolkhovitina 1953) Schulz 1967
Velosporites sp. A	Sensu Paterson and Mangerud 2015
Verrucosisporites spp.	

Pollen

Alisporites spp.	
Angustisulcites klausii	(Freudenthal 1964) Visscher 1966
Araucariacites australis	Cookson 1947
Bisaccate pollen	
Chasmatosporites apertus	(Rogalska 1954) Pocock and Jansonius 1969
Chasmatosporites hians	Nilsson 1958
Chasmatosporites spp.	
Classopollis spp.	
Cycadopites spp.	
Ephedripites spp.	
Eucommiidites spp.	
Granasporites magnus	Quian Lijun, Zao Cenghua and Wu Jinjun 1983
Illinites chitinoides	Klaus 1964
Lunatisporites spp.	
Ovalipollis ovalis	Krutzsch 1955
Ovalipollis pseudoalatus	(Thiergart 1949) Schuurmann 1976
Ovalipollis spp.	
Podosporites amicus	Scheuring 1970
Podosporites spp.	
Protodiploxypinus macroverrucosus	Bjærke and Manum 1977
Protodiploxypinus minor	Bjærke and Manum 1977
Protodiploxypinus spp.	
Pseudoquadrisaccus irregularis	Liu 1981
Retisulcites perforatus	(Mädler 1964) Scheuring 1970)
Schizaeoisporites worsleyi	Bjærke and Manum 1977
Staurosaccites quadrifidus	Dolby and Balme 1976
Steevesipollenites spp.	
Striatoabieites balmei	(Klaus 1964) Scheuring 1978
Striatoabieites multistriatus	(Balme and Henelly) Hart 1964
Striatoabieites spp.	

Tetrasaccus spp.

Triadispora crassa Klaus 1964 Pl. 3, 3.

Triadispora spp.

Triadispora verrucata (Schulz) Scheuring, 1970 Pl. 3,1.

Vitreisporites pallidus (Reissinger) Nilsson, 1958

Acritarchs

Baltisphaeridium spp.

Leiosphaeridia sp.

Micrhystridium spp.

Veryhachium spp.

Chlorococcales

Botryococcus spp.

Crassosphaera spp.

Plaesiodictyon mosellanum Brenner 1994

Tasmanites spp.

Appendix II: Range chart core 7830/3-U-1

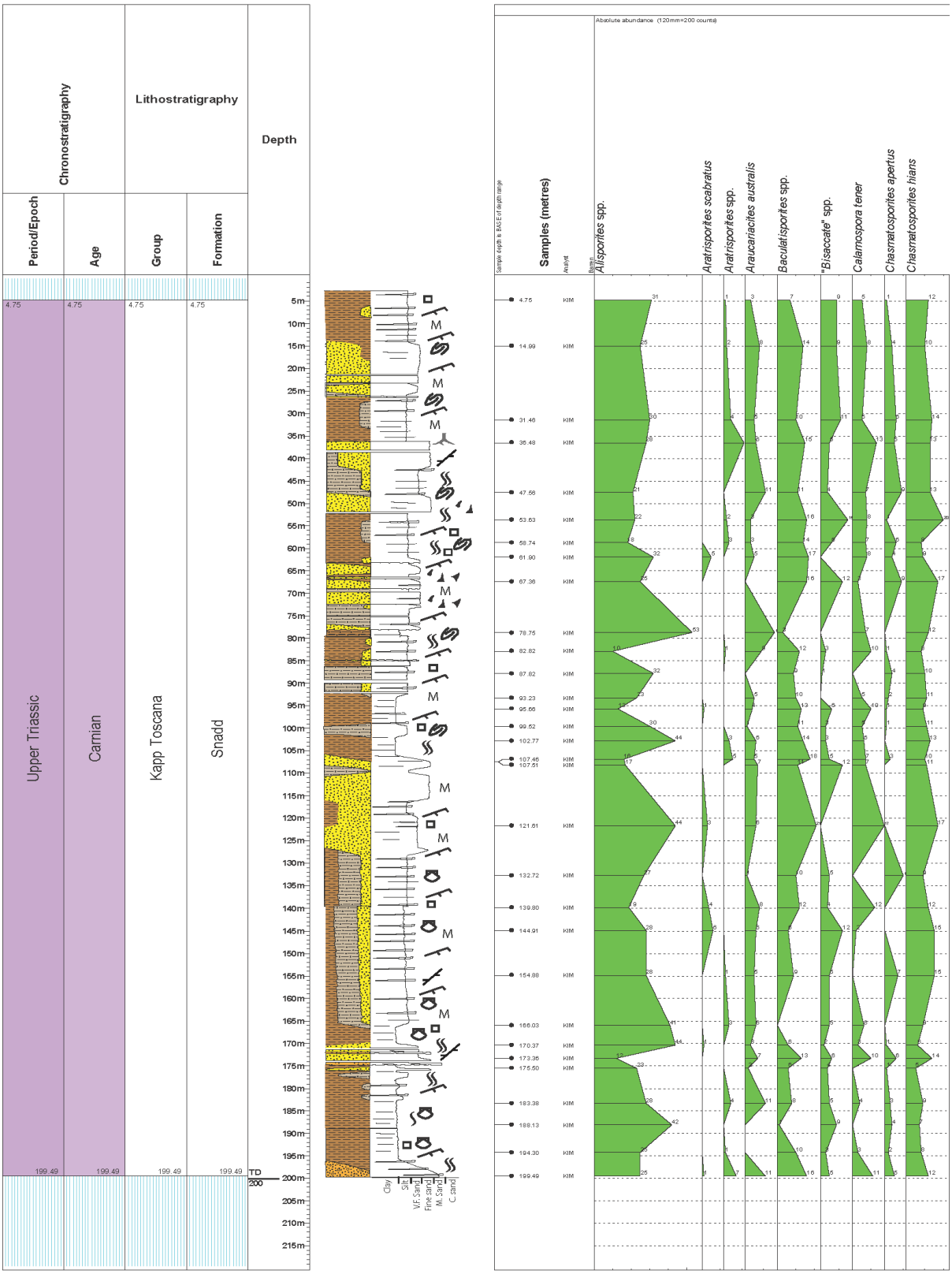

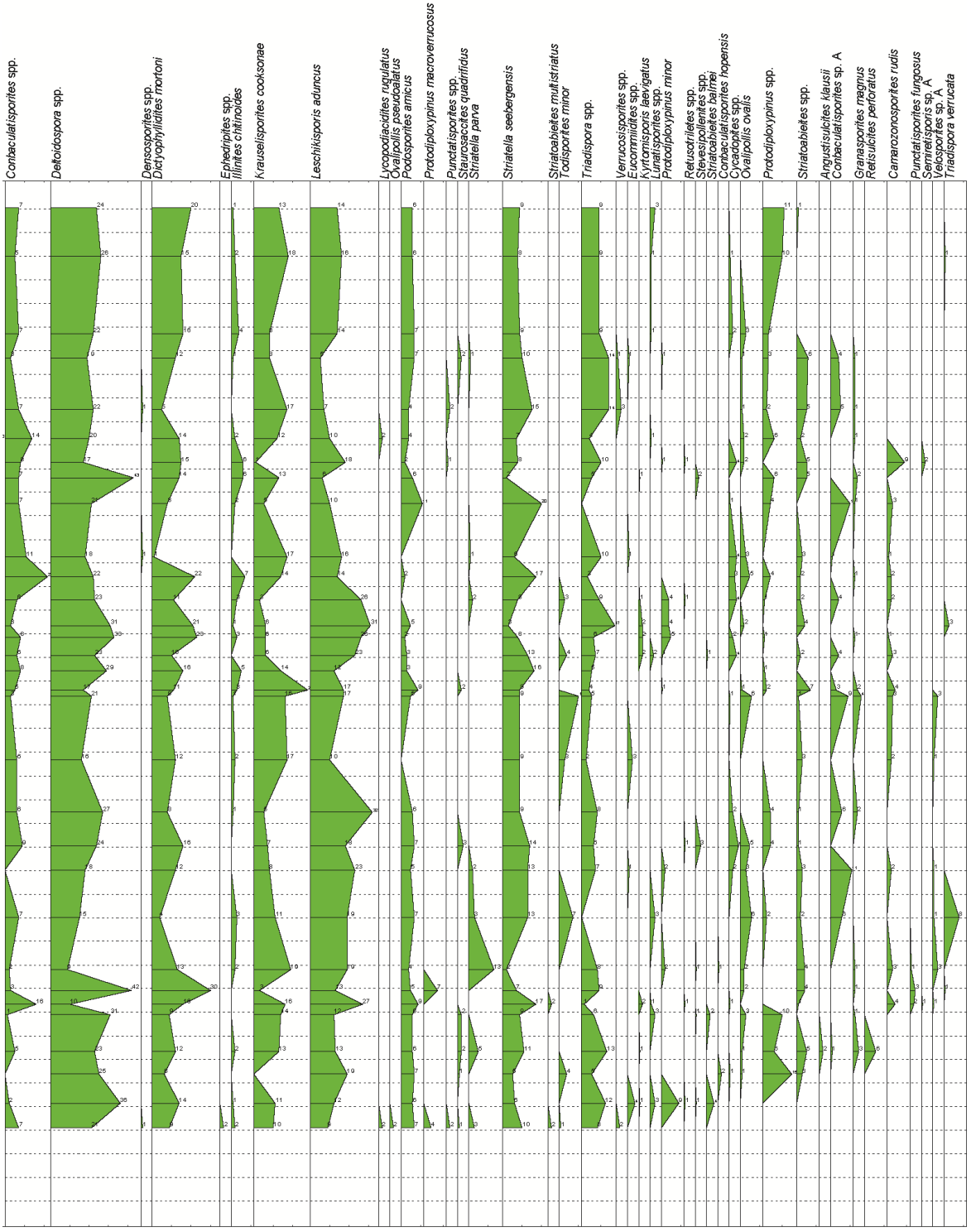
Conbaculatisporites spp.
Deltoidospora spp.
Densosporites spp.
Dictyophyllidites mortoni
Ephedripites spp.
Inaperturopollenites chitinoides
Krauselisporites cooksonae
Leschiksporis aduncus
Lycopodiacidites rugulatus
Ovalipollis pseudoalatus
Podosporites amicus
Protodiploxypinus macroverrucosus
Punctatisporites spp.
Staurosaccites quadrifidus
Striatella parva
Striatella seebergensis
Striatoabieites multistriatus
Todisporites minor
Triadispora spp.
Verrucosisporites spp.
Eucommiidites spp.
Kyrtomisporis laevigatus
Lunatisporites spp.
Protodiploxypinus minor
Retusotriletes spp.
Stevesipollenites spp.
Striatoabieites balmei
Conbaculatisporites hopensis
Cycadopites spp.
Ovalipollis ovalis
Protodiploxypinus spp.
Striatoabieites spp.
Angustisulcites klausii
Conbaculatisporites sp. A
Granasporites magnus
Reticulcites perforatus
Camarozonosporites rudis
Punctatisporites fungosus
Semiretisporis sp. A
Velosporites sp. A
Triadispora verrucata

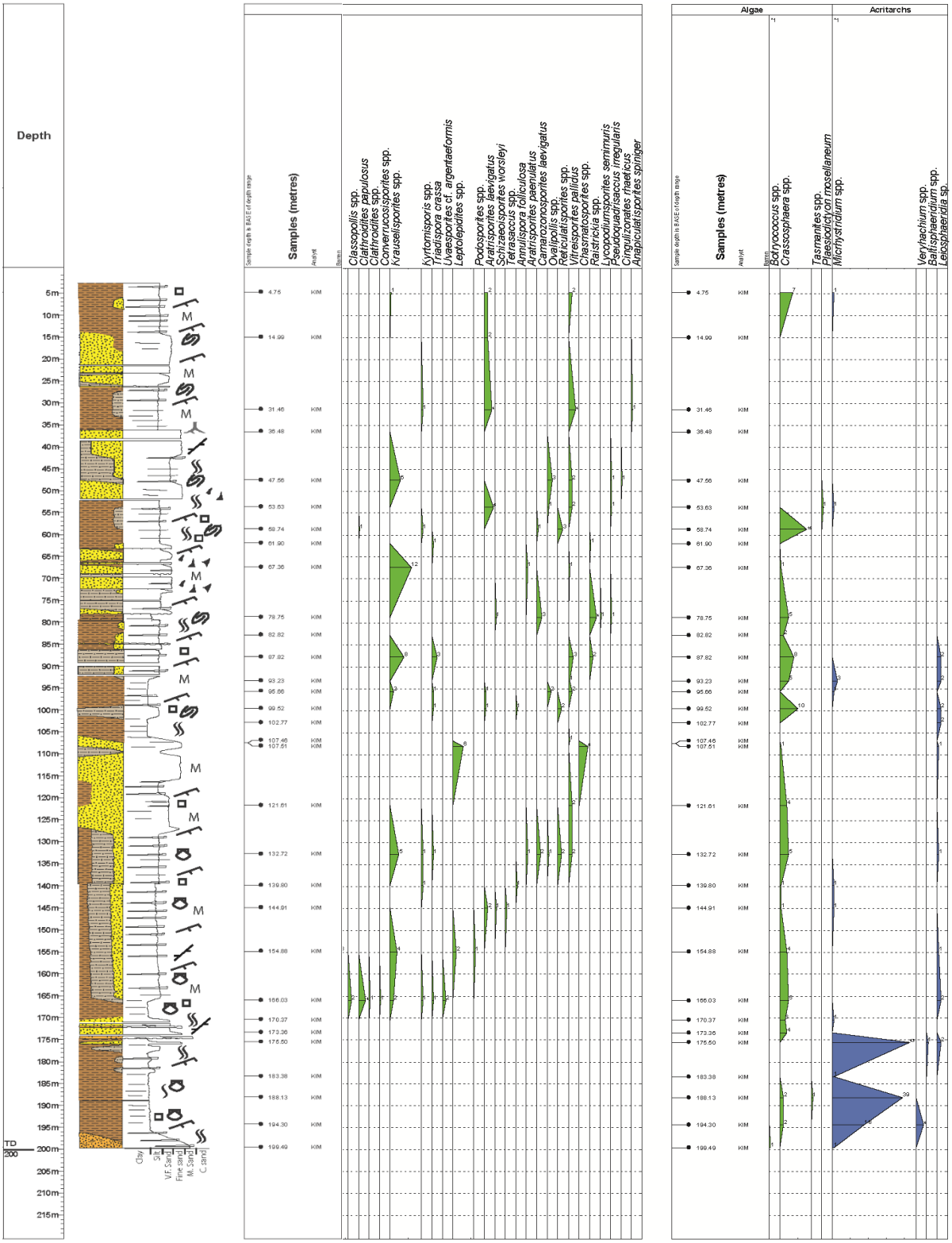
Depth
Samples (metres)
Algae
Acritarchs
Clay
Silt
V.F. Sand
Fine sand
M. Sand
C. sand
TD
Classopollis spp.
Callialasporites segmentatus
Callialasporites spp.
Cerebropollenites macroverrucosus
Cerebropollenites spp.
Kraeuselisporites spp.
Kyrtomisporis spp.
Triadispora crassa
Uvaesporites cf. argentaeformis
Leptolepidites spp.
Podosporites spp.
Aratrisporites laevigatus
Schizaeoisporites worsleyi
Tetrasaccus spp.
Annulispora folliculosa
Aratrisporites paenulatus
Camarozonosporites laevigatus
Osmundacidites spp.
Osmundacidites wellmanii
Vitreisporites pallidus
Chasmatosporites spp.
Raistrickia spp.
Lycopodiumsporites semimuris
Pseudoquadrisaccus irregularis
Cingulizonates rhaeticus
Anapiculatisporites spiniger
Botryococcus spp.
Crassosphaera spp.
Tasmanites spp.
Plaesiodictyon mosellanaeum
Micrhystridium spp.
Veryhachium spp.
Baltisphaeridium spp.
Leiosphaeridia sp.

Appendix III: Range chart, including palynofacies estimates

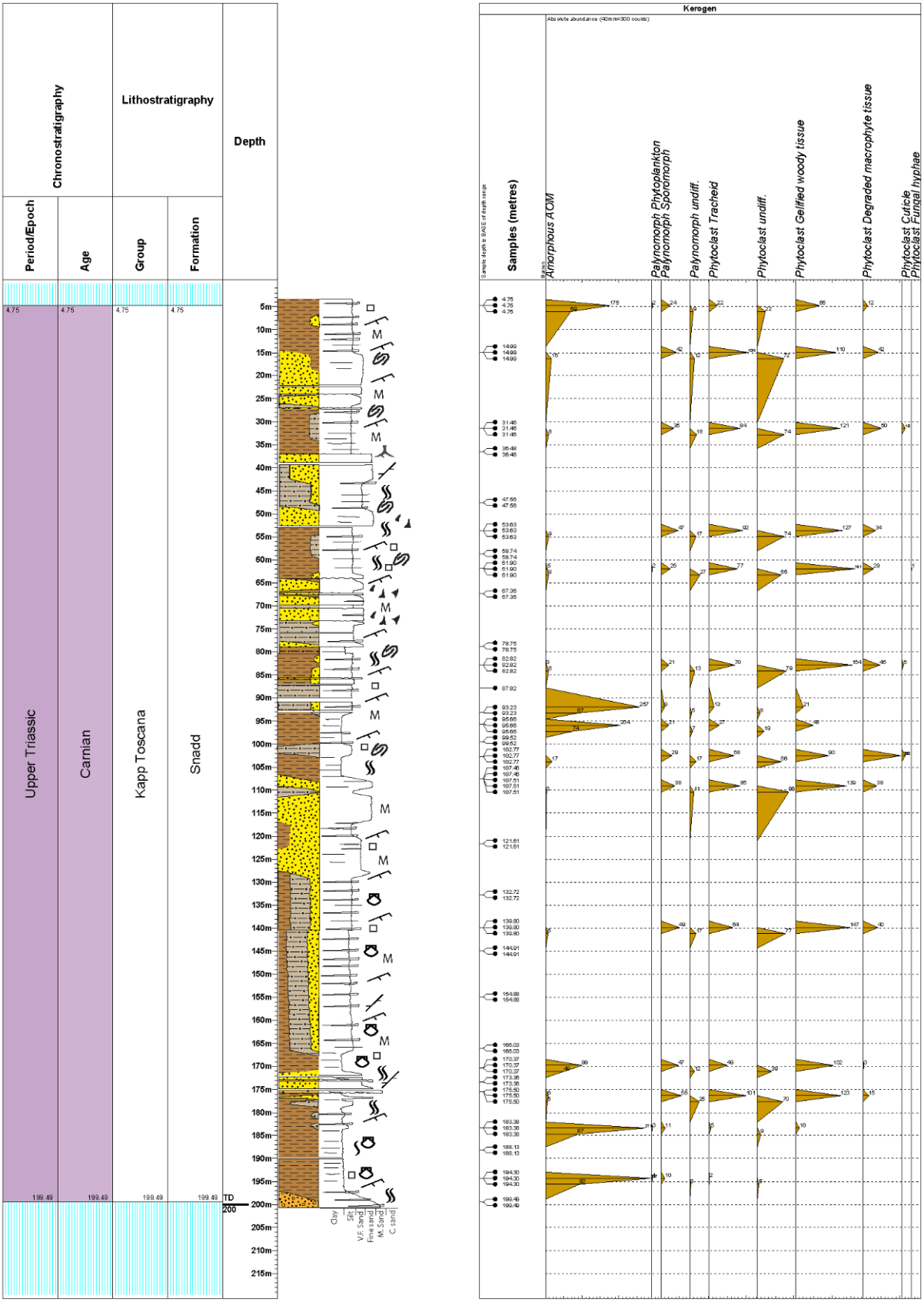

Appendix IV: Plates

Plates of selected palynomorphs recorded from core 7830/3-U-1. The genus/species are followed by the sample depth and the England Finder coordinates. All slides were analysed with the label to the right.

Plate 1

1 *Deltoidospora* sp. 58.74 m, T43-4

2 *Deltoidospora* sp. 67.36 m, G47

3 *Cyathidites* sp. 58.74 m, S56

4 *Dictyophyllidites mortonii* 47.56 m, P56-3

5 *Dictyophyllidites mortonii* 183.38 m, W47-2

6 *Striatella parva* 87.82 m, C48-4

7 *Striatella parva* 121.61 m, R44

8 *Striatella seebergensis* 99.52 m, M47

9 *Striatella seebergensis* 183.38 m, C38

10 *Striatella seebergensis* 99.52 m, M48

11 *Retusotriletes* sp. 99.52 m, T46

12 *Retusotriletes* sp. 47.56 m, R45-3

13 *Camarozonosporites rudis* 36.48 m, N45

14 *Camarozonosporites rudis* 99.52 m, L53-4

15 *Camarozonosporites rudis* 188.13 m, E44-1

16 *Lycopodiacidites rugulatus* 166.03 m, M54-2

Plate 1

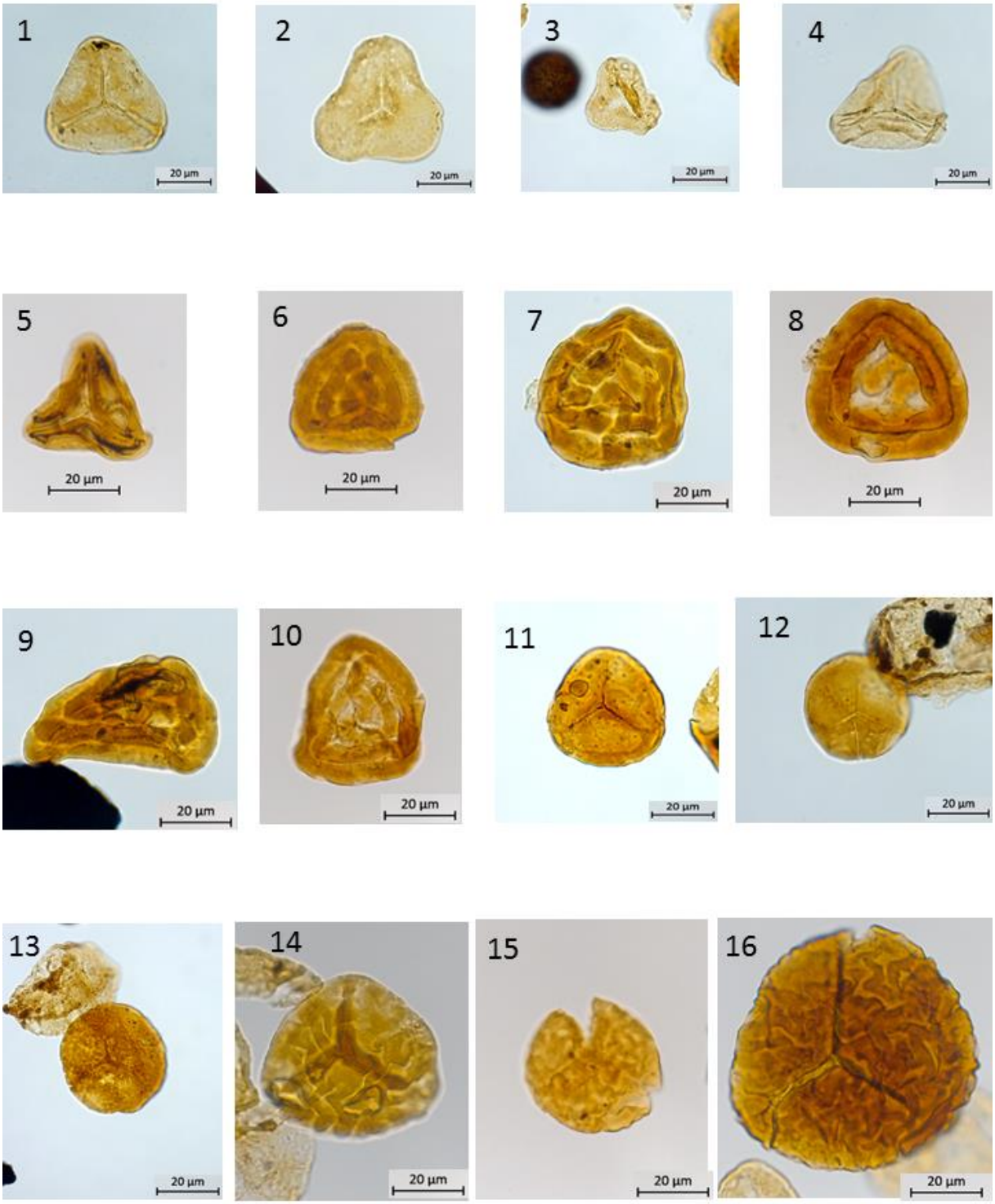
1
20 µm
2
20 µm
3
20 µm
4
20 µm
5
20 µm
6
20 µm
7
20 µm
8
20 µm
9
20 µm
10
20 µm
11
20 µm
12
20 µm
13
20 µm
14
20 µm
15
20 µm
16
20 µm

Plate 2

1. *Clathroidites fuscus* 47.56 m, P56
2. *Conbaculatisporites* sp. 78.75 m, N55
3. *Conbaculatisporites* sp. 99.52 m, O57-3
4. *Conbaculatisporites* sp. 194.30 m, W36-4
5. *Clathroidites papulosus* 132.72 m, O-55
6. *Clathroidites papulosus* 87.82 m, D50-1
7. Spore sp. A 78.75 m, N55
8. Spore sp. A 58.74 m, J52-1
9. Spore sp. A 132.72 m, H56-4
10. Spore sp. A 58.74 m, T-56
11. *Baculatisporites* sp. 194.30 m, D47
12. *Jerseyiaspora punctispinosa* 31.46 m, W38-3
13. *Leschikisporis aduncus* 47.56 m, P49
14. *Leschikisporis aduncus* 78.75 m, T55
15. *Baculatisporites* sp. 194.30 m, D47

Plate 2

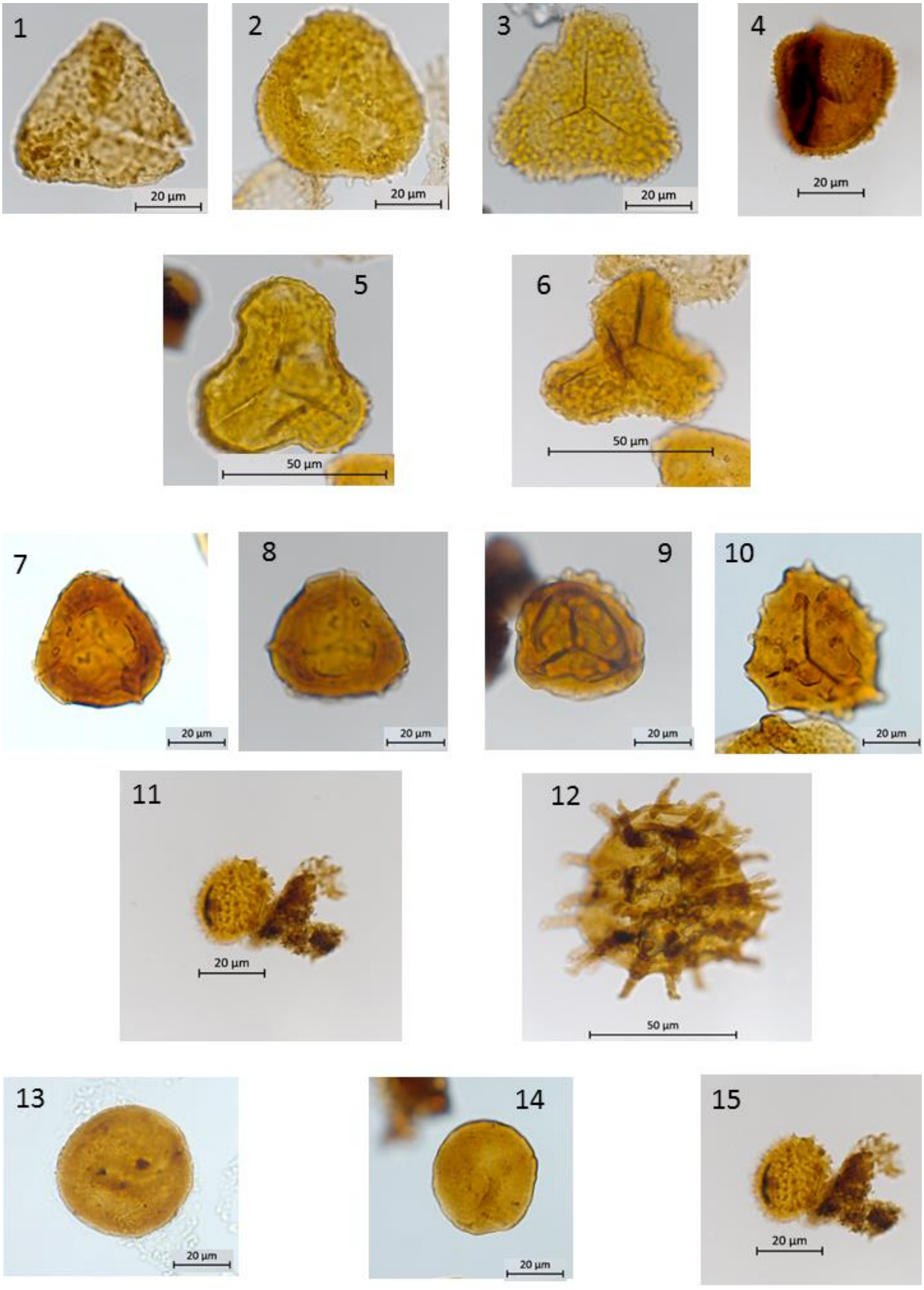
1
20 µm
2
20 µm
3
20 µm
4
20 µm
5
50 µm
6
50 µm
7
20 µm
8
20 µm
9
20 µm
10
20 µm
11
20 µm
12
50 µm
13
20 µm
14
20 µm
15
20 µm

Plate 3

1 *Kraeuselisporites* spp. 132.72 m, M45

2 *Kraeuselisporites cooksonae* 58.74 m, S41-4

3 *Kraeuselisporites* sp. *58.74* m, Q 47

4 *Semiretisporis* spp. 47.56 m, H51-4

5 *Semiretisporis* spp. 58.74 m, U41-3

6 *Velosporites* sp. 36.48 m, W55

7 *Cordaitina* sp.? 78.75 m, T55-3

8 *Aratrisporites* sp. 99.52 m, V50

9 *Aratrisporites* sp. 166.03 m, G40-2

10 *Calamospora tener* 99.52 m, R47-1

11 *Calamospora tener* 166.03 m, X39

Plate 3

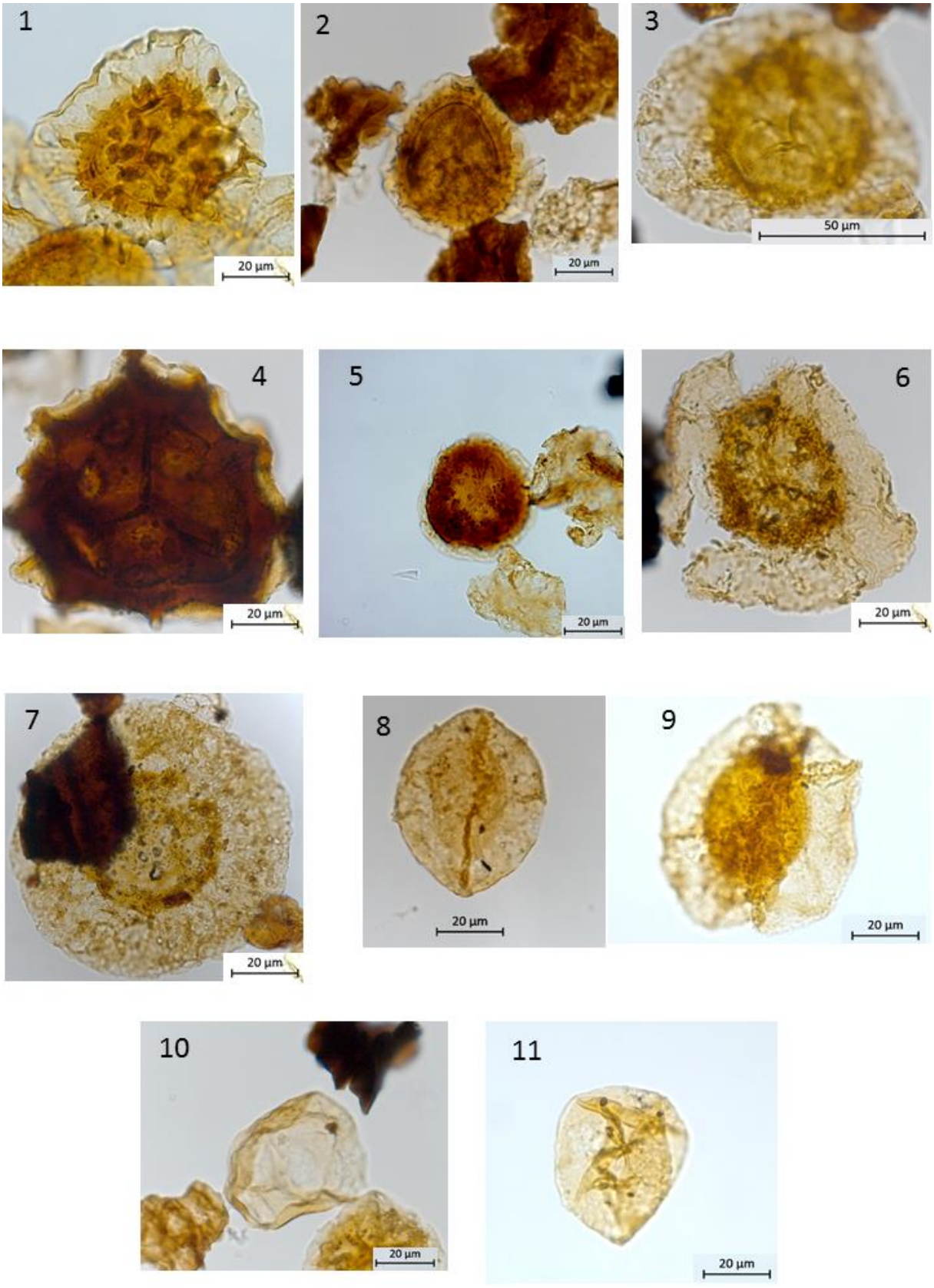
1
20 µm
2
20 µm
3
50 µm
4
20 µm
5
20 µm
6
20 µm
7
20 µm
8
20 µm
9
20 µm
10
20 µm
11
20 µm

Plate 4

1 *Chasmatosporites* sp. 36.48 m, H57-3

2 *Chasmatosporites hians* 99.52 m, N48-4

3 *Chasmatosporites hians* 188.13 m, M51-2

4 *Chasmatosporites* sp. 36.48 m, H55

5 *Illinites chitinoides* 58.74 m, T40-1

6 *Illinites chitinoides* 58.74 m, O43-1

7 *Staurosaccites quadrifidus* 188.19 m, V48-2

8 *Staurosaccites quadrifidus* 166.03 m, W46

Plate 4

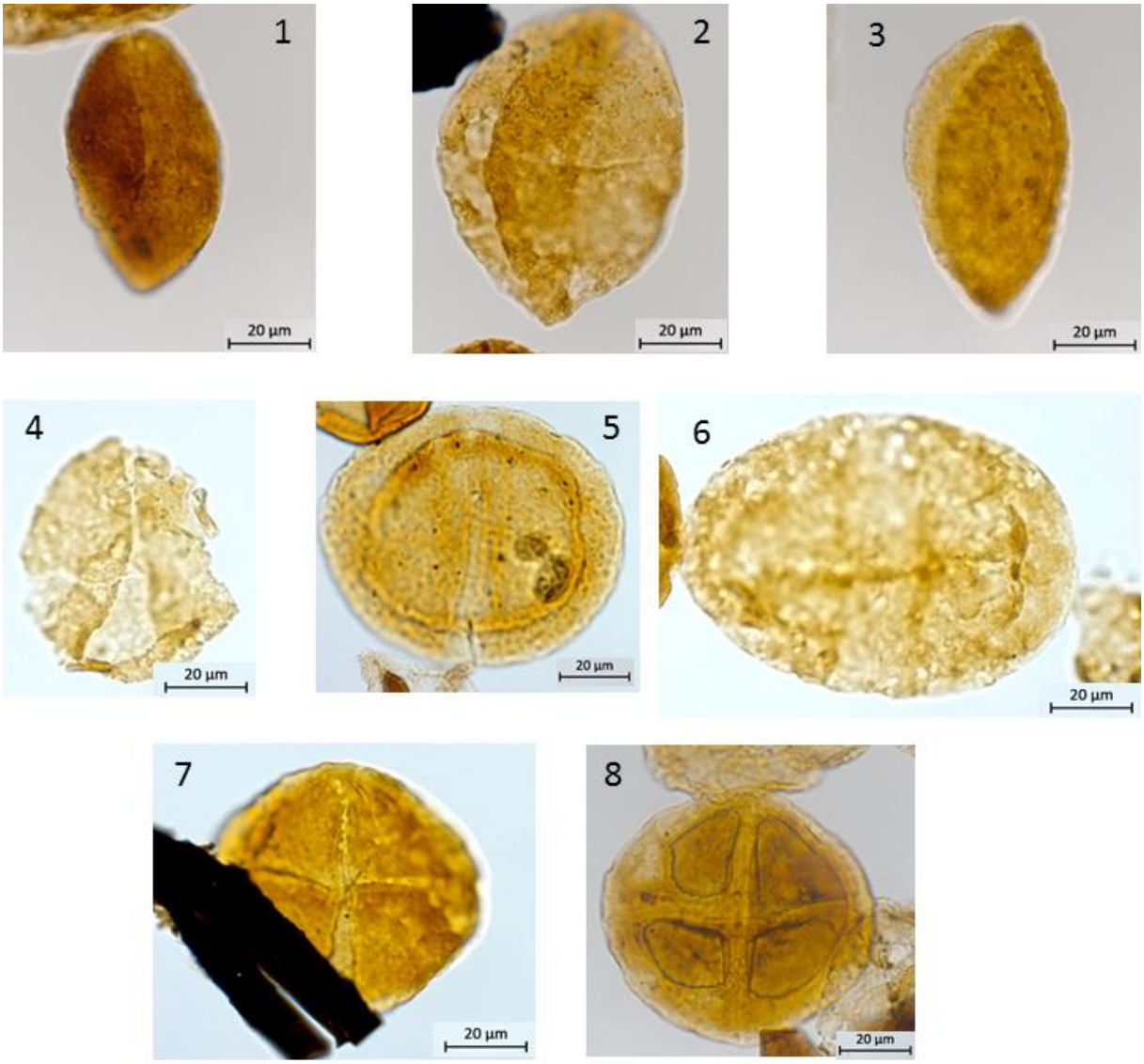

Plate 5

1 *Vitreisporites pallidus* 194.30 m, U41-4

2 *Alisporites* sp. 36.48 m, P45-3

3 Bisaccate pollen *36.48 m, L51*

4 *Protodiploxypinus* sp. 99.52 m, J50

5 *Protodiploxypinus* sp. 188.13 m, P50-3

6 *Protodiploxypinus* sp. 132.72 m, L45

7 *Striatoabieites balmei?* 99.52 m, O54-3

8 *Striatoabieites multistriatus* 99.52 m, T55-4

9 *Striatoabieites multistriatus* 194.30 m, Q41-1

10 *Striatoabieites* sp.36.48 m, G55

11 *Podosporites amicus* 58.74 m, T40-1

12 *Podosporites amicus* 188.13 m, E50-4

13 *Podosporites amicus* 36.48 m, F53-2

Plate 5

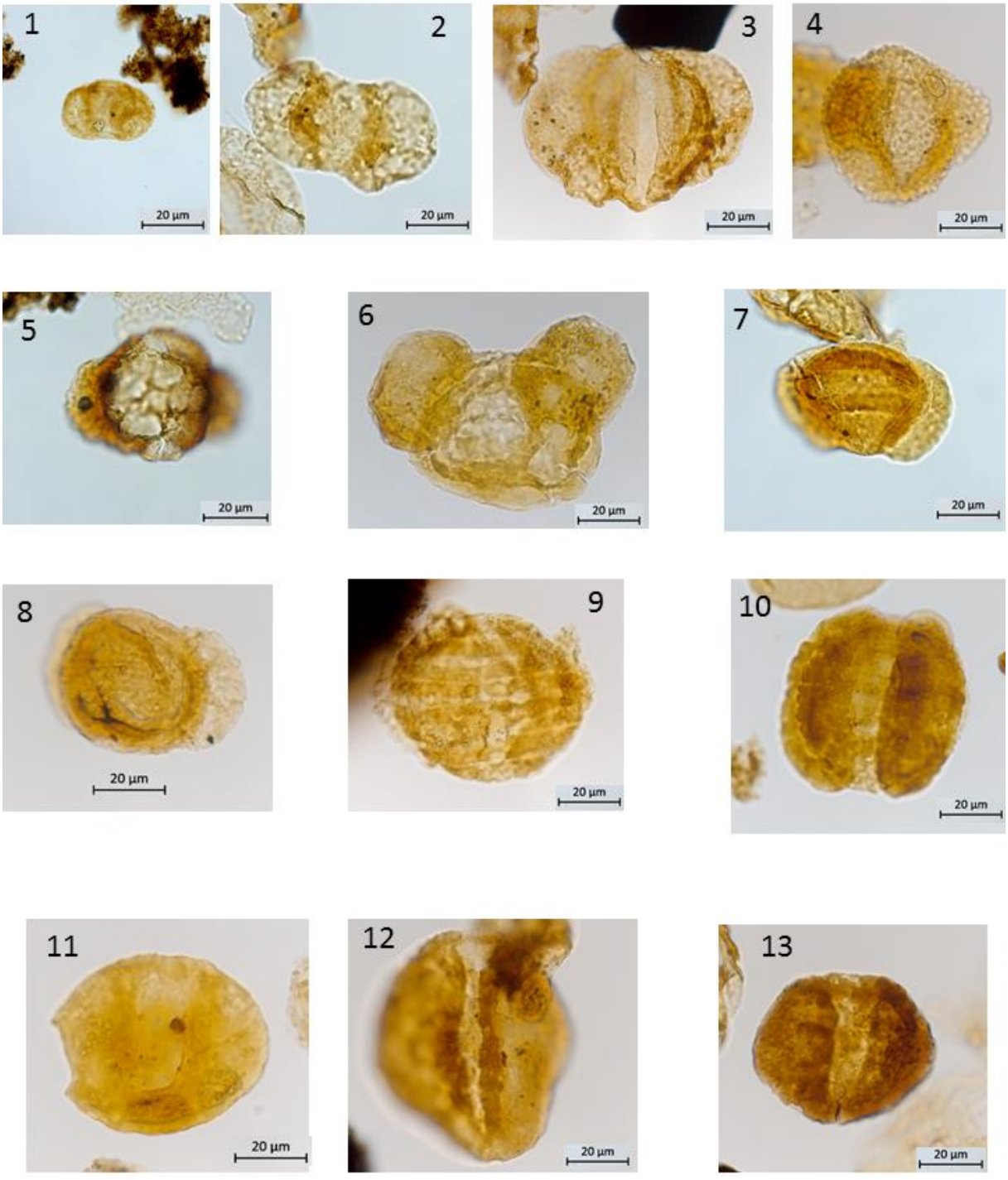
1
20 µm
2
20 µm
3
20 µm
4
20 µm
5
20 µm
6
20 µm
7
20 µm
8
20 µm
9
20 µm
10
20 µm
11
20 µm
12
20 µm
13
20 µm

Plate 6

1 *Echinitosporites iliacoides?* 183.38 m, T34-1

2 *Triadispora* sp. 58.74 m, Q47

3 *Triadispora* sp. 99.52 m, O55

4 *Angustisulcites klausii?* 166.03 m, L38

5 *Angustisulcites klausii*? 188.13 m, G45-4

6 *Araucariacites australis* 99.52 m, J53

7 *Araucariacites australis* 99.52 m, J54

8 *Illinites chitinoides* 31.46 m, O48-2

9 *Illinites chitinoides* 58.74 O43-1

10 *Ovalipollis* sp. 31.46 m, O48-2

11 *Ovalipollis ovalis* 166.03 m, P38-2

12 *Ovalipollis* sp. 99.52 m, S45

Plate 6

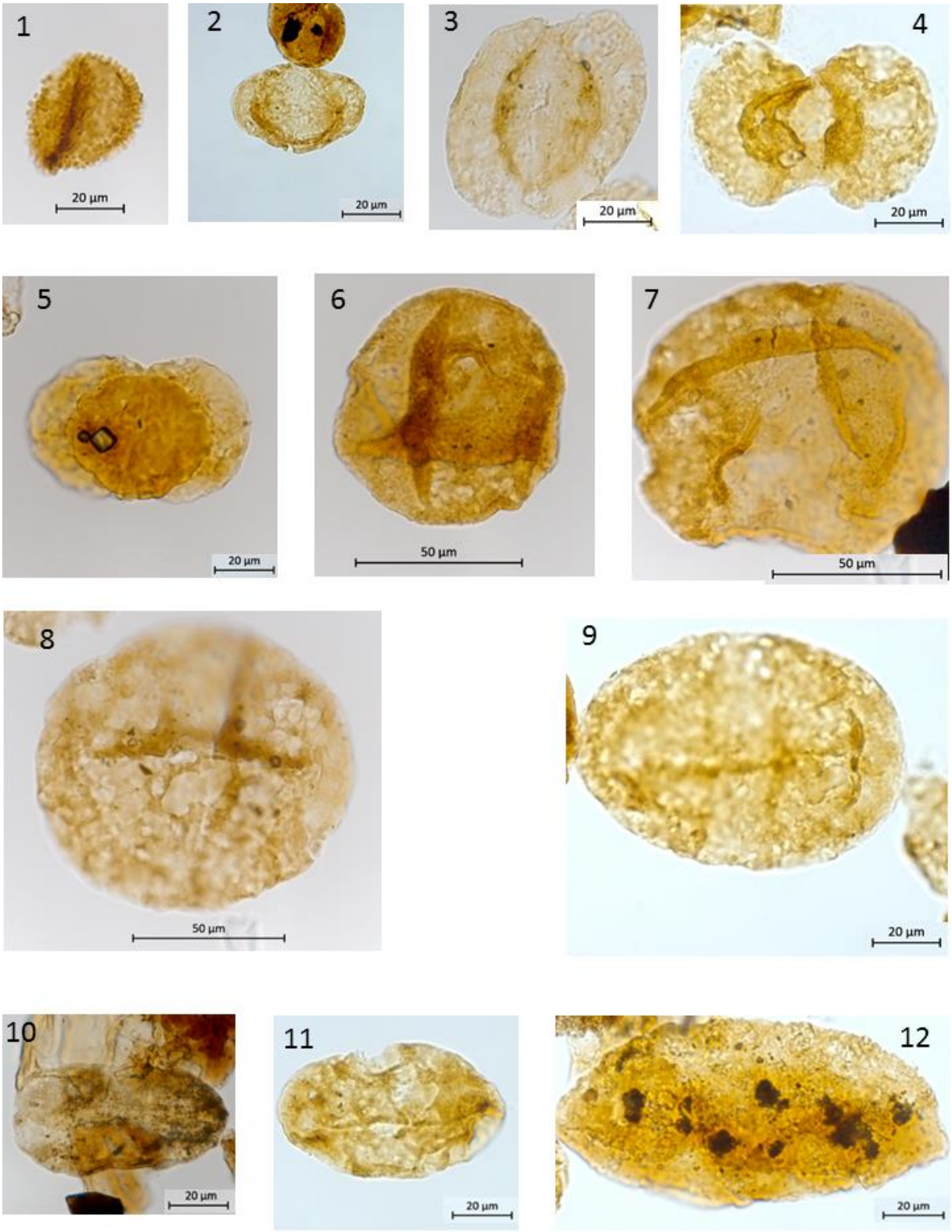
1
20 µm
2
20 µm
3
20 µm
4
20 µm
5
20 µm
6
50 µm
7
50 µm
8
50 µm
9
20 µm
10
20 µm
11
20 µm
12
20 µm

Plate 7

1 *Crassosphaera* sp. 58.74 m, S41-4

2 *Crassosphaera* sp. 99.52 m, S47-4

3 *Leiosphere* sp. 166.03 m, S44-3

4 *Baltisphaeridium* sp. 99.52 m, V50

5 *Baltisphaeridium* sp. 194.30 m, G49-2

6 *Baltisphaeridium* sp. 166.13 m, Q49-2

7 *Baltisphaeridium* sp. 188.13 m, J51-4

8 *Micrhystridium* sp. 188.13 m, J50-4

9 *Micrhystridium* sp. 194.30 m, D44-3

10 *Micrhystridium* sp. 194.30 m, U41-4

11 *Pterospermella* sp. 194.30 m, D49-2

12 *Veryhachium* sp. 194.30 m, D42-1

13 *Veryhachium* sp. 194.30 m, R43-2

14 *Veryhachium* sp. 194.30 m, X54

15 *Plaesiodictyon mosellanum* 194.30 m, R 42-4

Plate 7

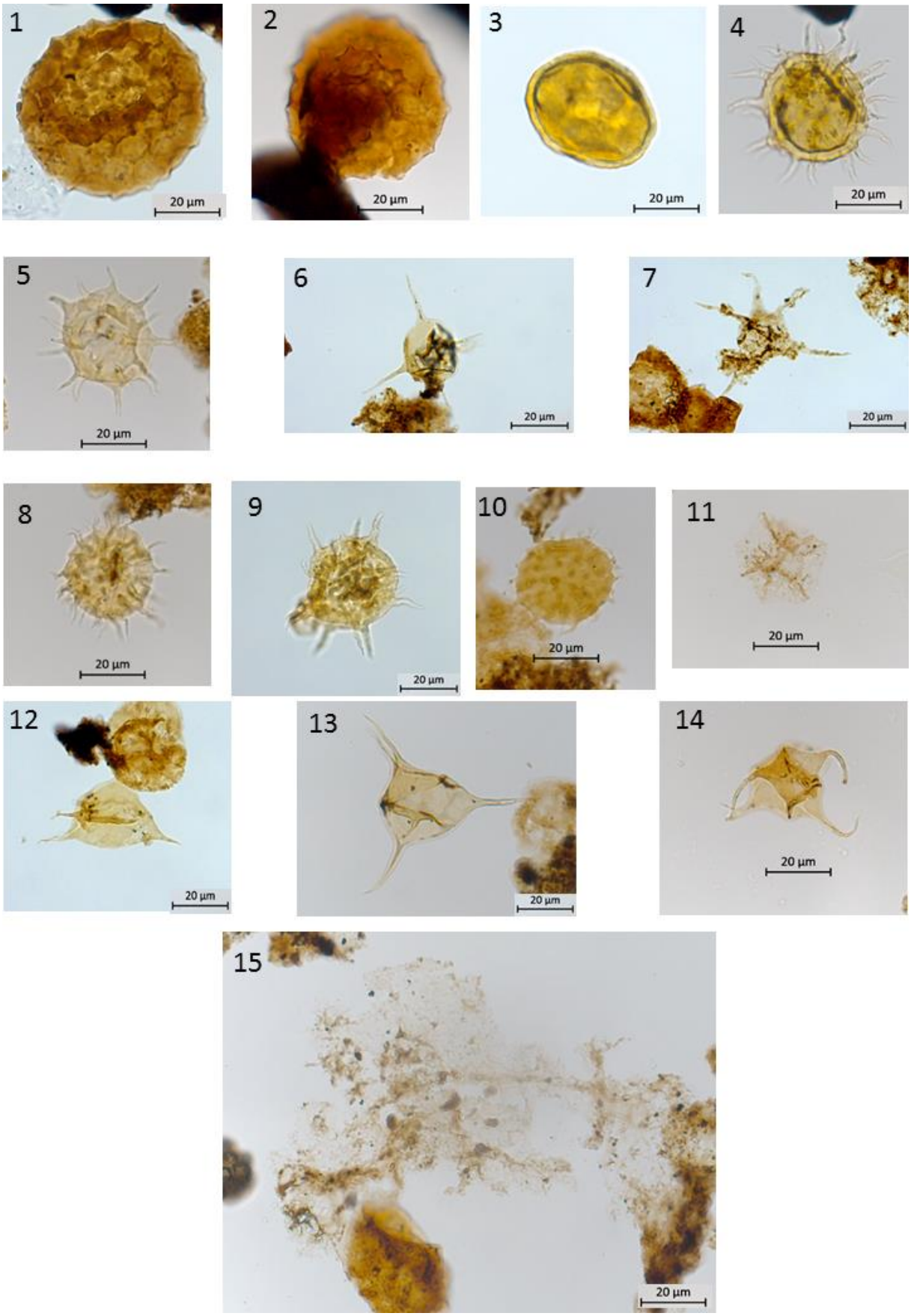
1
20 µm
2
20 µm
3
20 µm
4
20 µm
5
20 µm
6
20 µm
7
20 µm
8
20 µm
9
20 µm
10
20 µm
11
20 µm
12
20 µm
13
20 µm
14
20 µm
15
20 µm